EVOLUTION OF TERTIARY PLUTONIC AND VOLCANIC ROCKS NEAR RAVENNA, GRANITE COUNTY, MONTANA

by

BRUCE KEVIN REITZ

B.S., Wright State University, 1978

A MASTER'S THESIS

submitted in partial fulfillment of the

requirements of the degree

MASTER OF SCIENCE

Department of Geology

KANSAS STATE UNIVERSITY
Manhattan, Kansas

1980

Approved by:

Sambhudas Chaudhuri
Major Professor

THIS BOOK
CONTAINS
NUMEROUS PAGES
WITH THE ORIGINAL
PRINTING BEING
SKEWED
DIFFERENTLY FROM
THE TOP OF THE
PAGE TO THE
BOTTOM.

THIS IS AS RECEIVED
FROM THE
CUSTOMER.

CONTENTS

FIGURES

TABLES

ACKNOWLEDGEMENTS

The assistance and support of numerous people have been instrumental in all phases of this project. Dr. Sambhudas Chaudhuri served as major professor and assisted greatly in all aspects of the study. Members of the supervisory committee include Dr. H.V. Beck, Dr. J.L. Copeland, and Dr. R.L. Cullers. Dr. J.R. Underwood also provided constructive editorial remarks.

Dr. C.W. Wallace of the U.S. Geological Survey suggested the problem and aided in field orientation. Insights on the lithium metaborate fusion technique for atomic absorption and emission analyses were provided by Joseph P. Smalley of Kansas State University and Dr. James Gutmann of Weslyan University. Trace-element analyses by X-ray fluorescence were kindly done by Dr. Gerard James of the Kansas Geological Survey. Dr. Paul Pushkar, Wright State University, aided in manuscript preparation and provided moral support. The cooperation of the kind Montanans who provided access to their property, particularly the Weston family, was necessary for the completion of field work. Special thanks are due to my wife, Malia who assisted in ways too numerous to mention.

Financial support was provided by grants-in-aid of research from Sigma Xi, the Scientific Research Society of North America, and the Geological Society of America.

I N T R O D U C T I O N

STATEMENT OF THE PROBLEM

The Ravenna area, central-western Montana, contains a series of plutonic and volcanic rocks which range in composition from basaltic to rhyolitic. The purpose of this study is to define more precisely the areal extent and physical relations of these bodies, examine the geochemical relations of the rock types present, determine approximate ages of emplacement, and examine the petrogenetic histories of the igneous bodies. In order to procure data to attain these goals, the following investigations have been conducted: (1) geologic mapping and sampling of the igneous features surrounding Ravenna, (2) petrographic analyses of the volcanic and plutonic rocks, (3) major and trace-element analyses of the major igneous rock types by spectrophotometry, (4) trace-element and rare-earth element analyses of selected igneous samples by instrumental neutron activation analysis, and (5) strontium isotope compositions by mass spectrometry and Rb and Sr concentrations by X-ray fluorescence.

REGIONAL AND TECTONIC SETTING

The study area is located thirty miles east of Missoula in ranges fifteen and sixteen west, township eleven north, of the Ravenna and Bearmouth quadrangles. It occupies a segment of the northern Sapphire

Mountains on the Lolo National Forest and covers approxiamately thirty square miles (Fig. 1). The Clark Fork River is the approximate northern boundary, with Tyler Creek and Gillespie Creek forming approximate eastern and western boundaries, respectively.

Major structural and tectonic features in the area include the northern boundary of the Sapphire tectonic block and a portion of one of the Lewis and Clark lineaments. Beltian sediments comprise the Sapphire block, which has been thrust eastward approximately 25 km in response to the rise of the Idaho batholith 70 to 80 million years ago (Hyndman et al., 1975; Hyndman, 1979). Boundaries of the Sapphire block are marked by imbricate thrust faults and shearing of the brittle Precambrian units and large-scale structural deformation of the underthrust Paleozoic sediments. The Lake-Basin lineament, as defined by Smith (1965), passes beneath this area and is thought to represent a fundimental subsurface fault zone (Fig. 2). Other sources define this lineament as the Lewis and Clark line (Desormier, 1975), the Coeur d'Alene lineament (Montgomery, 1958), or the Montana lineament (Weidman, 1965).

RELATED LITERATURE

Northern portions of the Ravenna area were initially mapped by J.T. Pardee (1918). He defined a granodiorite intrusion and a pre-Tertiary gabbro sill overlain by mid-Tertiary dacite. In 1957, Joel Montgomery mapped the geology of the Nimrod area which included the eastern two-thirds of the present study area. Montgomery (1958) defined the Precambrian units as portions of the Belt Series and included brief petrographic descriptions of the major volcanic and plutonic units. Magmatic differentiation and textural zonations in the gabbro sill were

THIS BOOK CONTAINS NUMEROUS PAGES WITH DIAGRAMS THAT ARE CROOKED COMPARED TO THE REST OF THE INFORMATION ON THE PAGE.

THIS IS AS RECEIVED FROM CUSTOMER.

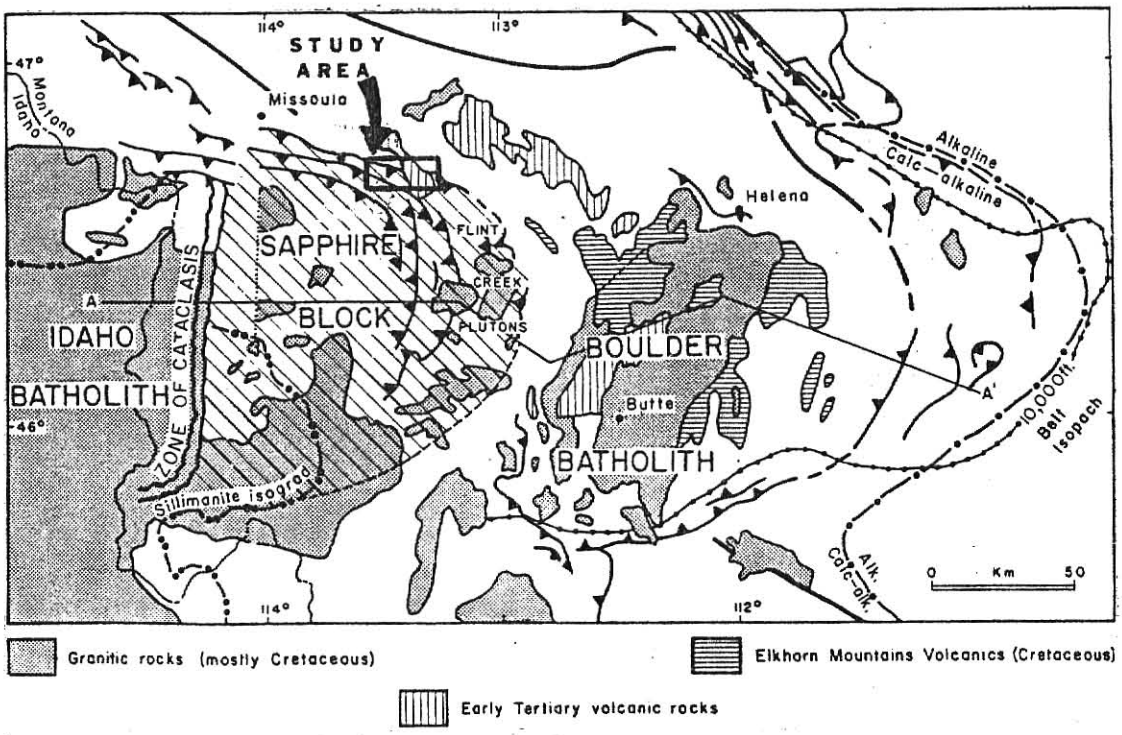

Figure 1. General geology of the central-western Montana area with the location of the present study area. From Hyndman, Talbot, and Chase (1975).

detailed by Montgomery (1958). William Desormier (1975) mapped a section of the northern boundary of the Sapphire tectonic block and surficially examined the igneous rocks in the western portion of the present study area.

GEOGRAPHY

The Ravenna area lies to the south of the Garnet Range and to the east of the axis of the Sapphire Mountains. Maximum elevation in the study area is 1980 m (6500 ft), maximum relief is 820 m (2700 ft). The region is mountainous and maturely dissected by erosion.

Coniferous forests of white pine, larch, ponderosa pine, and lodgepole pine cover the area, although extensive logging has occured in the last fifteen years. Logging roadcuts provide numerous exposures of

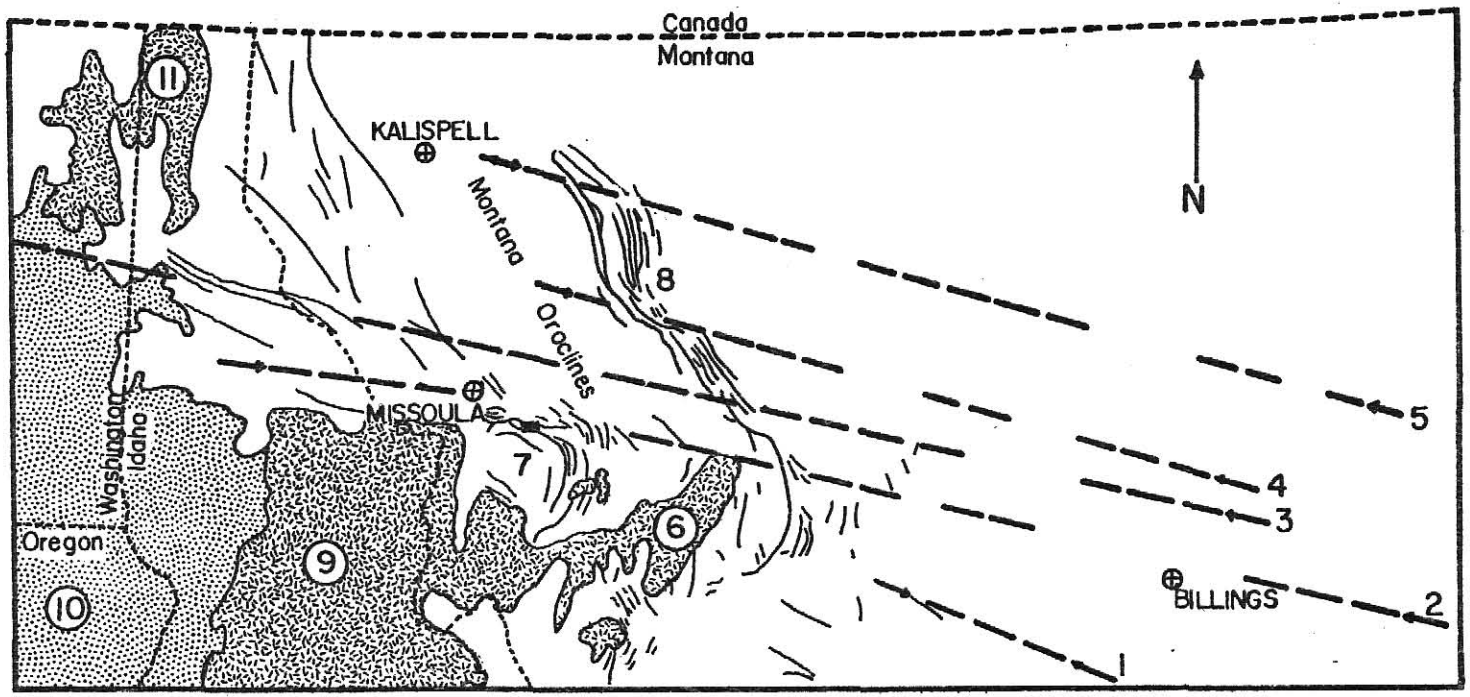

LEWIS AND CLARK LINEAMENTS

1 Nye-Bowler Lineament

2 Lake Basin Lineament

3 Osburn Lineament

4 Big Snowey Lineament

5 Cat Creek Lineament

IGNEOUS BODIES AND CONSTITUENT STRUCTURES

6 Boulder Batholith

7 Sapphire Tectonic Block

8 Disturbed Belt

9 Idaho Batholith

10 Columbia River Basalt Plateau

11 Loon Lake Batholith

Cordilleran Folds and Thrust Faults

Study Area

Figure 2. Major structural and tectonic features in the Montana area.

relatively fresh portions of rock units.

The climate is cool and semi-arid, but has wide daily and seasonal temperature variations. Winter temperatures rarely drop below -37° C (-35° F), and summer temperatures seldom exceed 35° C (95° F) with nighttime temperatures commonly dropping below 5° C (41° F). Annual rainfall averages 32 cm (12.5 in.).

Access is excellent within most portions of the study area. A major interstate highway, I-90, follows the Clark Fork River in the northern portions of the area. An extensive network of recent logging roads provides access to the more mountainous southern regions of the thesis area.

MAPPING AND SAMPLING TECHNIQUES

During four weeks of field work, the boundaries of the igneous bodies were defined, structural relations and internal variations of igneous units were described, and samples were collected. Geologic data were recorded on a U. S. Forest Service seven and a half minute quadrangle map. Aerial photographs taken in 1959 were obtained from the U. S. Department of Agriculture and aided in geologic interpretation. Igneous contacts were walked out laterally and numerous traverses across the igneous bodies were made. Hand samples were selected form the freshest portions of outcrops and trimmed to remove weathered surfaces. The locations of contacts and faults within Paleozoic and Precambrian sediments were obtained from a U. S. Geological Survey open file report (Wallace et al., 1978). Samples from several Precambrian units were taken near the boundaries of igneous units.

G E O L O G Y

STRATIGRAPHY

Volcanic and plutonic rocks within the study area include dacite porphyry, rhyodacite, granodiorite, basalt and gabbro. A Tertiary age has been assigned to the majority of the igneous rocks, although Pardee (1918) and Montgomery (1958) defined the large diabase (gabbro) sill as pre-Tertiary or Upper Cretaceous.

Igneous outcrops tend to lie parallel to the strike of the Precambrian formations (Fig. 3). Thrust faults and shear zones within and between the sedimentary units represent fundamental planes of weakness along which the igneous rocks have apparently intruded (Fig. 4). No deformation within the igneous units has been noted, placing the maximum age of igneous activity after the emplacement of the Sapphire tectonic block.

Sedimentary strata within the study area consists primarily of slightly metamorphosed sediments of Precambrian age and minor Paleozoic sedimentary rocks. The Precambrian rocks consist of the middle Belt carbonate unit and the Missoula Group of the Belt Supergroup. Paleozoic sediments occur primarily in the northern part of the study area, and are overthrust by the Precambrian series. Precambrian units occur in broadly northwest-trending belts bounded on the north by the Bearmouth thrust fault. A series of south to southwest dipping thrust faults seperates the Beltian units.

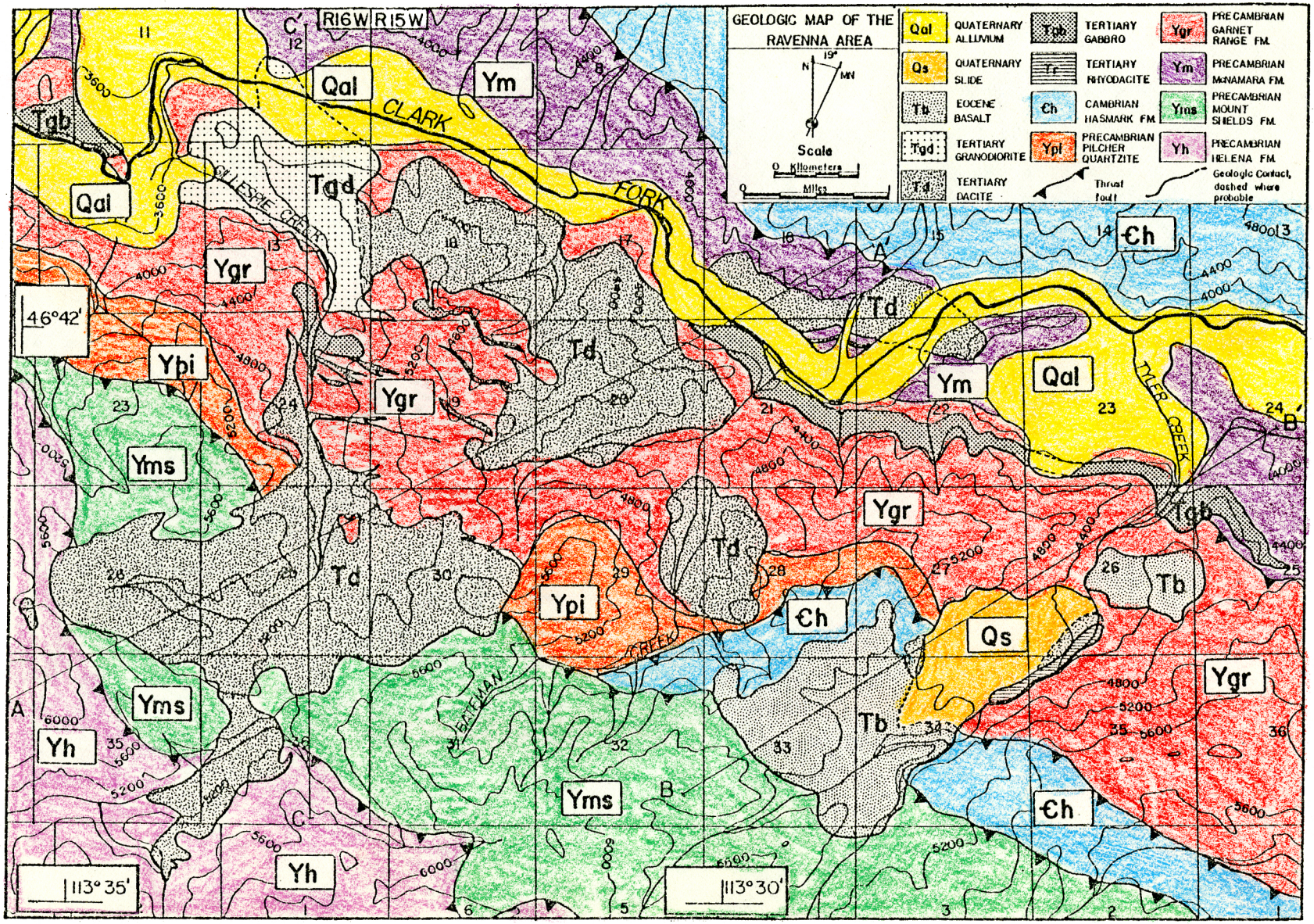

Figure 3. Geologic map of the Ravenna area.

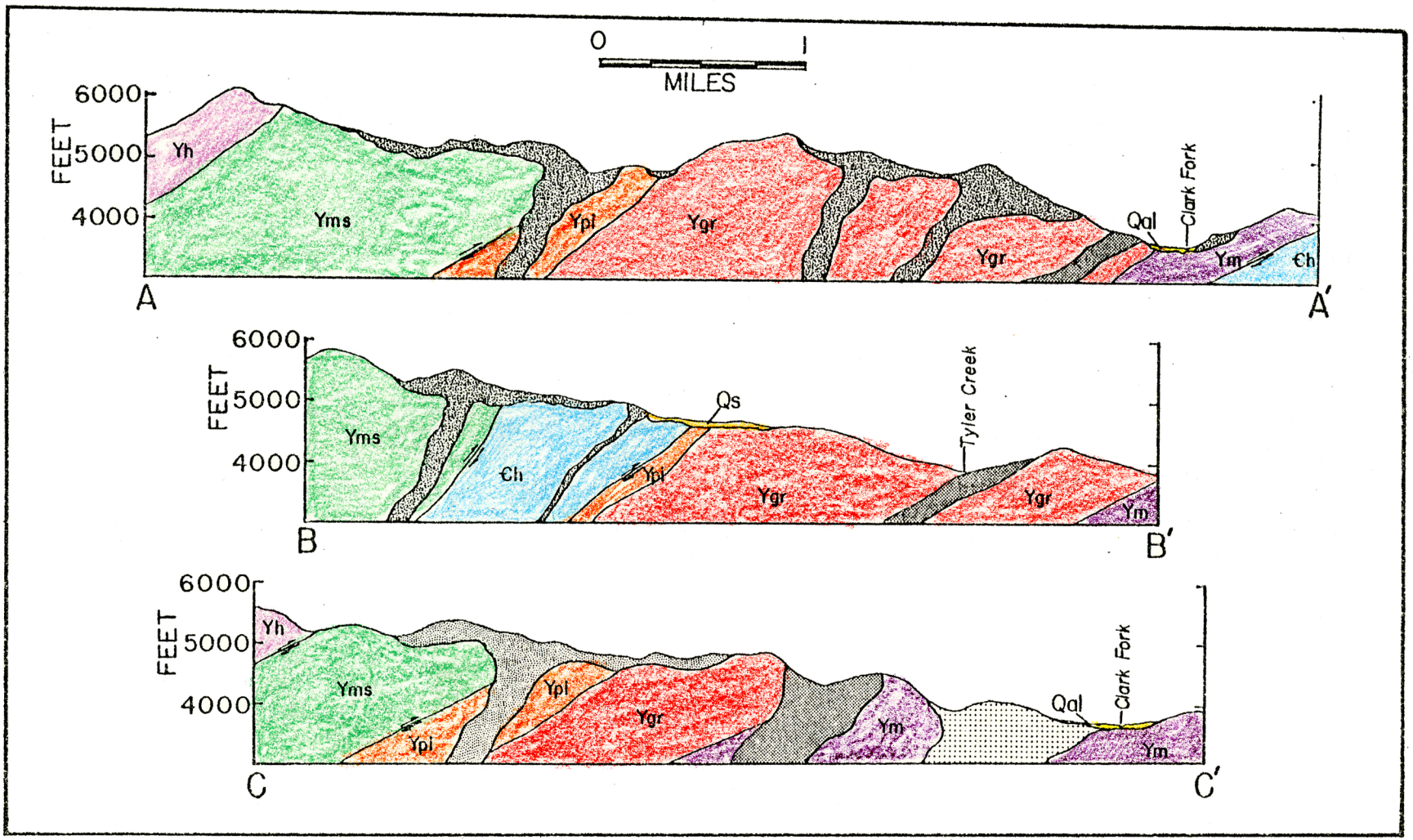

Figure 4. Geologic cross-sections through the Ravenna area (vertical exaggeration 2 times).

Tertiary Volcanic Rocks

Basalt

Two basaltic flows occur in the eastern portion of the study area (R. 15 W.). The smaller eastern unit in section 26 is poorly exposed and highly weathered. Sections 33 and 34 contain a more extensive flow with a massive lower flow capped by numerous scoriaceous units.

Basalt outcrops in section 26 are patches of massive, jumbled blocks, a few of which have coherent joint patterns. Blocks average half a meter in size, tend to be slightly rounded and are heavily covered with lichen. In hand specimen, fresh surfaces are very dense, black, and aphanitic with about ten percent of reddish-brown, altered olivine phenocrysts 0.5 to 1.0 mm in diameter. Weathered faces are light gray to gray.

Western portions of the larger basalt flow in sections 33 and 34 appear to be very young. At least six horizontal scoriaceous flows, one to two meters thick, cap a massive, aphyric basalt unit at least 18 m thick. The scoriaceous units have well-defined brecciated zones at the top and base, and are covered by poorly developed soils and sparse vegetation. Dark-red to rust-red amygdaloidal basalt with abundant secondary calcite is the major rock type within the scoriaceous units. The massive aphyric unit is well-exposed in several road cuts and displays poorly developed joint patterns. Fresh surfaces display sparse megaphenocrysts of fresh olivine up to 3 mm long in a dense, black matrix. Weathered surfaces of the lower massive flow are yellow to yellow-brown.

Southeastern portions of the larger basalt flow are highly weathered and poorly exposed. Outcrops adjacent to Tyler Creek consist of sub-

horizontal flows which fracture into platey fragments 1 to 5 cm thick.

Stratigraphic positions of the basalt in relation to the other igneous bodies could not be determined. In section 27 basalt lies at a higher topographic elevation than dacite but the relation between the two units is unclear. Similar basaltic units nearby have been dated at 45 ± 2 m.y. by K-Ar techniques (Williams, 1975). The fresh upper scoriaceous units of the larger basalt flow indicate emplacement has taken place more recently than extrusion of the dacite, and for this reason, an Eocene age is assigned to the basalts.

Rhyodacite

Massive, bulbous outcrops of pink rhyodacite form a steep slope on the western bank of Tyler Creek in sections 26, 34, and 35 (R. 15 W.). The lateral extent of this unit may be considerably greater since a large landslide has covered the western portion of the rhyodacite.

Hand samples of rhyodacite are red to pink to light gray and contain five to ten percent phenocrysts set in an aphanitic groundmass. Euhedral biotite, hornblende fragments and fractured sanidine phenocrysts are less abundant than plagioclase phenocrysts.

Stratigraphic position of the rhyodacite in relation to the other igneous units is impossible to determine. Although the rhyodacite is overlain by dacite, the dacite is unconsolidated and is primarily slide debris.

Gabbro

Four gabbro plugs and sills are intruded in a northwest-trending belt parallel to the strike of the Precambrian Garnet Range Formation. The largest gabbro body is a sill 6.5 km long and from 90 to 170 m thick.

Massive, blocky outcrops with poorly defined columnar jointing are characteristic of the sill. Weathered portions are a dark, rusty-brown very similar to the weathered appearance of the Garnet Range Formation. The sill is concordant with the Garnet Range Formation but does not display the thrust faults apparent in the Precambrian unit. No structural or stratigraphic relations between the sill and other igneous bodies are apparent, although location and mineralogic criteria indicate genetic relations between the sill and the gabbro intrusions to the west.
A small concordant sill in sections 18 and 19 (R. 15 W.) ranges in thickness from 10 to 30 m. Outcrops are generally poor and highly weathered.
Gillespie Creek bisects a gabbro plug in sections 13 and 24 (R. 16 W.). Exposures along the creek are massive and extend up to 120 m steeply from the creek bed. This intrusion cuts across several small dacite porphyry dikes, and there is limited thermal metamorphism at the intrusive contacts.

Gabbro also comprises the southern portion of Beavertail Hill (sec.10, R. 15 W.). Several sharp faces up to 20 m high form the eastern contact. Talus aprons of massive gabbroic blocks cover the bases of the vertical faces. Several large granodiorite or dacite xenoliths are visible in the walls of a road cut through the gabbro intrusion. Thermal metamorphism and ground water alteration has altered the leucocratic xenoliths to kaolinite.

Hand samples of the gabbro are medium- to coarse-grained and equigranular with interlocking crystals of plagioclase and augite as long as 3 cm. Fresh surfaces are light gray to gray whereas weathered portions are dark, rusty brown to black.

Hybrid rocks

Hybrid rocks crop out of the upper portions of the large gabbro sill. In hand specimen, one type appears to be a fine- to medium-grained holocrystalline syenite, composed primarily of orthoclase and biotite or hornblende. Pods of orthoclase- and muscovite-rich material occur near and at the upper contact of the sill and locally intrude the Garnet Range Formation. The second major type of hybrid rock is a medium-grained, holocrystalline, equigranular rock composed primarily of plagioclase and minor amounts of carbonate and pyrite. Outcrops of the plagioclase-rich rock occur at the upper contact of the sill and within the sill as a finely jointed, 1.5 m thick lens or pod. Planar joint patterns parallel to the upper and lower contacts of the body indicate the unit may have been intruded after the sill solidified. Montgomery (1958) called the plagioclase-rich lens a differentiated portion of the sill rather than a late-stage intrusion.

Dacite

Tertiary dacite porphyry is the most voluminous igneous rock type in the study area (Fig. 3). Features formed by dacite porphyry include dikes, flows, and vent areas.

Dacitic dikes ranging in width from 5 to 15 m and a maximum of 1 km in length occur in sections 19 (R. 15 W.) and 24 (R. 16 W.) of the western part of the area (Fig. 3). Vertical joints are displayed in the majority of the dikes. Orientations are predominantly parallel or subparallel to the strike of the Garnet Range Formation.

Major flows are found in sections 26 and 36 (R. 16 W.), and in sections 30,

18, 28, and 29 (R. 15 W.) of the western portion of the study area. Joint patterns displayed by the dacitic flows are horizontal or have slight dips. Several thin units have been eroded to expose thin ash flows and the Precambrian units beneath. The exposure of dacite in sections 28 and 29 appears to be an erosional remnant of a flow from the larger body to the north.

Vent remnants show two characteristic features: (1) nearly vertical joint patterns, and (2) numerous xenoliths over large vertical distances. Vertical jointing apparently occurred when magma cooled and contracted within a vent. Extensive vertical thicknesses of dacite and Precambrian xenoliths imply large-scale upwelling of dacitic magma, presumably from a vent area. Traces of vents are found in sections 25, 17, and 20. These are all near the central portions of major dacitic units. The vent near the center of section 25 displays poorly developed joint patterns and a vertical thickness of 50 m of highly xenolithic dacite porphyry. Vents or feeder dike remnants in sections 17 and 20 have extremely well-developed vertical joint patterns and contain minor quantities of xenolithic material. The remnants occur as spires of dacite porphyry up to 70 m high surrounded by aprons of slabby talus. The dacite porphyry body north of the Clark Fork River in sections 15 and 16 also exhibits vertical jointing and may be an extension of the extrusive center to the west.

The dacite porphyry has relatively homogeneous texture and mineralogy within the study area. Hand samples contain 5 to 20 percent plagioclase phenocrysts (2 mm - 2 cm) occasionally rimmed with orthoclase, and up to three percent euhedral biotite and hornblende phenocrysts (1 to 2 mm) set in a light gray, aphanitic groundmass. Quartz phenocrysts (2 to 3 cm) are sparse. Xenoliths of Precambrian material, gabbro, and dacite porphyry are locally abundant.

At least two periods of dacitic volcanism have occurred within the study area. Older dacite porphyry xenoliths can be found in younger dacite porphyry units in sections 26 and 20. The two phases cannot be distinguished on the basis of mineralogy, textures, or structural criteria utilizing the field data presently available.

Granodiorite

Granodiorite occurs as a hypabyssal intrusion in section 13 (R. 16 W.). A gradational contact between the medium-grained, holocrystalline granodiorite and the dacite porphyry flows to the east indicate that the intrusion may have been the source of some of the volcanic flows within the study area.

In hand sample, the granodiorite is a fine- to medium-grained, equigranular rock with abundant plagioclase, orthoclase, biotite, and hornblende. Quartz is also present in lesser amounts. Several road cuts along Gillespie Creek in section 13 expose thick, massive sections of granodiorite a minimum of 25 m thick. The road cuts also expose large Precambrian xenoliths imbedded in granodiorite near the igneous contact. Granodiorite is cut by gabbro intrusions in two locations in a road cut north of I-90 and in a road cut through the southern end of Beavertail Hill.

Igneous Stratigraphic Relations

Igneous stratigraphic succession from oldest to youngest appears to be: (1) granodiorite and dacite porphyry, (2) gabbro and hybrid rocks, (3) dacite porphyry, (4) basalt and perhaps rhyodacite. Numerous pulses of volcanism have occurred over an extended period of time in the study area.

Paleozoic Sedimentary Rocks

The Cambrian Hasmark Formation is exposed in the northeastern and southeastern portions of the study area. Thin- to medium-bedded light gray dolomite and limestone are the predominant lithologies of the Hasmark Formation. It weathers to light gray, light brown, or tan. The upper boundary of the Hasmark Formation is a fault contact with the Precambrian McNamara Formation in the northeastern portion of the study area, but an isolated block of the Hasmark Formation bounded by thrust faults crops out to the southeast.

Precambrain Belt Supergroup

Middle Belt carbonate rocks exposed in the study area have been termed the Helena Formation by Wallace et al. (1978) and the Wallace Formation by Montgomery (1958) and Desormier (1975). The Helena Formation consists of impure limestone and dolomite commonly interbedded with carbonaceous argillite, siltite, and quartzite. Weathered surfaces are gray or brown to tan and may be reddish-brown. Minimum thicknesses of the Helena Formation near the study area are 730 to 1,590 m (Desormier, 1975).

The Mount Shields Formation (Wallace et al., 1978) has also been called the Miller Peak Formation by Montgomery (1958) and Desormier (1975). The Mount Shields Formation is the lowest unit of the Missoula Group exposed in the study area (Fig. 5). Dominant lithologies are argillite, siltite, and quartzite. Detrital mica is common throughout the section and some quartzite contains abundant feldspar. The formation weathers easily and forms rounded

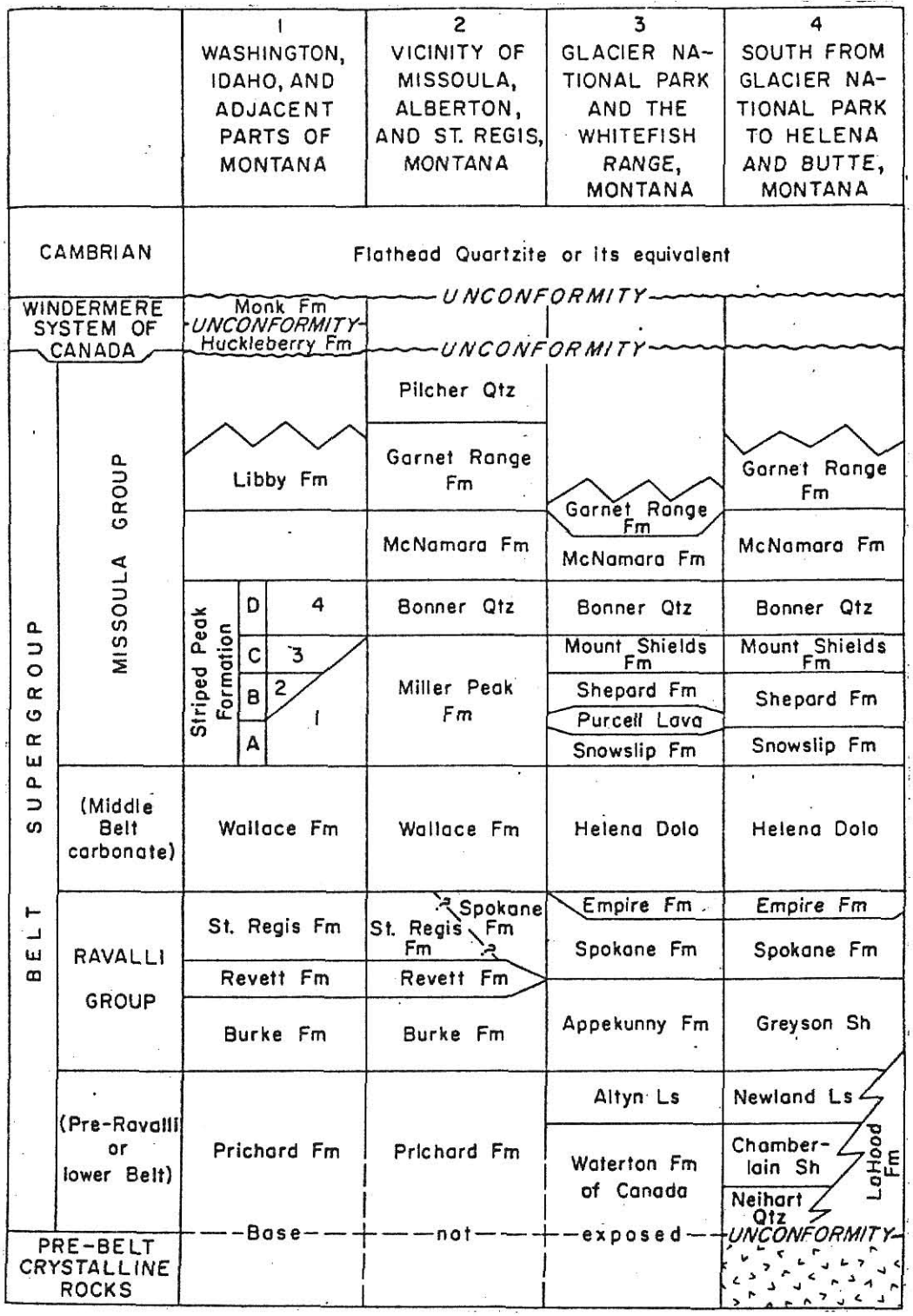

Figure 5. Recommended terminology for the Belt Supergroup, western Montana. Names in parentheses are used informally. From Desormier (1975).

hills and slopes which are light purple, tan and gray. Maximum thickness in the study area is 1,569 m (Desormier, 1975).

The McNamara Formation is composed of argillite, siltite, and quartzite. Quartz and detrital mica are the most common minerals but minor feldspar is also found. Desormier (1975) calculated a thickness of 430 m near the study area.

The Garnet Range Formation conformably overlies the McNamara Formation. Argillites, thin-bedded greenish-brown quartzitic sandstone, and quartzite are the major lithologies which form the Garnet Range Formation. Colors are commonly dark rust to greenish-gray. Quartz and detrital mica are the major minerals in the Garnet Range Formation. Calculated thickness is 760 m in the study area (Desormier, 1975).

The Pilcher Quartzite has also been termed the Sheep Mountain Formation (Montgomery, 1958). Pilcher Quartzite lies conformably above the Garnet Range Formation and is the uppermost unit of the Missoula Group. Medium-grained quartzite is the major lithology, although some interbeds of argillite and siltite are present. The formation is pink, purple, or gray and weathered surfaces are dark red-gray. Thickness ranges from 430 to 760 m (Desormier, 1975).

EXPERIMENTAL METHODS

PETROGRAPHY

Standard covered thin sections were prepared on equipment available at Kansas State University. A total of 26 sections were obtained from the freshest hand specimens. A Zeiss binocular petrographic microscope was used to examine the completed slides. Petrographic study included identification of constituent minerals and estimates of relative volume percents of the major mineralogic components in each slide.

SAMPLE PREPARATION FOR CHEMICAL ANALYSES

The freshest samples for major element, trace element, and isotopic analyses were selected by petrographic examination. Weathered portions of samples were removed prior to initial grinding with a hardened steel mortar and pestle. Fragments were then placed in a steel-carbide lined mill and ground in a Spex ball mill for fifteen to twenty-five minutes. This procedure reduced the specimen to less than 200 mesh. The sample was removed from the mill and stored for future use in a clean glass vial.

SPECTROPHOTOMETRY PROCEDURES

Major element and several trace element analyses were obtained by Atomic Absorption and Emission Spectrophotometry utilizing a method similar to those described by Medlin et al. (1969), Suhr and Ingamells (1966), and Gutmann (1979, personnal communication). A Perkin-Elmer 305-B Atomic Absorption Spectrophotometer with a chart recorder was used for the analyses.

A total of thirty samples were analyzed. These include 17 basic to silicic samples for this study, and 13 analyses of five U.S. Geological Survey standard rocks. Ten samples and a blank were processed in each of three groups, with the U.S. Geological Survey standard rocks acting as checks on the accuracy and precision of the results.

Rock samples were prepared for analysis (Fig. 6) by adding 0.1000 $\pm$ 0.0002 g of powdered samole to 0.5000 $\pm$ 0.0002 g of lithium meteborate ($LiBO_2$, anhydrous, reagent grade), thoroughly mixing, and placing the mixture in a 9 ml graphite crucible (Spex part number 7152). The mixture was fused at 1000° C for 15 minutes in a muffle furnace. Wetting of the crucible did not occur, and if properly mixed the sample was entirely digested. Crucibles may be used several times without contamination (Suhr and Ingamells, 1966). After fusion, the molten material was immediately added to 40 ml of four percent HCl solution in a teflon beaker. Solution loss by spattering was rare. Solutions were stirred by a magnetic stirrer until visual inspection showed the samples to be totally dissolved. Finally, graphite flakes were removed by vacuum filtration and the solution was transferred to a clean polyethylene bottle.

A total of four dilutions were made to bring the various elements within their linear range (Figure 6). Three were prepared with a one percent La solution (La'A') and one with distilled deionized water. The high La and Li concentration prevented flame interference during analyses.

Due to minor amounts of major- and trace-element contaminants in the $LiBO_2$, blank solutions were prepared utilizing the same technique as outlined above. Similar dilutions were also made on the blank solutions.

A set of three synthetic standards were mixed during dissolution of the rock samples (Figure 7). Solution I was used to analyze Si only, although it contained the other major elements. Solution II was used to analyze Al, Fe, Ca, Mg, Na, Mn, Ti, and K. Standard solution III was used

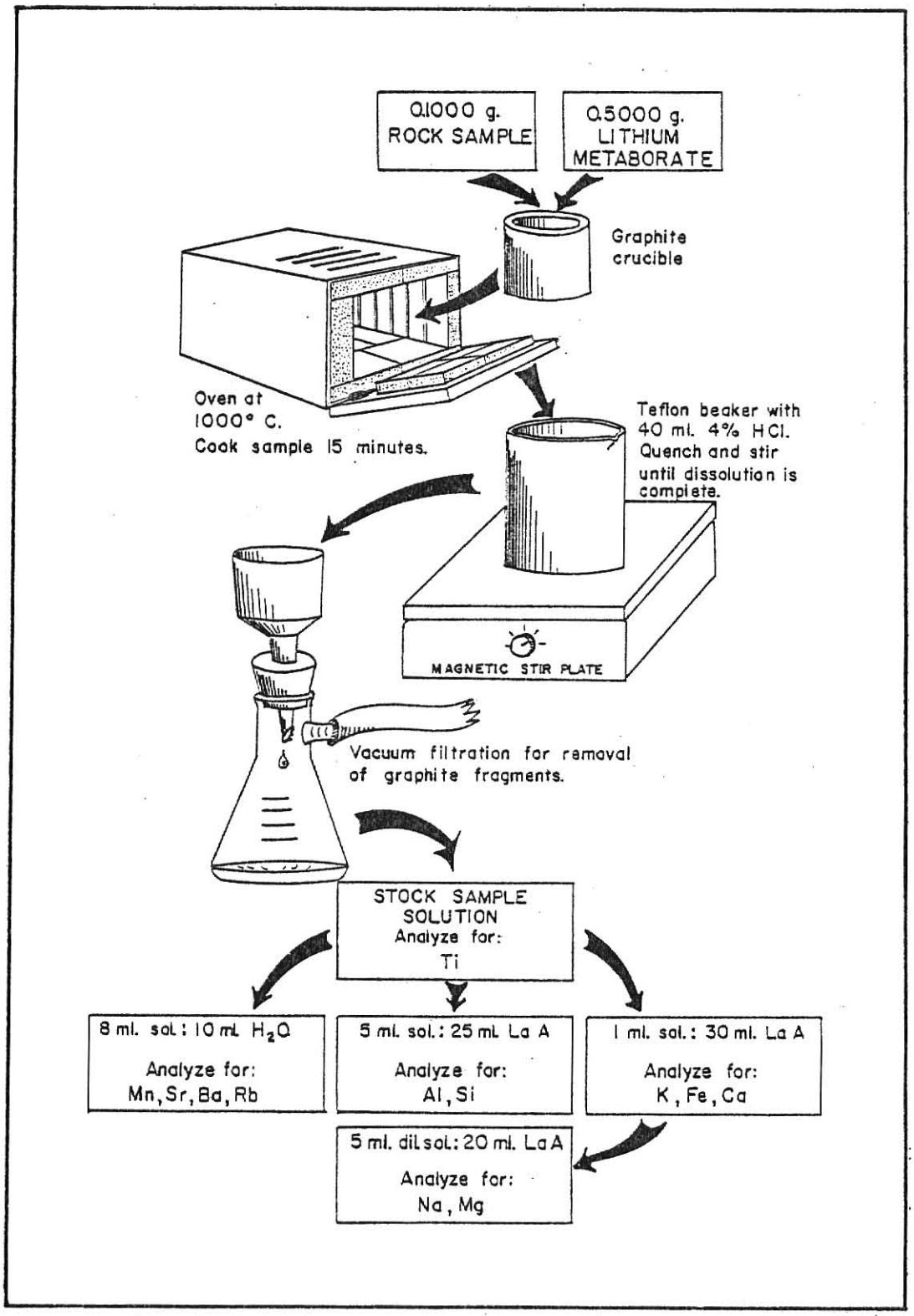

Figure 6. Schematic diagram of spectrophotometric sample preparation and dilution procedures.

to analyze Ba, Rb, and Sr and contained a concentration of lithium equal to that in the rock sample solutions.

Basic instrument settings for spectrophotometric analyses are similar to those of Koch (1978), with minor modifications (Table 1). Peak sizes in the output were one half to one third of the width of the chart paper for greater measurement precision. Titanium and manganese, however did not yield peaks of this size due to low elemental concentrations in the samples. Every sample was run in triplicate for each element. The sequence of analysis was as follows: standard - standard - blank - 3 samples - standard - standard - blank.

Chart output data were reduced by graphically determining the heights of both standards and the blank at every sample peak. The blank peak height, which could be as great as fifty percent of the sample solutions, was initially subtracted from the sample peak height. A linear regression line through 0,0 was constructed using the standard peak heights verses the standard concentrations. Unknown elemental concentrations were then determined by substituting the sample peak height into the equation of the linear regression line. Three concentrations for each sample were averaged and oxide percents (or ppm) calculated.

A total of thirteen analyses on five different U.S. Geological Survey standard rocks are summarized in Table 3. Averaged results for major elements show good agreement to the recommended values of Flanagan (1973). Ba, Rb, and Sr values do not appear to be as precise as the more abundant elements. This is probably due to the trace elements' lower concentration and interferences which produce noisy chart outputs.

GRAVIMETRIC DETERMINATIONS

Adsorbed water and total volatile content of the samples were determined with equipment and techniques similar to those described by Kilbane (1978).

Element	Reagent Used	Low Standard	High Standard
Si	Stock	90.0	150.0
Al	Stock	30.0	50.0
Fe	Stock	2.0	5.0
Ca	Stock	2.0	7.0
Mg	Stock	0.1	0.5
Na	Stock	0.1	1.0
K	Stock	0.5	2.0
Ti	Stock	2.0	15.0
Mn	Stock	1.0	3.0
Ba	Stock	0.5	1.0
Rb	RbCl	0.1	0.3
Sr	Stock	0.1	0.4

Standard Solution I (in La solution, for Si analysis only)	Standard Solution II (in La solution, for all other major elements)	Standard Solution III (in deionized H_2O for Ba, Rb, and Sr analysis)
Si	Al	Ba
Al	Fe	Rb
Fe	Ca	Sr
Ca	Mg	LiCl- added to equal the Li concentration in the samples.
Mg	Na	
Na	Mn	
Mn	Ti	
Ti	K	
K		

Figure 7. Standard solution concentrations and three standard solutions used for spectrophotometric analyses.

Table 1. Instrument settings for the Perkin-Elmer 305B used during spectrophotometric analyses.

Element	Wavelength Setting	Slit	Range	Function	Burner Width	Burner Height	C_2H_2	N_2O	Air
Si	251.7	3	UV	Abs.	2.5''	6.0	4.6	5.3	
Al	309.2	4	UV	Abs.	2.5''	7.0	5.0	5.2	
Fe	248.5	3	UV	Abs.	2.5''	7.0	5.0		5.0
Ca	211.4	4	Vis.	Abs.	2.5''	6.0	4.7		5.0
Mg	285.2	4	UV	Abs.	2.5''	5.0	5.0		5.3
Na	294.4	4	Vis.	Abs.	2.5''	6.0	6.0		5.0
K*	382.4	4	Vis.	Em.	2.5''	6.0	4.7		5.3
Ti	365.2	3	UV	Abs.	2.5''	7.0	4.7		5.3
Mn	279.5	3	UV	Abs.	2.5''	7.0	5.0		6.0
Ba	276.6	2	Vis.	Em.	2.5''	6.0	4.8	5.4	
Rb	389.6	5	Vis.	Em.	4.0''	5.0	9.0		9.0
Sr	230.2	4	Vis.	Em.	2.5''	7.0	4.7	5.0	

*Red Filter

Approximately one gram of sample was placed in a pre-ignited platinum crucible and dried at 110°C for one hour. The weight loss was recorded as H_2O^-, or adsorbed water. The crucible was then placed in a muffle furnace at 1000°C for 15 minutes, removed, and allowed to cool to room temperature in a dessicator. This weight loss was recorded as ignition loss. A total of five U.S. Geological Survey standard rocks were analyzed by this method to check the precision of this technique. The Fe-poor standards AGV-1, STM-1, and G2 show good agreement between the ignition loss and H_2O^+ and CO_2 values as reported by Flanagan (1973). BCR-1 and W-1 show poor agreement, probably due to the oxidation of FeO to Fe_2O_3 (Table 3). Kilbane (1978) has reported good quality of anlaysis utilizing similar equipment and procedures by determining the ignition weight loss of standard carbonate 400.

NEUTRON ACTIVATION ANALYSIS

Ten samples were chosed for INAA (instrumental neutron activation analysis) on the basis of atomic absorption data. Approximately 0.1 to 0.2 g of powdered rock sample was placed in a polyethylene vial which was then sealed with a warm soldering gun to prevent water infiltration during irradiation. Ten centimenters of iron wire to act as a flux monitor were wrapped symmetrically around the vial's exterior and secured with teflon tape. Six vials containing five samples and a standard were irradiated for four hours in the central core of a Triga Mark II nuclear research reactor at a neutron flux of approximately 1×10^{13} $N/cm^2/s$. Samples decayed for three to four days before their activity reached 200 mr/hr. When suitable radiation levels for handling were obtained, samples were removed from vials and poured into a small plastic bag (approximately 1 cm wide) and mounted symmetrically on a 3 x 5 index card. Iron wires were coiled symmetrically and similarly mounted.

If leakage occurred during irradiation, the slurry was vacuum filtered and the vial carefully rinsed to retrieve all radioactive material. Sample and filter paper were then placed in a plastic bag and symmetrically mounted.

A 25 cm^3 Ge(Li) detector was used to detect gamma rays emmitted by the irradiated samples. The gamma spectrum was collected and stored in 4096 channels by a Canberra model 8180 multichannel analyzer. Data from sample and standards were subsequently stored on 9 track magnetic tape with a model 8531A magnetic tape interface.

A computer program outlined by Jacobs et al. (1977) was used to retrieve data and determine each element's standard and sample peak areas, associated errors, and the ratio of sample to standard area. Kilbane (1978) presented a more detailed discussion of the theory and functions of this program. Final elemental concentrations were determined using the following equation:

$$Csa = Cst \times \frac{sa}{st} \times \frac{st\ wt}{sa\ wt} \times \frac{st\ Fe}{sa\ Fe}$$

where:

Csa = concentration of element in sample

Cst = concentration of element in standard

$\frac{sa}{st}$ = sample/standard peak area ratio

$\frac{st\ wt}{sa\ wt}$ = standard/sample weight ratio

$\frac{st\ Fe}{sa\ Fe}$ = standard/sample Fe specific activity

Because of interferences by elements with similar gamma energies, the following elements required further corrections:

ISOTOPES		INTERFERING PEAK	
^{175}Yb	396.1 kev	^{233}Th	398.5 kev
^{130}Tb	298.6 kev	^{233}Th	300.1 kev
^{141}Ce	145 kev	^{59}Fe	142 kev

MASS SPECTROMETRY

Strontium isotopic ratios were determined on a 15 cm radius, 60 degree sector, Nier-type mass spectrometer (Nuclide Corporation Model 6-60-S). Strontium nitrates were mounted onto a tantalum filament which served as a source of strontium during isotopic analysis.

Sample preparation procedures identical to those outlined by Kilbane (1978) were used to grind samples. Whole-rock samples were prepared following dissolution and strontium separation procedures outlined by Kilbane (1978).

X-RAY FLUORESCENCE

X-ray fluorescence was used to determine Rb and Sr concentrations for all samples on which Sr isotope data were obtained. Analyses were done on a Phillips 1410 X-ray spectrometer. A molybdenum target and LiF analyzing crystal were used. Other instrument settings were: Kilovolts = 50, milliamps = 50, baseline = 2.1, window = 2.1. The compton scattering peak was found at 30.00° 2θ, Rb at 38.00° 2θ, and Sr at 35.85° 2θ.

Five U.S. Geological Survey standard rocks (W1, G2, GSP-1, AGV-1, and BCR-1) with known Rb and Sr concentrations were initially analyzed in order to construct a linear regression of counts per second versus element concentration. Rb and Sr concentrations of 16 powdered whole-rock samples were determined using the constructed regression.

EXPERIMENTAL RESULTS

PETROGRAPHY

Brief descriptions of each major rock type are presented; locations of samples examined in detail are shown in Figure 8 and described in Appendix A. Mineral percentages of each rock type are visually estimated. Classifications are based on modal mineralogy using Q-A-P-F diagrams as outlined by Streckeison (in Hyndman, 1972) and on the basis of hand specimen descriptions. Table 2 summarizes the petrographic features of individual samples.

Dacite Porphyry (samples: 26, 12, 20, 58, 45, and 46-B)

The dacite porphyrys are composed of 20 to 50 percent plagioclase (An_{33} - An_{39}), 1 to 5 percent euhedral biotite, 1 to 3 percent hornblende, less than 3 percent orthoclase and quartz, and glassy to orthophyric matrices. Trace minerals include opaque minerals, carbonate, sericite, chlorite, and apatite. Plagioclase occurs as euhedral megaphenocrysts or glomerocrysts 1.5 to 5.0 mm in length (Fig. 9); zonation, carlsbad twins, and albite twins are common. Moderate to heavy sericitic alteration also is common in phenocryst cores and margins. Plagioclase microlites (0.01 to 0.1 mm) with carlsbad twins are found in orthophyric and hyalopilitic matrices. Biotite crystals with hexagonal or rectangular outlines range in size from 0.2 to 1.5 mm. Alteration to iron oxides, opaque minerals, and chlorite is common. Hornblende rhombs from 0.2 to 2.0 mm in length are

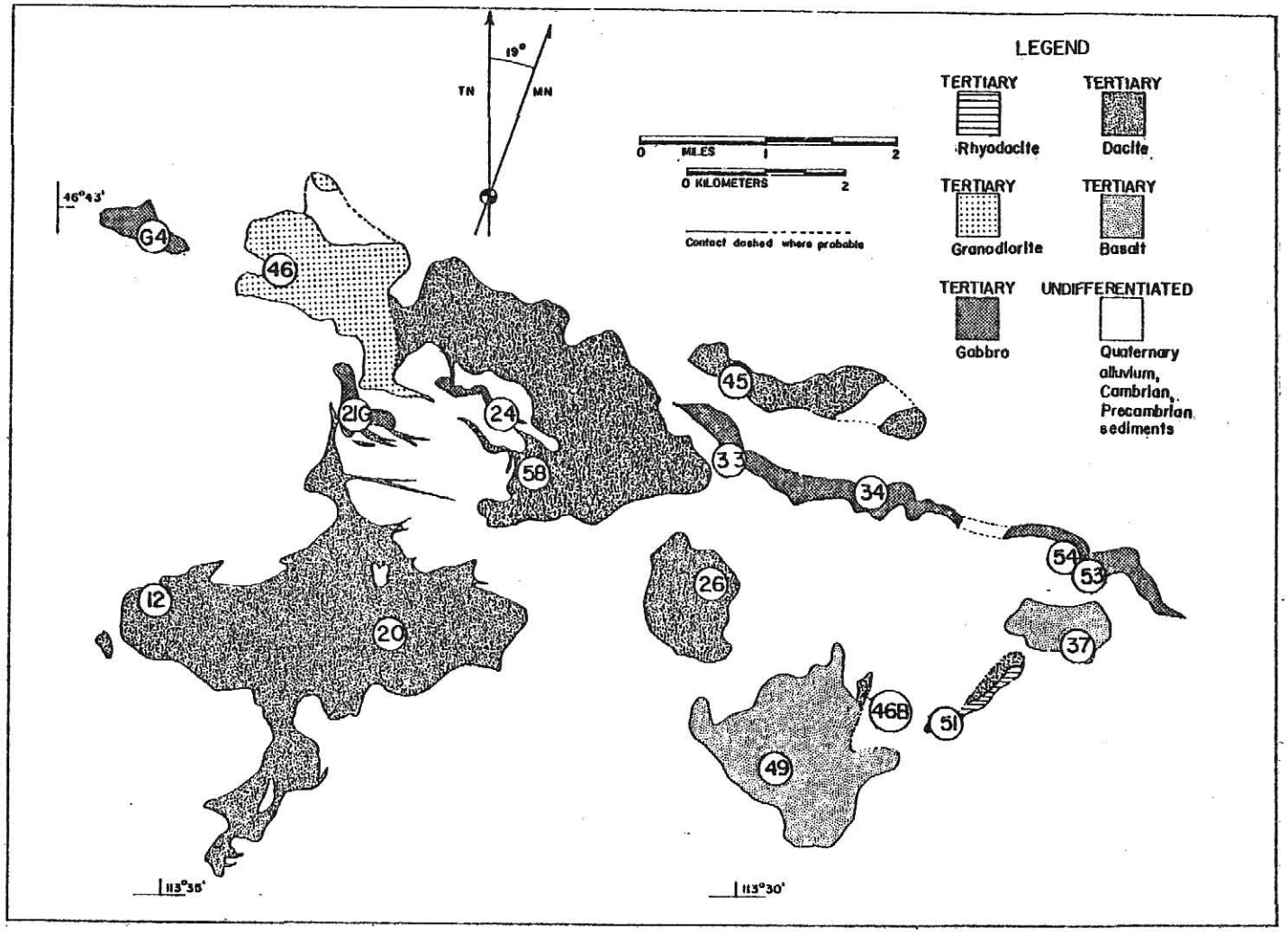

Figure 8. Locations of samples selected for petrographic and chemical analyses.

generally surrounded by alteration rims of iron oxides and opaque minerals. Hornblende is usually green to light green or tan and displays excellent cleavage. Low percentages of orthoclase phenocrysts are visible in some dacite specimens. Orthoclase crystals have subhedral outlines, are untwinned, and reach 1.0 mm in length. Sericitic alteration over whole grains is common. Quartz is a rare phenocryst mineral. Rounded, marginally resorbed grains up to 1.5 mm are the usual occurrence. Matrix material contains traces of apatite, finely disseminated opaque minerals, and secondary carbonate. Hyalopilitic or coarser orthophyric textures are typical.

Granodiorite (sample: 46)

This rock is a medium-grained, hypidiomorphic granular granodiorite composed of 50 percent plagioclase (An_{35}), 20 percent orthoclase, 20 percent quartz, 5 percent biotite, 3 percent hornblende, and 2 percent opaque minerals (Fig. 10). Euhedral plagioclase laths range from 0.2 to 4.0 mm in length, have well-developed carlsbad and albite twins, and are slightly altered to sericite. Orthoclase crystals are subhedral to anhedral interstitial grains which range in diameter from 0.2 to 1.0 mm and are occasionally altered to sericite. Anhedral, interstitial quartz occurs as fillings 0.2 to 0.4 mm across. Rectangular books and euhedral crystals of biotite 0.2 to 0.4 mm wide are imbedded in orthoclase and quartz. Some biotite shows extensive alteration to opaque minerals, iron oxides, and chlorite. Prismatic hornblende crystals up to 1.5 mm long are heavily altered to chlorites and iron oxides. Finely dissiminated opaque minerals less than 0.1 mm in diameter are scattered in interstices and concentrated in and around altered ferromagnesian minerals. The sequence of crystallization is: first: plagioclase, hornblende and biotite,

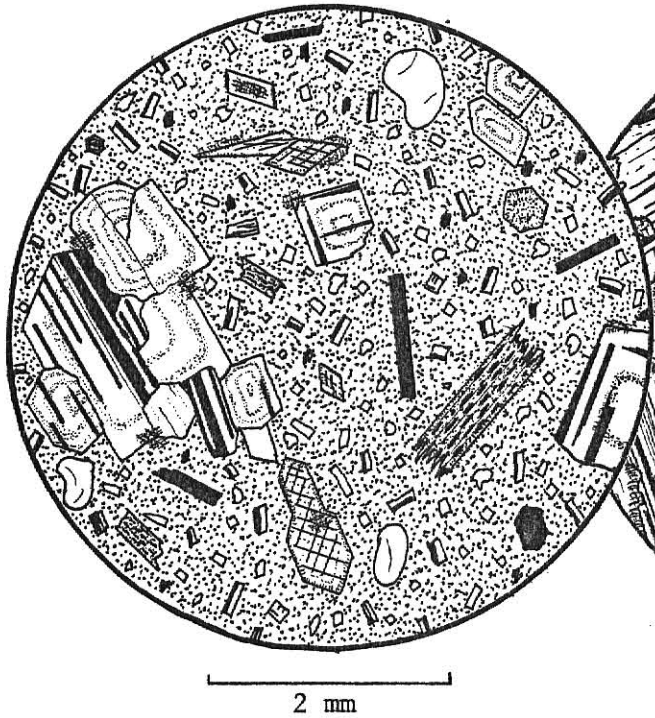

Figure 9. Petrographic view of dacite porphyry. Plagioclase glomerocryst, partially resorbed quartz grains, hornblende and biotite phenocrysts are dispersed in an orthophyric matrix.

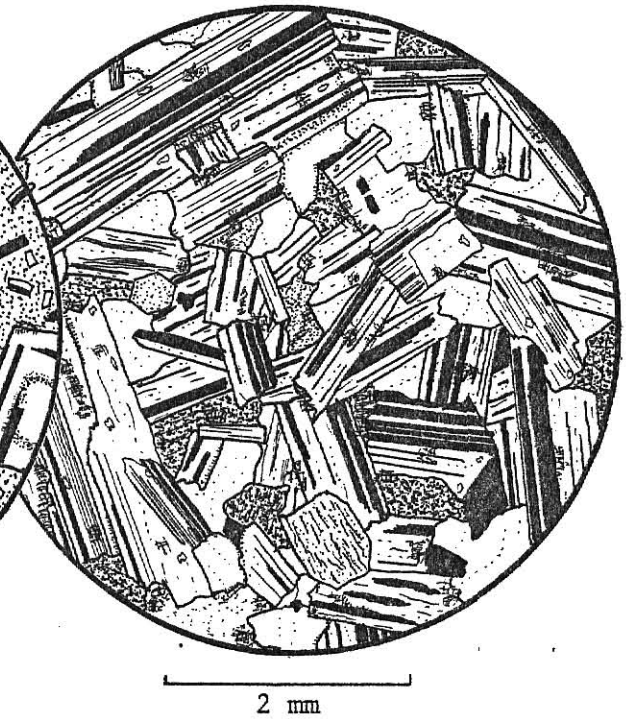

Figure 10. Petrographic view of granodiorite. Hypidiomorphic-granular texture. Minerals are euhedral plagioclase laths, interstitial orthoclase and quartz, and altered hornblende and biotite.

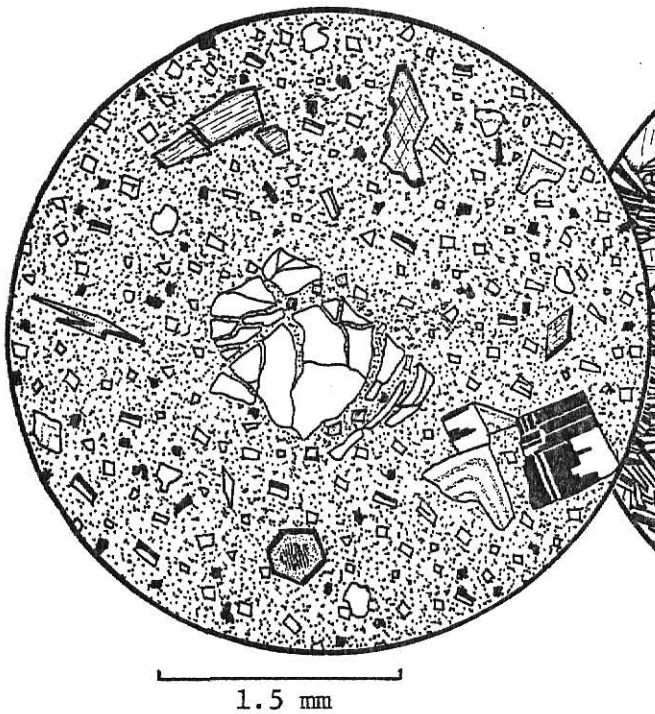

Figure 11. Petrographic view of rhyodacite. Fragmented sanidine phenocryst with plagioclase, hornblende and biotite phenocrysts set in a vitrophyric matrix.

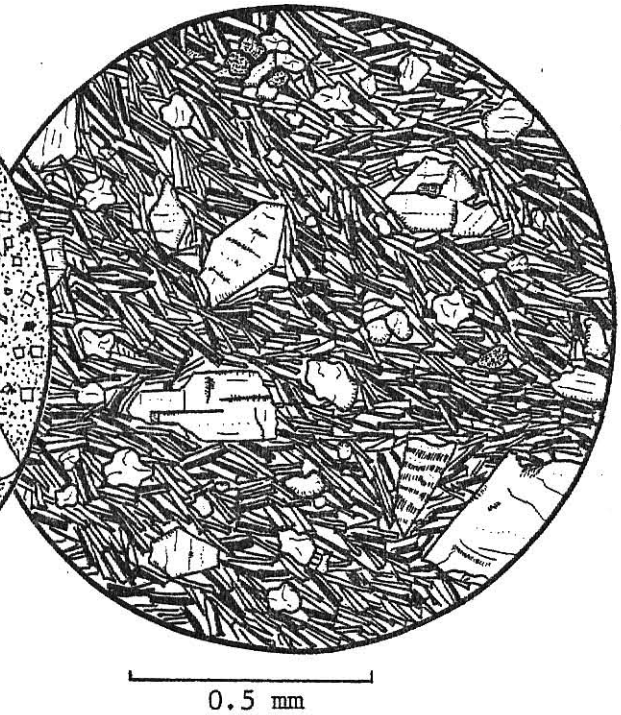

Figure 12. Petrographic view of alkali-olivine basalt. Microporphyry composed of fluidal plagioclase microlites, olivine microphenocrysts. and interstitial augite and opaque minerals.

orthoclase, quartz, and fianlly opaque minerals followed by alteration of feldspathic and ferromagnesian minerals.

Rhyodacite (sample: 51)

This vitrophyric rhyodacite is composed of 35 percent plagioclase (An_{45}), 4 percent sanidine, 3 percent quartz, 2 percent hornblende, 1 percent biotite, and 1 percent opaque minerals. The remainder of the rock (55 percent) is glassy (Fig. 11). Plagioclase occurs as stubby, rectangular microlites averaging 0.1 mm long and as megaphenocrysts 0.5 to 2.5 mm long. Microlites occasionally display carlsbad twins, while fragmental, subhedral megaphenocrysts have carlsbad, albite, and pericline twins, and exhibit faint zonation. Megaphenocrysts and fragmented megaphenocrysts compose about 10 percent of the entire rock. Fractured subhedral sanidine fragments are up to 2.0 mm wide. Rounded quartz crystals 0.1 to 0.4 mm across are scattered throughout the matrix. Euhedral crystals and books of biotite are altered to opaque minerals and chlorite and range in width from 0.4 to 0.8 mm. Rhombic hornblende fragments range from 0.2 to 0.4 mm in length, have clear cleavage, and show alteration similar to biotite. Finely disseminated opaque minerals in the matrix are less than 0.1 mm in diameter. Opaque minerals also occur as alteration rims on the ferromagnesian minerals.

Alkali-olivine Basalt (sample: 37)

This rock is a microporphyritic, pilotaxitic basalt composed of 5 percent plagioclase (An_{37}), 1 percent olivine phenocrysts, 30 percent augite, and 5 percent opaque minerals (Fig. 12). Plagioclase microlites, averageing 0.2 mm long, exhibit fluidal textures and display carlsbad twins. Euhedral to subhedral olivine phenocrysts 0.1 to 0.8 mm across are usually surrounded by deuteric iddingsite alteration rims. Intergranular augite microlites

less than 0.1 mm wide occur as subhedral to anhedral grains. Opaque minerals 0.01 to 0.08 mm in diameter are also displayed in interstices. Iron oxides occur as secondary or deuteric alterations of olivine, augite, and opaque minerals.

Olivine Tholeiite (sample: 49)

This vitrophyric basalt consists of 10 percent euhedral olivine megaphenocrysts, 5 percent opaque minerals, and 85 percent glass (Fig. 13). Olivine crystals 0.3 to 4.0 mm across have minor iddingsite alteration. Large numbers of fractures near crystal boundaries are indicative of thermal shock due to rapid cooling. Opaque minerals 0.01 to 0.1 mm wide are finely disseminated throughout the mesostasis.

Gabbro (samples: 34, G-4, 24, and 21-G)

Mineralogic abundances within the gabbros are relatively homogeneous, but a considerable variance in textural characteristics is noted (Fig. 14a and 14b). The gabbros are composed of 45 to 55 percent plagioclase (An_{50} - An_{54}), 35 to 40 percent augite, up to 4 percent hornblende, up to 5 percent quartz, up to 5 percent opaque minerals and traces of apatite, biotite, iron oxides, ilmenite, uralite, and chlorite. Average lengths of euhedral plagioclase laths range from 1.0 to 4.0 mm. The plagioclase typically displays well-developed carlsbad and albite twins. Augite displays the greatest textural variability as some samples have euhedral prismatic augite grains up to 8 mm long while other gabbros have anhedral intergranular augite grains less than 1.0 mm long. Pleochroic green hornblende commonly occurs as a secondary or deuteric alteration product at grain boundaries or within augite crystals. Myrmekitic, interstitial intergrowths of quartz and

albite are characteristic of all gabbros. Opaque minerals occur as intergranular crystals and range from microscopic to 5.0 mm wide. Apatite crystals are commonly less than 0.1 mm long and are commonly associated with quartz-albite intergrowths. Hornblende, biotite, chlorite, opaque minerals, and iron oxides are alteration products of augite, whereas plagioclase shows moderate to intense alteration to sericite. Sequence of crystallization is: first: plagioclase, augite, myrmekite and opaque minerals, and finally secondary and deuteric alteration.

Hybrid rocks (samples: 33, 53, and 54)

Two types of hybrid rocks were sampled in the upper sections of the sill. The first (samples 53 and 54) is composed of 79 to 87 percent plagioclase (An_6 - An_9), 11 percent quartz, up to 7 percent carbonate, up to 8 percent chlorite, up to 2 percent opaque minerals, and traces of zircon, apatite, sericite, iron oxides, and natrolite. Hypidiomorphic-granular textures are displayed by the plagioclase-rich hybrid rocks (Fig. 15). Euhedral to subhedral plagioclase crystals range in length from 0.1 to 4.0 mm and form an interlocking fabric cut by veinlets of calcite. Plagioclase shows very minor alteration to sericite, and displays some albite, carlsbad, and pericline twins. Quartz occurs as fine-grained (0.1 to 0.5 mm) crystals. Intergranular sub-parallel aggregates of chlorite may be deuteric alterations of hornblende. The chlorite contains zircon with pleochroic halos and numerous apatite crystals. Sample 53 contains radiating, acicular aggregates of natrolite which average 0.5 mm in diameter. Intergranular opaque minerals 0.2 to 0.5 mm across are visible in both samples.

The second major type of hybrid rock (sample 33) found in association with the sill is composed of 50 percent muscovite-sericite, 28 percent orthoclase, 13 percent quartz, and 9 percent chlorite. A very heavily

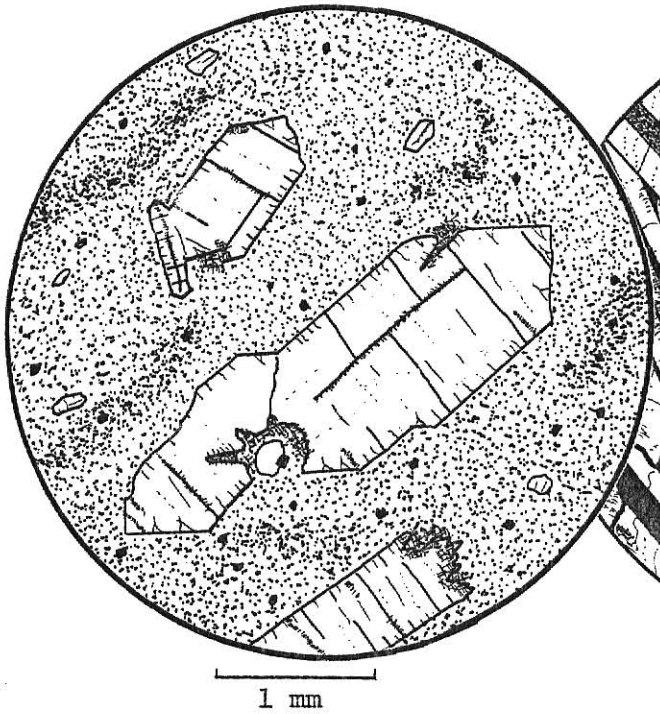

Figure 13. Petrographic view of olivine tholeiite. Megaphenocrysts of olivine are embedded in a glassy mesostasis.

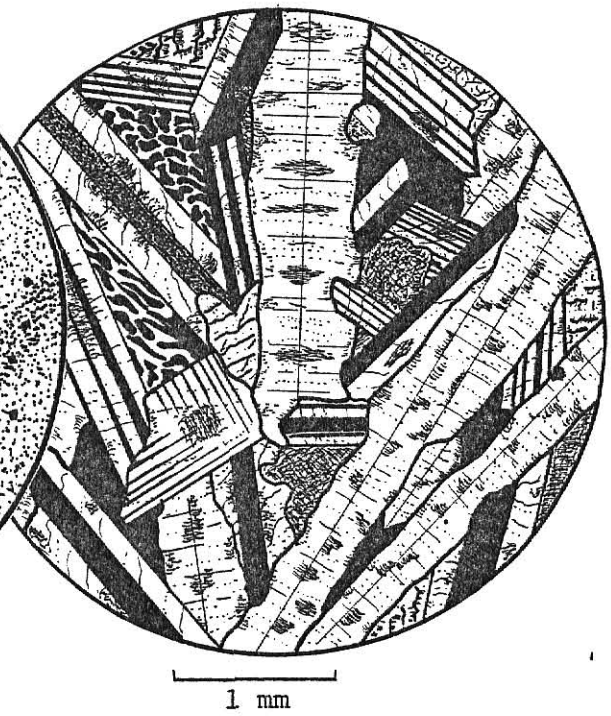

Figure 14a. Petrographic view of Gabbro G-4. Euhedral augite and plagioclase with interstitial augite, myrmekite, and opaque minerals.

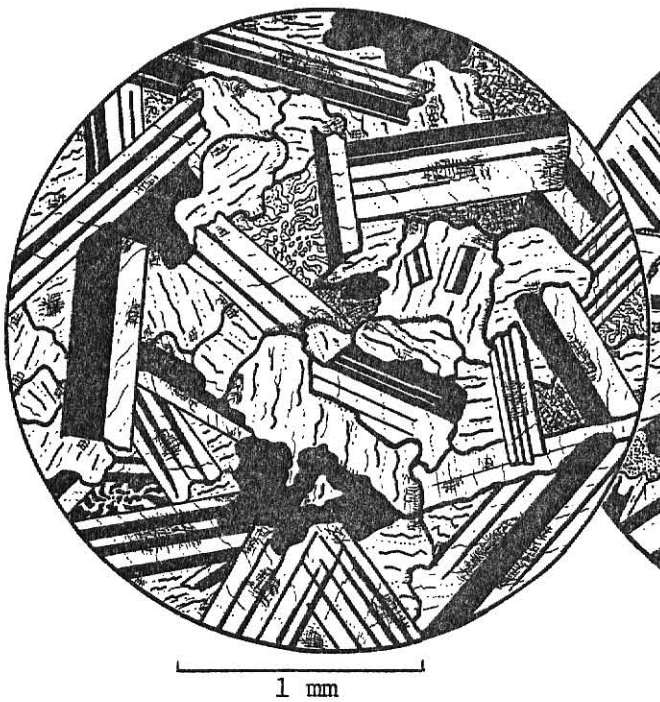

Figure 14b. Petrographic view of Gabbro 34. Plagioclase laths with anhedral augite, interstitial myrmekite, and opaque minerals.

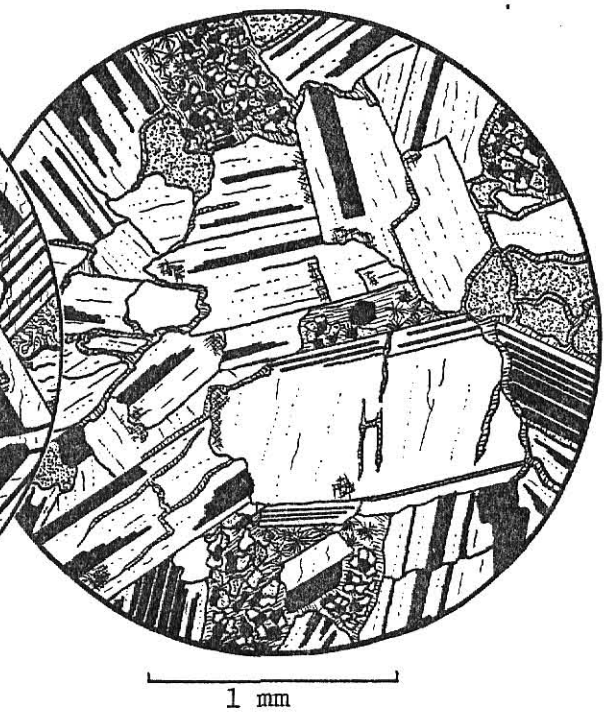

Figure 15. Petrographic view of Hybrid Rock 54. Subhedral palgioclase is cut by calcite veinlets which contain quartz, natrolite, and minor opaque minerals.

altered appearence is characteristic, with anhedral quartz and altered orthoclase grains set in a muscovite-sericite groundmass. Orthoclase grains range from 0.1 to 0.8 mm across and are highly altered to sericite. Anhedral quartz crystals are 0.1 to 0.5 mm wide. Chlorite minerals (0.02 to 0.1 mm) are finely disseminated in the muscovite-sericite groundmass. Subhedral books of muscovite up to 1.0 mm wide have ragged and heavily altered edges. Sericitization is intense and tends to mask most petrographic features. Traces of opaque minerals a maximum of 0.1 mm wide, zircon with pleochroic halos, iron oxides, and natrolite are also present.

Table 2. Summary of petrographic results for rocks on which chemical data have been obtained.

Sample Number	Rock Name (Classification)	Phenocrysts	Groundmass	Alteration	Texture-comments
37	Alkali-olivine Basalt (Normative, Hyndman, 1972)	10% ol	55% plag, 30% aug, 5% opaque min.	Very slight. Ol to iddingsite, fe oxides	Microporphyritic, pilotaxitic, intergranular- An_{37}
49	Olivine Tholeiite (Normative, Hyndman, 1972)	10% ol	85% glass, 5% opaque mins.	Very slight. Ol to iddingsite	Megaporphyritic, vitrophyric- ol shows thermal shock fractures.
12	Dacite porphyry (Hand Specimen Description)	5% plag, 4% hb, 2% bt	40% plag, 3% qtz 1% opaque mins, 40% glass	Heavy. Hb, bt to chlorite, fe oxides, opaque mins; plag to sericite	Hyalopilitic, orthophyric, porphyritic- An_{37}, zoned plag
20	Dacite Porphyry (Hand Specimen Description)	5% plag, 1% hb, 1% bt	30% plag, 1% qtz, 2% opaque mins, 60% glass, minor apatite	Heavy. Hb, bt to chlorite, fe oxides opaque mins; plag to sericite	Hyalopilitic, porphyritic- An_{37}, zoned plag
26	Dacite Porphyry (Hand Specimen Description)	10% plag, 3% hb, 1% bt	35% plag, 5% qtz, 1% opaque mins, 45% glass	Slight. Hb, bt to chlorite, opaque mins; plag to sericite	Hyalopilitic orthophyric- An_{37}, zoned plag
45	Dacite Porphyry (Hand Specimen Description)	5% plag, 1% bt, 1% hb	35% plag, 2% opaque mins, 1% qtz, 55% glass	Moderate. Hb, bt to chlorite, fe oxides, opaque mins; plag to sericite; carbonate	Orthophyric, hyalopilitic, porphyritic- An_{35}, zoned plag
46-B	Dacite Porphyry (Hand Specimen Description)	10% plag, 1% hb, 1% bt	50% plag, 2% qtz, 1% opaque mins, 35% glass	Moderate. Hb, bt to chlorite, fe oxides, opaque mins; plag to sericite	Hyalopilitic, orthophyric, porphyritic- An_{39}, zoned plag
58	Dacite Porphyry (Hand Specimen Description)	10% plag, 2% hb, 2% bt	35% plag, 4% qtz 2% opaque mins, 45% glass	Moderate. Hb, bt to chlorite, fe oxides, opaque mins; plag to sericite	Hyalopilitic, porphyritic- An_{37}, zoned plag
46	Granodiorite (Streckeisen)	-	50% plag, 20% or, 20% qtz, 5% bt, 3% hb, 2% opaque mins, minor apatite, carbonate	Moderate. Hb, bt to chlorite, fe oxides; plag to sericite	Hypidiomorphic-granular- An_{35}

Table 2 (cont.). Summary of petrographic results for rocks on which chemical data have bpen obtained.

Sample Number	Rock Name (Classification)	Phenocrysts	Groundmass	Alteration	Texture-Comments
51	Rhyodacite (Hand Specimen Description)	5% plag, 5% sanidine, 1% bt, 1% hb	30% plag, 10% qtz, 1% opaque mins, 47% glass	Slight. Hb, bt to chlorite, fe oxides, opaque mins	Porphyritic, vitrophyric, orthophyric- An_{35}, zoned plag
G-4	Gabbro (Streckeisen)	-	55% plag, 35% aug, 5% hb, 5% opaque mins, minor qtz, apatite	Slight. Pyx to hb, bt, chlorite; plag to sericite	Intergranular, holocrystalline- An_{50}
21-G	Gabbro (Streckeisen)	-	55% plag, 35% aug+ hb+bt, 7% opaque mins, 3% qtz	Heavy. Pyx to hb, bt, chlorite, opaque mins; plag to sericite	Intergranular, holocrystalline- An_{53}
24	Gabbro (Streckeisen)	-	55% plag, 35% aug, 5% opaque mins, 5% qtz, minor apatite	Moderate. Pyx to hb, bt, chlorite, opaque mins, fe oxides; plag to sericite	Intergranular, holocrystalline, inequigranular- An_{53}
34	Gabbro (Streckeisen)	-	50% plag, 40% aug, 8% opaque mins, 2% qtz, minor apatite	Slight. Pyx to hb, bt, chlorite, fe oxides, opaque mins; plag to sericite	Intergranular, holocrystalline. equigranular- An_{54}
33	Hybrid Rock (Hand Specimen Description)	-	50% musc+sericite, 30% or, 10% qtz, 10% chlorite, minor opaque mins, zircon,	Very heavy. Or to sericite, musc; secondary natrolite	Holocrystalline, inequigranular, fine-grained
53	Hybrid Rock (Hand Specimen Description)	-	80% plag, 10% qtz, 8% carbonate, 2% opaque mins, minor apatite	Very slight. Plag to sericite; opaque mins to oxides; secondary natrolite	Holocrystalline, inequigranular, coarse-grained- An_{9}
54	Hybrid Rock (Hand Specimen	-	80% plag, 10% qtz, 2% opaque mins, minor apatite, carbonate, zircon	Moderate. Hb to chlorite	Holocrystalline, equigranular, medium-grained- An_{6}

MAJOR ELEMENTS

Rocks analyzed for major elements consist of the seventeen samples on which detailed petrography has been completed. Weight percent of major element oxides and CIPW normative minerals are reported in Table 4. Repeated analyses on five different U.S. Geological Survey standard rocks were used to check the accuracy of the experimental techniques. Experimental results for STM-1, W-1, AGV-1, G-2, and BCR-1 are given in Table 3. The average analyses obtained in this study are in excellent agreement with published standard analyses. Estimated maximum deviations of the major elements are as follows: SiO_2, Al_2O_3, K_2O: ± 1 percent; Fe_2O_3, Na_2O: ± 2 percent; CaO, MnO: ± 3 percent; MgO: ± 4 percent; and TiO_2: ± 8 percent.

Major-element oxides versus SI (solidification index) are plotted in Figure 16. Three distinct fields are recognized: the gabbro, the basalt, and the dacite-granodiorite-rhyodacite groups. Hybrid rocks, while showing large degrees of scatter in the Al_2O_3, Na_2O, K_2O, and CaO plots, tend to fall within the dacite-granodiorite-rhyodacite field with respect to SiO_2, MgO, and Fe_2O_3 compositions. The dacite-granodiorite-rhyodacite group increases with SI in the MgO and Fe_2O_3 plots, decreases with SI in the SiO_2 diagram, has constant K_2O, CaO and Na_2O compositions, and displays a concave downward trend with SI in the Al_2O_3 plot. The gabbro group increases with SI in the MgO, Fe_2O_3, and CaO plots, decreases with SI in the Al_2O_3 diagram, and has constant SiO_2, K_2O, and Na_2O compositions. The basalt bodies differ from the gabbro in that they have a higher SI, higher MgO, Al_2O_3, K_2O and Na_2O contents, and much lower Fe_2O_3 values.

Table 3. Multiple major-element analyses (weight percent) of five U.S. Geological Survey standard rocks.

STANDARD:	STM-1 Neph. seyenite	STM-1	W-1 Diabase	W-1	AGV-1 Andesite	AGV-1	G-2 Granite	G-2	BCR-1 Basalt	BCR-1
REFERENCE:	(1)*	(2)	(1)*	(3)	(1)*	(3)	(1)**	(3)	(1)**	(3)
SiO_2	59.68	59.54	52.41	52.46	59.23	59.00	68.90	68.96	53.59	54.50
Al_2O_3	18.47	18.60	15.07	15.00	17.11	17.25	15.26	15.18	13.55	13.61
Fe_2O_3	5.21	5.14	11.52	11.09	6.77	6.76	2.46	2.44	13.42	13.40
MgO	0.084	0.10	6.69	6.62	1.51	1.53	0.76	0.75	3.49	3.46
CaO	1.07	1.16	11.04	10.96	4.92	4.90	1.92	1.88	6.73	6.92
Na_2O	8.76	8.96	2.16	2.15	4.27	4.26	4.08	4.19	3.22	3.27
K_2O	4.24	4.24	0.64	0.64	2.85	2.89	4.52	4.55	1.64	1.70
TiO_2	0.11	0.14	1.13	1.07	1.01	1.04	0.43	0.47	2.14	2.20
MnO	0.21	0.22	0.17	0.17	0.093	0.097	0.033	0.034	0.17	0.18
H_2O^-	0.025	0.18	0.14	0.16	0.87	0.16	0.070	0.11	0.57	0.80
Ignition	1.54	---	0.09	---	0.08	---	0.60	---	0.44	---
H_2O+CO_2	---	1.57	---	0.59	---	0.87	---	0.63	---	0.80
TOTAL:	99.40	99.85	101.06	101.09	99.43	98.76	99.03	99.19	98.96	100.84

*Average of three analyses.
**Average of two analyses.
(1) This study.
(2) Flanagan (1976).
(3) Flanagan (1973).

Table 4. Major-element analyses (weight percent) and CIPW normative mineral compositions (percent) of the Ravenna area igneous rocks.

SAMPLE:	37 Basalt	49 Basalt	12 Dacite	20 Dacite	26 Dacite	45 Dacite	46-B Dacite	58 Dacite
SiO_2	48.38	51.79	59.62	62.84	65.07	65.90	64.60	64.45
Al_2O_3	14.97	15.71	15.17	16.92	16.54	15.42	16.41	15.84
Fe_2O_3	8.34	8.58	3.22	3.17	2.09	2.31	1.80	2.87
MgO	9.58	8.26	3.06	2.34	1.48	1.31	1.13	1.84
CaO	8.86	8.07	4.67	3.18	3.80	2.82	2.49	2.97
Na_2O	3.30	3.73	3.53	3.83	4.17	2.67	4.02	3.68
K_2O	1.84	1.76	3.07	3.24	2.77	3.52	2.79	4.23
TiO_2	0.97	0.94	0.41	0.45	0.32	0.28	0.26	0.41
MnO	0.15	0.14	0.10	0.050	0.026	0.027	0.023	0.034
H_2O^-	0.62	0.19	0.74	0.53	0.88	1.23	1.61	1.18
Ignition	1.84	0.34	4.32	2.64	1.49	1.56	1.92	1.27
TOTAL:	98.85	99.51	97.91	99.19	98.64	97.05	97.05	98.77
q	---	---	13.16	16.95	19.40	28.12	22.98	17.12
c	---	---	---	1.33	---	2.09	2.25	---
or	10.86	10.39	18.21	19.12	16.35	20.78	16.47	24.97
ab	21.41	31.54	29.84	32.38	35.25	22.57	33.99	31.11
an	20.59	20.91	16.47	15.76	18.22	13.98	12.34	14.20
ne	3.52	---	---	---	---	---	---	---
di	18.61	15.28	5.33	---	0.50	---	---	0.42
wo	---	---	---	---	---	---	---	---
ol	15.46	13.18	---	---	---	---	---	---
hy	---	1.57	7.32	7.77	4.70	4.90	3.93	5.96
mt	3.39	3.60	1.50	1.54	1.00	1.03	0.86	1.48
il	1.85	1.79	0.78	0.86	0.61	0.53	0.50	0.78
SI*	42.65	38.03	24.17	18.92	14.27	13.58	11.75	14.80

*Solidification Index ($100xMgO/MgO+FeO+Fe_2O_3+Na_2O+K_2O$)

Table 4 (cont.). Major-element analyses (weight percent) and CIPW normative mineral compositions (percent) of the Ravenna area igneous rocks.

SAMPLE:	46 Grano-diorite	51 Rhyodacite	G-4 Gabbro	21-G Gabbro	24 Gabbro	34 Gabbro	33 Hybrid Rock	53 Hybrid Rock	54 Hybrid Rock
SiO_2	65.29	71.31	52.13	49.36	50.34	50.03	63.84	66.62	64.83
Al_2O_3	16.68	14.06	14.46	13.84	13.27	12.18	18.71	13.99	14.09
Fe_2O_3	4.07	1.62	16.50	16.15	16.41	16.89	3.21	1.23	4.16
MgO	1.35	0.32	5.05	4.37	4.96	6.18	2.04	0.80	1.14
CaO	3.35	3.16	7.97	7.28	9.10	9.22	0.082	4.67	2.84
Na_2O	4.37	3.65	2.66	2.48	2.55	2.39	1.38	7.17	6.69
K_2O	3.69	2.35	0.69	0.71	0.78	0.67	6.96	0.069	0.068
TiO_2	0.61	0.19	1.46	2.33	2.34	2.38	0.36	0.51	0.55
MnO	0.071	0.058	0.23	0.23	0.23	0.24	0.021	0.027	0.037
H_2O^-	0.39	0.82	0.10	0.91	0.080	0.080	0.29	0.086	0.090
Ignition	0.92	1.04	---	1.99	0.040	0.040	2.43	3.79	2.98
TOTAL:	100.79	98.58	101.19	99.65	100.12	100.30	97.96	98.96	97.48
q	15.89	33.36	5.28	6.12	3.99	3.34	24.92	17.41	18.11
c	---	---	---	---	---	---	8.90	---	---
or	21.78	13.87	4.07	4.19	4.60	3.96	41.08	---	---
ab	36.95	30.86	22.49	20.97	21.56	20.21	11.67	60.62	56.56
an	14.99	15.03	25.46	24.52	22.44	20.51	---	5.99	8.41
ne	---	---	---	---	---	---	---	---	---
di	1.32	0.53	11.46	9.66	18.84	20.80	---	4.29	4.68
wo	---	---	---	---	---	---	---	4.86	---
ol	---	---	---	---	---	---	---	---	---
hy	4.91	1.79	22.69	20.25	17.29	19.78	6.87	---	3.21
mt	2.14	0.71	5.51	5.29	5.46	5.45	1.71	0.61	1.96
il	1.16	0.36	2.78	4.42	4.45	4.53	0.69	0.97	1.05
SI*	10.21	4.09	21.38	19.47	21.17	24.91	15.25	8.71	9.68

*Solidification Index ($100 \times MgO/MgO+FeO+Fe_2O_3+Na_2O+K_2O$)

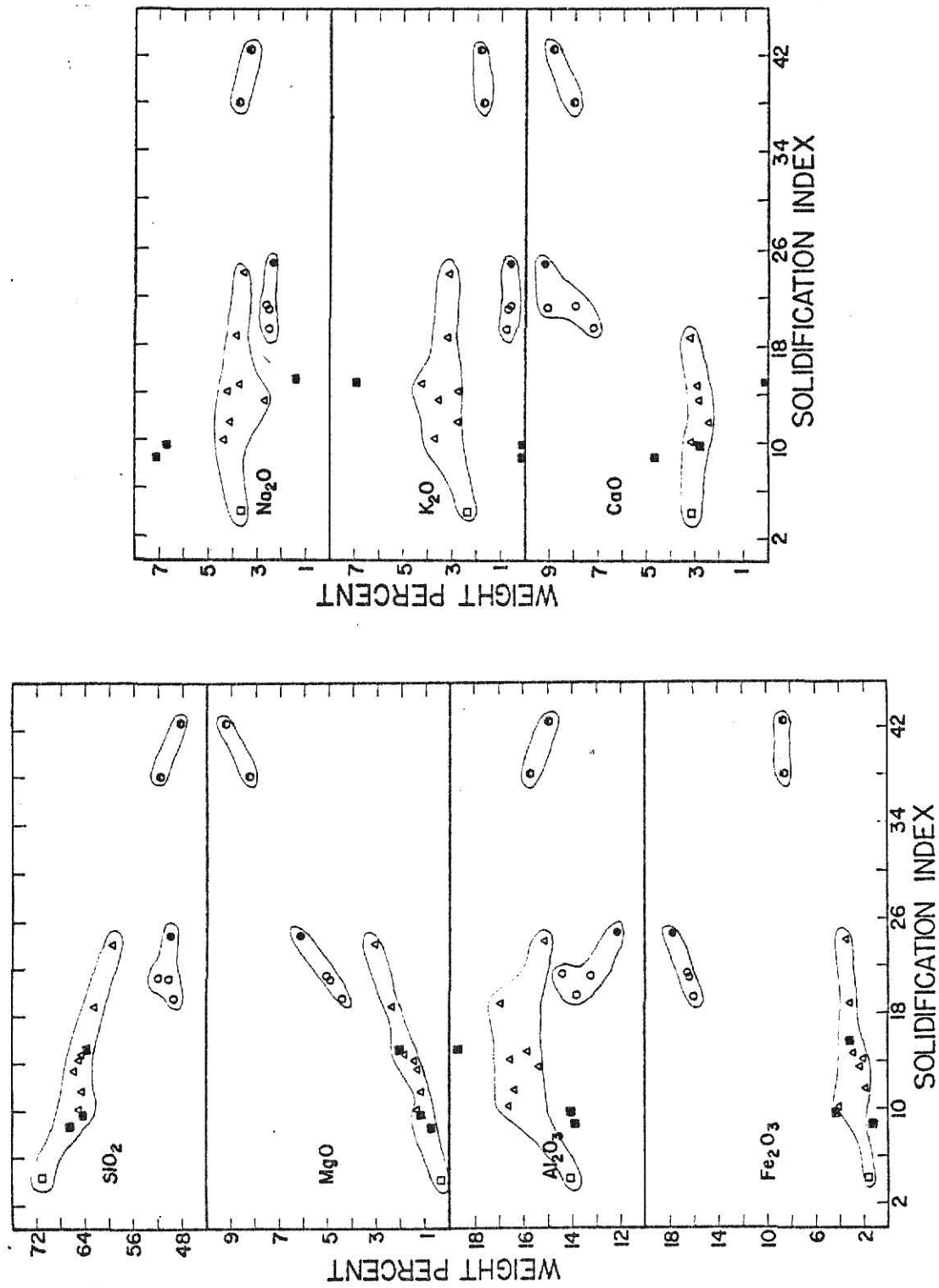

Figure 16. Major element oxides versus solidification index: (□) Rhyodacite, (△) Dacite and Granodiorite, (■) Hybrid Rocks, (◑) Basalts, and (○, ●) Gabbro and Gabbro sill, respectively.

Figure 18 is a ternary plot of K_2O versus Na_2O versus CaO which demonstrates the lack of chemical continuity between the three rock groups. The gabbro, basalt, and dacite-granodiorite-rhyodacite plot as distinct groups. Hybrid rocks have very large degrees of scatter due to exceptionally low CaO and K_2O contents of the two hybrid types.

Figure 18 is an AFM diagram which further magnifies the chemical dissimilarity of the three major rock groups. The compositions of gabbro, basalt, and dacite-granodiorite-rhyodacite again plot as distinct groups which lack intermediate compositions. The hybrid rocks are again scattered but plot in the proximity of the dacite-granodiorite-rhyodacite field.

Figure 19 is a plot of CaO and K_2O+Na_2O versus SiO_2 for the dacite - granodiorite -rhyodacite which yields the alkali-lime index as defined by Peacock (1931). An index of about 57 given by the intersecting trends shows the silicic units are calc-alkaline, although the index could range from 55 to 59 because of data scatter.

TRACE ELEMENTS

General

Trace element concentrations were obtained using three analytical techniques: instrumental neutron activation, atomic emission spectrophotometry, and X-ray fluorescence. Instrumental neutron activation data are given in Table 6. Atomic emission and X-ray fluorescence data are given in Table 7.

Three U. S. Geological Survey standard rocks were analyzed by instrumental neutron activation analyses. Results are compared to values given by Flanagan (1973) in Table 5. Standard data compares favorably to the published values. Estimated maximum deviations of trace element values were determined by comparison of accepted and calculated standard

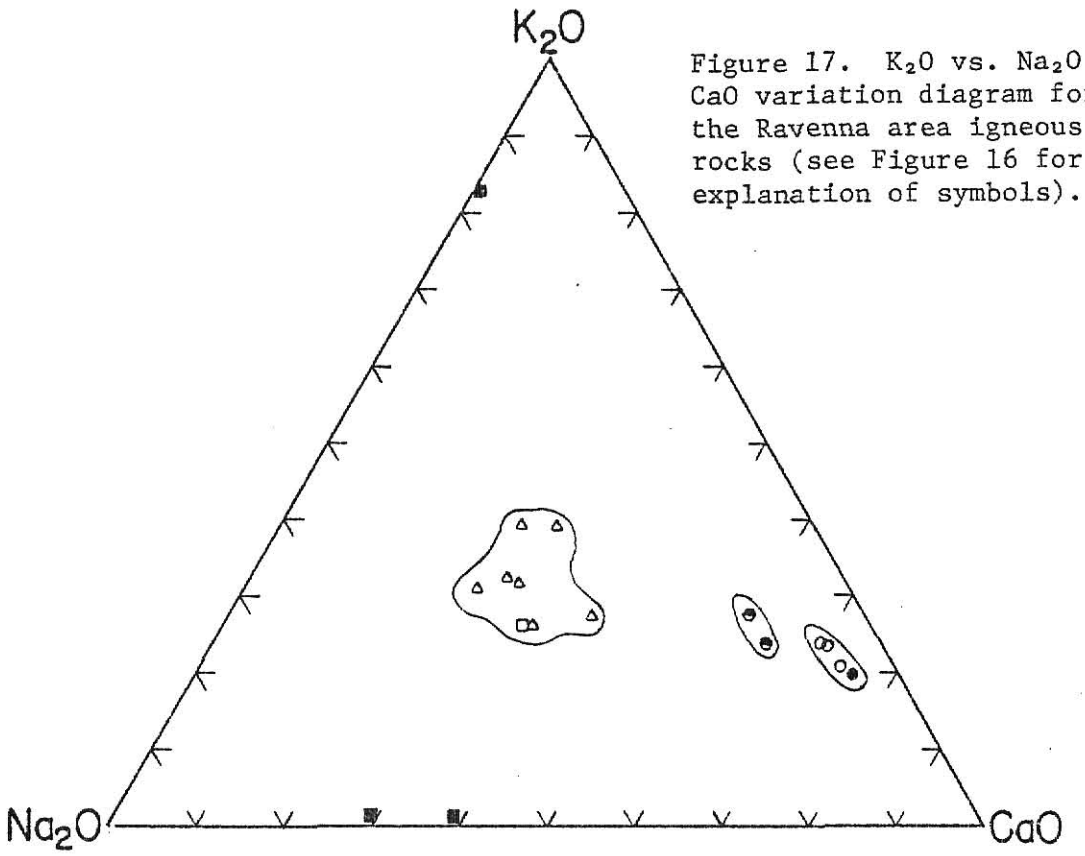

Figure 17. K_2O vs. Na_2O vs. CaO variation diagram for the Ravenna area igneous rocks (see Figure 16 for an explanation of symbols).

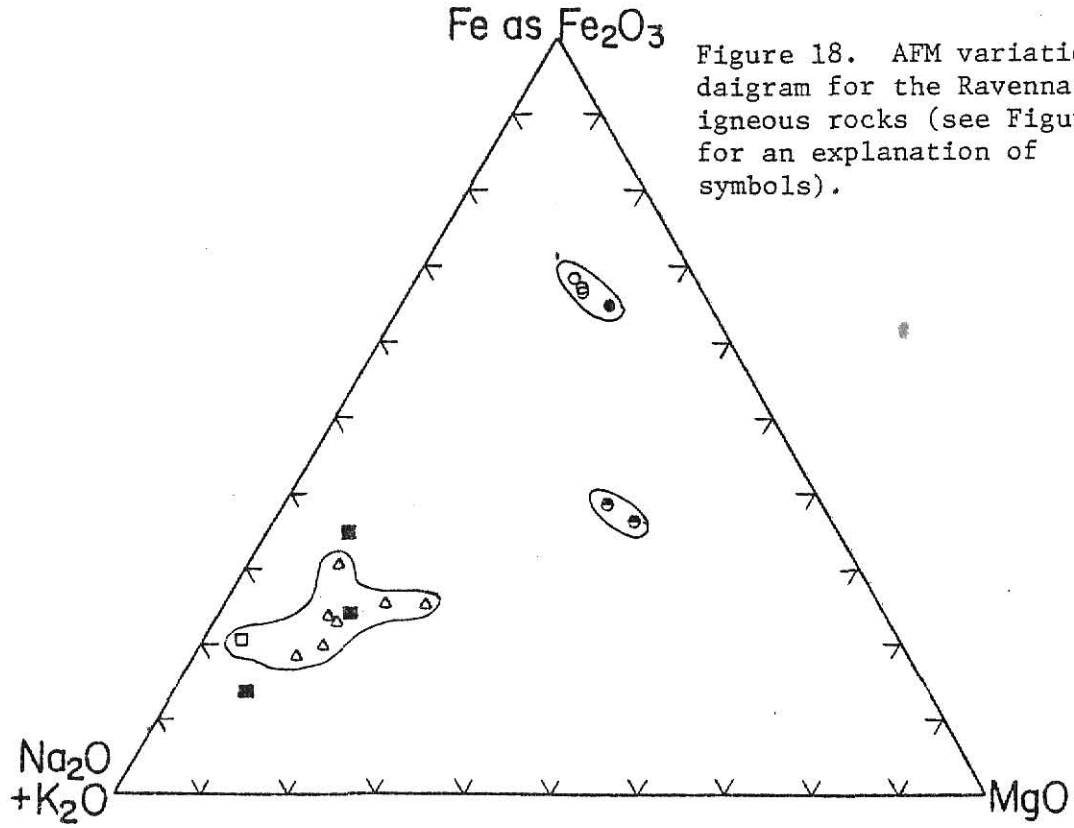

Figure 18. AFM variation daigram for the Ravenna area igneous rocks (see Figure 16 for an explanation of symbols).

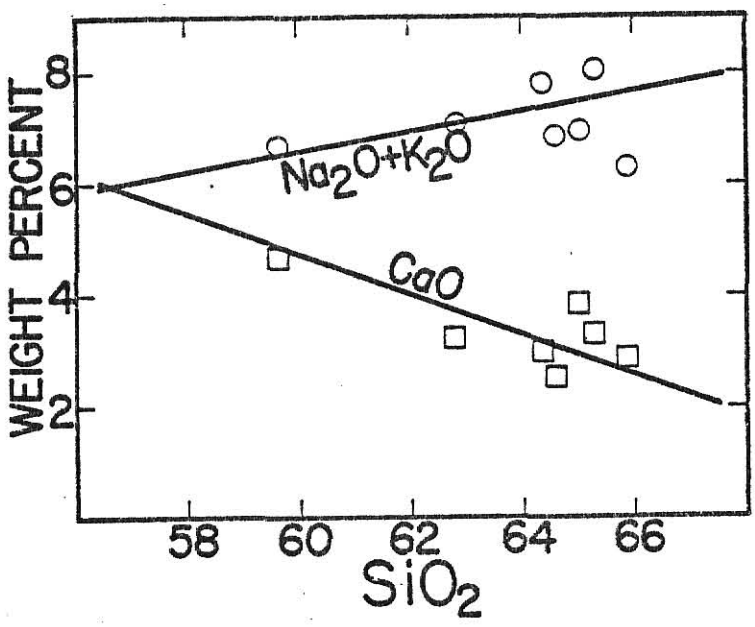

Figure 19. Alkali lime index for the dacite, granodiorite, and rhyodacite (○ = $Na_2O + K_2O$, □ = CaO).

concentrations and are as follows: Co, Hf, Ce, La, Sm: ± 5 percent; Ba, Fe, Na, Sb, Sc, Th, Eu, Lu, Nd, Yb: ± 10 percent; Cr, Ta, Tb: ± 15 percent; Cs, Rb: ± 20 percent; U, Zn, Se: greater than ± 25 percent.

Accuracy of flame emission analyses of Ba, Rb, and Sr was monitored by the analysis of five U.S. Geological Survey standard rocks. The results are in fair agreement with published standard values. Ba concentrations determined for STM-1 and W-1 were consistantly high, whereas samples with higher Ba concentrations (AGV-1, G-2, and BCR-1) showed better correlations. Variable data may be the result of interference caused by high lithium and lanthanum concentrations in the sample and standard solutions.

The accuracy of X-ray fluorescence data was not determined in this study, however S. Chaudhuri (personal communication) has reported accuracies of ± 5 percent for Rb and Sr utilizing the same equipment and techniques. For this reason, in future discussions, X-ray fluorescence data will be used in preference to Rb and Sr values determined by flame emmision.

Table 5. Analytical results of instrumental neutron activation analyses for U.S. Geological Survey standards (ppm, unless otherwise noted).

ELEMENT	AGV-1* Andesite	AGV-1**		BCR-1* Basalt	BCR-1**		W-1* Diabase	W-1**	
Ba	1097	1208	R	599	675	R	88	160	R
Co	13.8	14.1	A	35	38	M	52	47	A
Cr	11.2	12.2	A	14.1	17.6	A	164	114	A
Cs	1.0	1.4	M	0.62	0.95	R	0.66	0.90	R
Fe***	6.16	6.76	R	12.68	13.40	R	13.02	11.09	R
Hf	5.1	5.2	A	4.7	4.7	A	3.20	2.67	A
Na***	4.02	4.26	R	3.27	3.27	R	2.58	2.15	R
Rb	81	67	R	120	46.6	R	25	21	R
Sb	4.5	4.5	A	0.58	0.69	A	---	1.0	R
Sc	10.7	13.4	A	31	33	M	40.9	35.1	A
Se	0.82	0.14	A	0.33	0.10	M	0.22	0.13	M
Ta	1.1	0.9	R	0.76	0.91	R	0.51	0.50	R
Th	6.90	6.41	R	6.6	6.0	R	3.18	2.42	R
U	1.83	1.88	A	1.0	1.74	A	0.17	0.58	A
Zn	60	84	R	74	120	R	120	86	R
La	34	35	M	24	26	A	12.6	9.8	A
Ce	59	63	A	47.6	53.9	R	23	23	M
Nd	38	39	A	30	29	R	18	15	R
Sm	5.4	5.9	A	6.2	6.6	A	3.7	3.6	A
Eu	1.4	1.7	A	1.60	1.94	R	1.15	1.11	R
Tb	0.48	0.70	R	0.79	1.0	R	0.65	0.71	R
Yb	1.5	1.7	A	3.16	3.16	A	2.4	2.1	R
Lu	0.25	0.28	A	0.51	0.55	R	0.41	0.35	A

*This study.
**Flanagan (1973).
***Na as Na_2O, Fe as Fe_2O_3

R = recommended USGS value.
A = average USGS value.
M = magnitude of USGS value.

Table 6. Analytical results of instrumental neutron activation analyses for Ravenna area igneous rocks.

ELEMENT	37 Alk.-ol. Basalt	49 Thol. Basalt	12 Dacite	45 Dacite	58 Dacite	46 Grano-diorite	51 Rhyo-dacite	G-4 Gabbro	34 Gabbro	33 Hybrid Rock	53 Hybrid Rock
Ba	1343	665	1198	1338	2005	1628	1270	90	60	1090	---
Co	44	40.7	10.5	11.9	14.1	18.2	12.4	54.6	55.9	8.5	15.6
Cr	790	383	54.6	39.6	62.4	103	18.3	45.5	158	29.8	20.8
Cs	1.5	1.1	1.4	4.0	2.8	4.2	2.0	2.6	0.97	10	0.27
Fe*	9.50	8.79	3.26	2.79	3.43	4.08	1.96	16.11	17.52	3.28	1.30
Hf	5.2	3.6	4.4	4.2	5.8	4.8	2.9	4.1	5.0	13	10
Na*	3.93	3.56	3.33	4.10	4.33	3.97	3.97	2.73	2.23	0.97	7.05
Rb	36	44	73	121	120	100	54	30	108	314	---
Sb	0.13	---	---	0.05	---	2.8	0.47	---	---	---	0.20
Sc	22	23	5.9	5.0	6.3	8.2	3.6	35	46	11	8.9
Se	1.6	1.5	0.4	1.7	1.0	0.04	0.89	4.6	1.7	1.2	0.96
Ta	2.8	1.7	1.5	1.3	2.8	3.8	3.4	2.4	2.0	3.7	5.2
Th	14	7.9	10	12	14	16	6.8	2.8	3.1	25	11
U	2.6	1.7	2.2	4.0	3.3	2.5	2.7	0.91	5.7	5.3	2.5
Zn	76	46	67	53	65	52	39	81	46	23	42
La	103	40	41	33	51	60	21	12	13	56	12
Ce	203	74	75	32	100	114	40	24	28	111	29
Nd	110	42	37	30	55	88	20	15	17	58	16
Sm	13	5.8	4.9	2.2	6.7	7.5	2.6	5.4	6.2	11	5.3
Eu	3.0	1.6	1.2	0.56	1.7	1.8	0.74	1.8	1.8	1.2	0.55
Tb	0.82	0.52	0.34	0.16	0.39	0.52	0.23	0.91	1.12	1.38	0.73
Yb	1.8	1.5	0.90	0.42	0.88	1.0	0.68	3.4	3.8	7.5	3.2
Lu	0.35	0.29	0.18	0.10	0.19	0.20	0.14	0.51	0.60	1.3	0.50
ΣREE	428	163	162	107	211	244	87	80	89	272	80

*Fe as Fe_2O_3, Na as Na_2O

Table 7. Trace element contents determined by atomic emission spectrophotometry and X-ray fluorescence.

ELEMENT	TECHNIQUE	37 Alk.-ol. Basalt	49 Thol. Basalt	12 Dacite	20 Dacite	26 Dacite	45 Dacite	46-B Dacite	58 Dacite	46 Grano-diorite
Ba	AES*	1404	760	1409	1493	1196	1259	1172	1926	1876
Rb	AES	45	43	72	76	64	119	67	132	91
	XRF**	29.6	35.0	69.3	75.4	---	88.4	61.2	90.8	88.3
Sr	AES	1522	675	806	851	908	482	720	992	1302
	XRF	1737	726	758	931	---	602	851	1134	1282
Rb/Sr	XRF	0.02	0.05	0.09	0.08	---	0.15	0.07	0.08	0.07

ELEMENT	TECHNIQUE	51 Rhyo-dacite	G-4 Gabbro	21-G Gabbro	24 Gabbro	34 Gabbro	33 Hybrid Rock	53 Hybrid Rock	54 Hybrid Rock	Garnet Range Fm.
Ba	AES	1133	202	212	208	203	996	92	124	---
Rb	AES	68	26	27	28	26	336	0.8	5	---
	XRF	46.6	24.8	26.4	---	25.0	260	13.6	13.3	171.4
Sr	AES	836	212	186	235	153	63	49	22	---
	XRF	928	169	148	---	134	58.6	8.2	11.5	57.8
Rb/Sr	XRF	0.05	0.15	0.18	---	0.19	4.44	1.67	1.16	2.96

*Atomic Emission Spectrophotometry
**X-ray Fluorescence

Elements which have been determined by two or more analytical techniques include Na, Fe, Ba, Rb, and Sr. The values of Fe and Na determined by atomic absorption and neutron activation are in excellent agreement. The concentrations of Ba, Rb, and Sr determined by atomic emmission, neutron activation, and X-ray fluorescence are in fair agreement.

Rare-Earth Elements

Chondrite-normalized REE concentrations versus REE atomic number are plotted in Figures 20a and 20b. The rhyodacite, dacite, granodiorite, and basalt display highly fractionated trends with chondrite-normalized La/Lu ratios of 14.0 to 30.9. Parallel to sub-parallel trends and lack of Eu anomaly characterize these rock types. The two gabbros analyzed have similar flat trends with chondrite-normalized La/Lu ratios of 2.2 to 2.5. Hybrid rocks have large negative Eu anomalies of similar magnitude and La/Lu ratios of 2.4 to 4.6. The extrapolated sums of the REE are listed in Table 6. The dacite-granodiorite-rhyodacite group ranges from 87 to 244 ppm, the gabbros have 80 and 89 ppm of REE, and the basalts 163 to 428 ppm.

Other Trace Elements

Concentrations of U, Th, Ta, Se, Hf, Cs, Cr, Co, Ba, Sr, Rb, and Zn versus SI are plotted in Figure 21. Trace-element concentrations tend to be similar within the basalt, gabbro, and dacite-granodiorite-rhyodacite groups, whereas the hybrid rocks have widely varied compositions compared to rocks with similar SI.

STRONTIUM ISOTOPES

Sixteen igneous samples were analyzed to determine $^{87}Sr/^{86}Sr$ ratios. The results are presented in Table 8, with the calculated $^{87}Sr/^{86}Sr$ initial

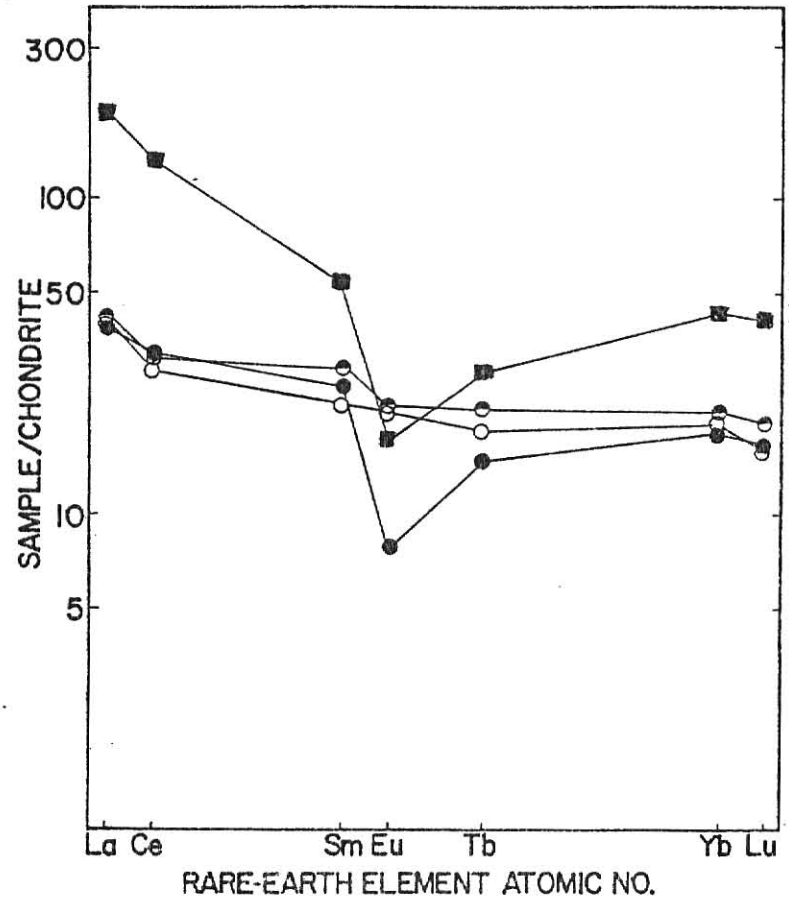

Figure 20a. Chondrite-normalized REE patterns for: (◓) Gabbro sill, sample 34; (○) Gabbro G-4; (■) Hybrid 33; (●) Hybrid 53.

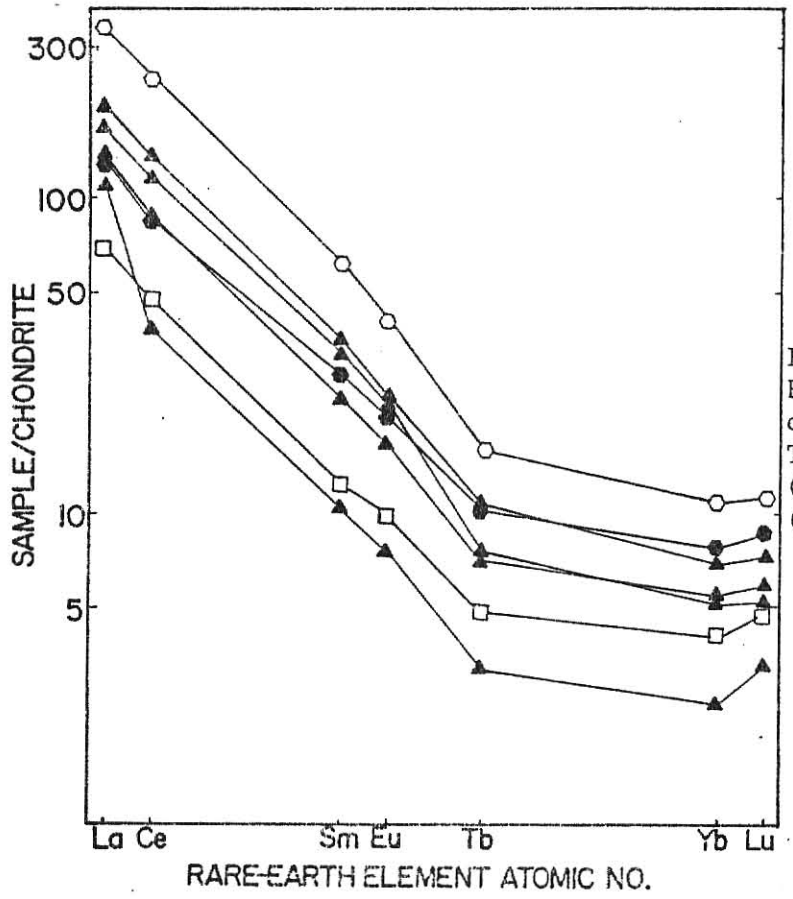

Figure 20b. Chondrite-normalized REE batterns for: (○) Alkali-olivine Basalt; (●) Olivine Tholeiite; (□) Rhyodacite; (△) Dacites and Granodiorite (uppermost).

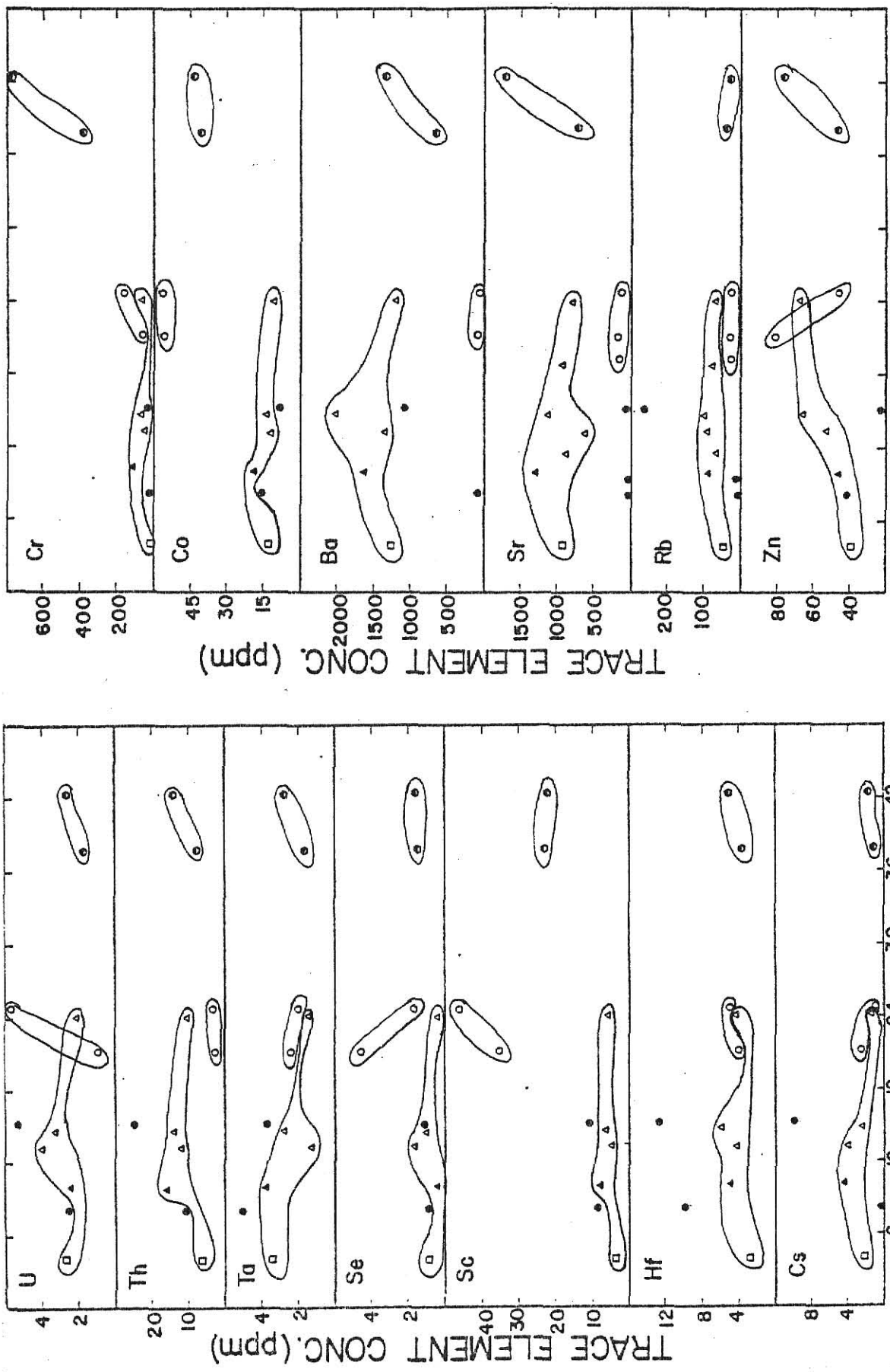

Figure 21. Trace element concentrations versus solidification index for igneous rocks of the Ravenna area; (□) Rhyodacite; (▲) Granodiorite; (●) Hybrids; (○) Gabbro; (◓) Basalt.

Table 8. Strontium isotope ratios determined by mass spectrometry.

Sample Number	Rock Name	$^{87}Sr/^{86}Sr$	$^{87}Sr/^{86}Sr_i$*	Rb/Sr (XRF)
37	Alk.-ol. Basalt	0.7060 ± 0.0005	0.7060 ± 0.0005	0.02
49	Thol. Basalt	0.7114 ± 0.0005	0.7113 ± 0.0005	0.05
12	Dacite	0.7208 ± 0.0005	0.7206 ± 0.0005	0.09
20	Dacite	0.7094 ± 0.0005	0.7092 ± 0.0005	0.08
45	Dacite	0.7083 ± 0.0005	0.7079 ± 0.0005	0.15
46-B	Dacite	0.7160 ± 0.0005	0.7158 ± 0.0005	0.07
58	Dacite	0.7067 ± 0.0005	0.7065 ± 0.0005	0.08
46	Granodiorite	0.7069 ± 0.0005	0.7067 ± 0.0005	0.07
51	Rhyodacite	0.7088 ± 0.0005	0.7087 ± 0.0005	0.05
G-4	Gabbro	0.7120 ± 0.0005	0.7116 ± 0.0005	0.15
21-G	Gabbro	0.7148 ± 0.0005	0.7143 ± 0.0005	0.18
34	Gabbro	0.7125 ± 0.0005	0.7120 ± 0.0005	0.19
33	Hybrid Rock	0.8730 ± 0.0005	0.8614 ± 0.0005	4.44
53	Hybrid Rock	0.7329 ± 0.0005	0.7286 ± 0.0005	1.67
53	(Leachate)	0.7261 ± 0.005		
54	Hybrid Rock	0.7364 ± 0.0005	0.7334 ± 0.0005	1.16
	Garnet Range Fm. (Argillaceous quartzite)	0.8229 ± 0.0005		2.96

*Strontium initial ratios calculated using an age of 45 m.y. for samples 37 and 49, and an age of 70 m.y. for all other samples.

ratios at time = 70 m.y. B.P. One sample of Precambrian Garnet Range Formation also was analyzed.

Precision of the $^{87}Sr/^{86}Sr$ ratios is estimated to be $\pm$ 0.0003 based on replicate analyses of the Eimer and Amend $SrCO_3$ standard (0.7081 $\pm$ 0.0003). The variance between analyses is assigned to instrumental error, as laboratory contaminations are considered negligible.

Most measured isotopic ratios of the granodiorite, dacite, and rhyodacite range from 0.7067 to 0.7094 although two dacites have higher values of 0.7160 and 0.7280. The gabbro has generally higher values of 0.7120 to 0.7148. The two basalts have disparate values of 0.7060 and 0.7114 whereas the hybrid rocks have ratios higher than 0.7329. Carbonate leached from one of the hybrid rocks has approximately the same isotopic value as the whole-rock sample. A sample of the Garnet Range Formation collected south of sample site 54 has a highly radiogenic value of 0.8229.

Figure 22 is a plot of $^{87}Sr/^{86}Sr$ versus $^{87}Rb/^{86}Sr$ in which the data points are widely scattered. No apparent linearities are observed which could permit the construction of an isochron.

Crustal contamination of the igneous rocks with a homogeneous contaminant could result in linear trends on a plot of $^{87}Sr/^{86}Sr$ versus 1/Sr (Fig. 23). A steeply positive linear trend with varied scatter is observed amoung the granodiorite, dacite, and rhyodacite.

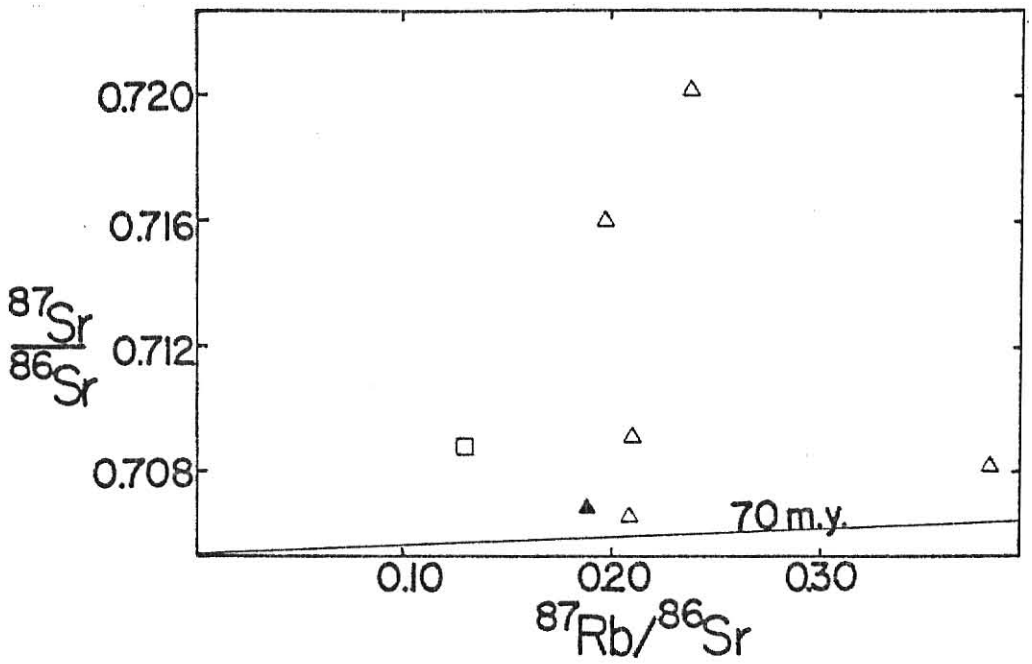

Figure 22. $^{87}Sr/^{86}Sr$ versus $^{87}Rb/^{86}Sr$ for the silicic units of the Ravenna area. Symbols: (□) Rhyodacite; (△) Dacite ; (▲) Granodiorite (the 70 m. y. line is a reference isochron).

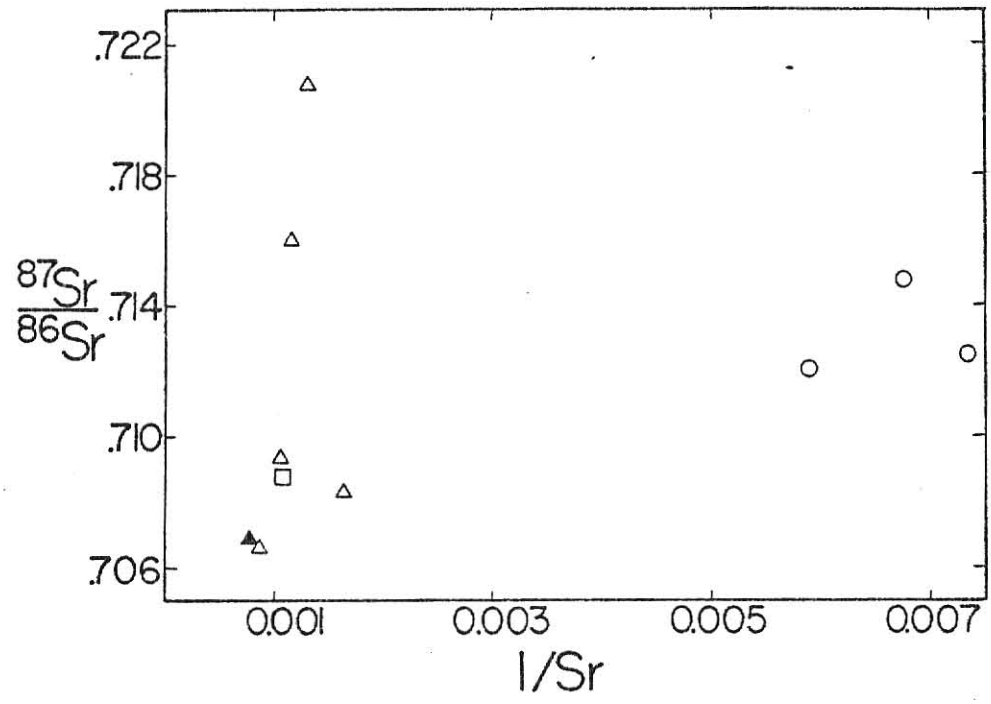

Figure 23. $^{87}Sr/^{86}Sr$ versus 1/Sr for the silicic and gabbroic units of the Ravenna area. Symbols: (△) Dacite ; (□) Rhyodacite; (▲) Granodiorite; (○) Gabbro .

D I S C U S S I O N

INTRODUCTION

Field evidence, major-element data, trace-element data, and strontium isotope data can be used to establish the genetic relations between the igneous units of the Ravenna area. Spatial relations and stratigraphic relations could show sequences of magma evolution. Smooth linear trends displayed on major-element diagrams may be indicative of genetic relations between various rock types. Major elements can also provide information on the mineralogic phases which may have fractionated to produce the observed chemical variations between related igneous units. Trace elements as a group can yield valuable information about the source composition, crystal fractionation, and processes of magma generation. The strontium isotope initial ratios can be indicators of the genetic and emplacement histories of the igneous rocks.

RELATIONS AMONG ROCK TYPES

Rocks of the Ravenna area petrographically and chemically form four distinct groups: (1) basalt group, (2) dacite-granodiorite-rhyodacite group, (3) gabbro group, and (4) hybrid group. Groups 1, 2, and 3 are the major igneous rock units in this area, whereas group 4 (i.e. hybrid rock group) constitute only a minute fraction of the total igneous mass. As the hybrid rocks appear to have formed from the interaction between a

magma and the very surficial Precambrian sedimentary rocks of the Belt Supergroup, the chemical evolutionary trends of these rocks will be treated separately.

Field relations suggest contemporaneous emplacement of the dacite-granodiorite-rhyodacite and gabbro groups. The basalt group tends to be much younger than either of the other major groups. The younger age is substantiated by the fact that they are relatively fresh and are possibly equivalent in age to the Eocene basalts from the nearby Bearmouth area (Williams, 1976).

The major-element variation trends among these major rock groups are distinct. The distinctions are illustrated in Figures 16, 17, and 18. Various trace-element contents, especially Th, Se, Sc, Co, Ba, Sr, and Rb plotted against solidification index further substiante the distinctions among these groups (Fig. 21). The REE patterns of the dacite-granodiorite-rhyodacite and gabbro groups are dissimilar. The dacite group with a La/Lu ratio of 10 to 30 are more fractionated than the gabbro group having La/Lu ratios of about 2. Although one of the basalt samples (the alkali-olivine basalt) has the highest total REE content among all the rocks analyzed, the REE trends of the basalt and the dacite are very similar (Fig. 20b).

The dacite-granodiorite-rhyodacite group, which has Rb/Sr ratios between 0.05 and 0.15, shows initial $^{87}Sr/^{86}Sr$ ratios between 0.7065 and 0.7206. In contrast to the dacite-granodiorite-rhyodacite group, the gabbro group has a limited range in $^{87}Sr/^{86}Sr$ ratios between 0.7116 and 0.7143 and high Rb/Sr values between 0.15 and 0.19. The basalt group tends to have the lowest Rb/Sr values of 0.02 and 0.05, whereas its initial $^{87}Sr/^{86}Sr$ ratios of 0.7060 and 0.7113 are within the range of values observed for the dacite-granodiorite-rhyodacite group. Although there is

considerable overlap in the strontium isotopic composition amoung the three major groups of rocks, the distinctions between them, especially between the dacite-granodiorite-rhyodacite and the gabbro groups, are apparent on the basis of either $^{87}Sr/^{86}Sr$ versus $^{87}Rb/^{86}Sr$ relationships or $^{87}Sr/^{86}Sr$ relationships (Figs. 22 and 23).

The isotopic diversity and the chemical dissimilarity of the igneous rocks in the Ravenna area require diverse evolutionary trends. Discussions and models which follow treat the genesis of the basalt, dacite-granodiorite-rhyodacite, gabbro, and hybrid rock groups separately.

DERIVATION OF THE MODEL

Elemental behavior can be predicted with a non-modal, aggregate liquid partial fusion model derived by Shaw (1970) and expressed by:

$$Cl/Co = 1/F \left[1 - (1 - PF/Do)^{1/P} \right]$$

where:

Cl = elemental concentration in the liquid
Co = elemental concentration in the source
F = fraction melted
P = proportionality coefficient
Do = overall distribution coefficient

Do and P can be further defined as:

$P = P\alpha K\alpha + P\beta K\beta + \ldots$

where:

$P\alpha,\beta$ = proportion of phase α,β in the liquid
$K\alpha,\beta$ = distribution coefficient of the element in the liquid

$Do = X\alpha D\alpha + X\beta D\beta + \ldots$

where:

$X\alpha,\beta$ = fraction of phase α,β in the source
$D\alpha,\beta$ = distribution coefficient of the element in the liquid.

The distribution coefficient D is defined as the concentration of the element in the derived phase divided by the concentration of the element in the source. Basaltic, intermediate, and silicic distribution coefficients used in the present modeling are compiled in Table 9.

Crystal fractionation of phenocryst minerals and the effect on the trace-element concentrations are predicted by the following equation of Haskin et al. (1970):

$$Cr/Ca = (1 - X)^{D-1}$$

where:

Cr/Ca = average elemental concentration in the residual phase divided by the same element's concentration in the system
X = fraction of crystallization
D = distribution coefficient of the element.

BASALT GENESIS

Numerous authors have discussed the genesis of alkalic and tholeiitic basalts. Theories to explain their origins include: (1) differentiation of tholeiitic parent to form alkali-olivine basalt (MacDonald and Katsura, 1964); (2) high pressure fractionation to form tholeiitic materials from the alkali-olivine melt (McBirney and Williams, 1969); (3) small degrees of partial melt of peridotite or eclogite to form alkali-olivine basalt and larger degrees to yield tholeiitic melts (Philpotts and Schnetzler, 1970a; 1970b; Leeman, 1976); and (4) high pressure melting of garnet peridotite to produce alkali-olivine basalts and low pressure melting to produce tholeiitic basalts (Leeman and Rogers, 1970).

Table 9. Partition coefficients used in trace-element melting models.

	Orthopyroxene		Clinopyroxene		Plagioclase		Garnet	
	B,I*	S**	B,I	S	B,I	S	B,I	S
La	0.020	0.13	0.10	0.25	0.14	0.30	0.027	0.28
Ce	0.024	0.15	0.15	0.50	0.12	0.27	0.028	0.35
Sm	0.054	0.27	0.50	1.67	0.067	0.13	0.29	2.7
Eu	0.054	0.17	0.51	1.56	0.34	2.2	0.49	6.5
Tb	0.12	0.27	0.53	1.57	0.067	0.13	1.0	12
Yb	0.34	0.86	0.62	1.58	0.067	0.049	11.5	40
Lu	0.42	0.90	0.56	1.54	0.060	0.046	11.9	42
Rb	0.001	0.003	0.001	0.032	0.01	0.041	0.001	0.01
Sr	0.017	0.027	0.12	0.10	2.2	4.4	0.012	0.015
Ba	0.001	0.003	0.001	0.13	0.023	0.31	0.002	0.017
Co	2	8	0.02	5	0.02	0.10	0.3	2.5
Cr	1.8	1	0.10	12	0.10	0.06	2	3.7
Sc	1.2	5	0.035	10	0.035	0.02	10	13.6

	Spinel	Olivine	Biotite		Hornblende		Ortho.	Quartz
	B,I	B,I	B,I	S	B,I	S	S	S
La	0.09	0.008	0.035	0.34	0.18	1.30	0.040	0.001
Ce	0.08	0.007	0.034	0.32	0.20	1.52	0.044	0.001
Sm	0.05	0.0066	0.031	0.26	0.52	7.77	0.018	0.001
Eu	0.03	0.0068	0.030	0.24	0.59	8.9	1.13	0.001
Tb	0.02	0.010	0.033	0.28	0.55	8.6	0.018	0.001
Yb	0.02	0.014	0.042	0.44	0.49	8.4	0.012	0.001
Lu	0.02	0.016	0.046	0.33	0.43	5.5	0.006	0.001
Rb	0.01	0.001	3.1	5.5	0.04	0.014	0.37	0.001
Sr	0.01	0.014	0.08	0.12	0.46	0.055	3.87	0.001
Ba	0.01	0.001	1.1	9.7	0.42	0.044	6.1	0.001
Co	10	3	20	20	4	10	0.01	0.001
Cr	10	2	17	12	2	2	0.01	0.001
Sc	10	0.03	11	11	10	15	0.06	0.001

*B,I: Basaltic and Intermediate coefficients
**S: Silicic coefficients
Compiled mainly from: Kilbane (1978), Philpotts and Schnetzler (1970a,b), Cox et al. (1979), and Schnetzler and Philpotts (1968; 1970).

Many previous investigators have used trace-element data to develop models explaining the genesis of different igneous rocks. This study has emphasized the use of REE to construct models of evolution for the rocks of the Ravenna area. The models will be further tested by isotopic, trace-element, and major-element data.

The REE patterns of the alkali-olivine basalt and tholeiitic basalt are sub-parallel to each other, the alkali-olivine basalt having the higher total REE content. High La/Lu ratios indicate the presence of garnet in the source, whereas the lack of an Eu anomaly eliminates the possibility of plagioclase fractionation.

The possibility of crystal fractionation of an alkali-olivine parent magma to produce tholeiitic compositions can be eliminated on the basis of REE data. Removal of ferromagnesian minerals with partition coefficients less than one could not produce the lower tholeiitic basalt REE patterns. Fractionation of large quantities of orthopyroxene could produce alkali-olivine magmas from tholeiitic parents (Green and Ringwood, 1967; Mc Birney and Williams, 1969), however, removal of 65 percent orthopyroxene from the analyzed tholeiitic REE composition sould produce La/Lu ratios of 20 instead of the observed ratio of 30 in the alkali-olivine basalt. The presence of only olivine phenocrysts in the analyzed tholeiitic basalt also tends to negate the possibility of fractionation to form an alkali-olivine derivative.

Assuming both basalts were produced from the same source, varied degrees of fusion of a suitable source could account for the observed REE patterns. An upper mantle assemblage of garnet peridotite composed of 53 percent olivine, 25 percent orthopyroxene, 20 percent clinopyroxene, and 2 percent garnet with a LREE (light rare-earth element) enriched chondrite-normalized pattern is the proposed source. Although most peridotites do not have such high REE contents, LREE enriched peridotites similar to the theoretical

source are known. The tholeiitic REE pattern could be produced by 18 percent melt of the proposed source, while the alkali-olivine REE pattern would require abour 4 percent fusion (Fig. 24). Alternatively, the two compositions could be produced by varied confining pressures during fusion and varied degrees of fusion of similar sourdes, although little is known about the change in distribution coeffieients with pressure variations (Frey, 1979).

Partitioning models can also be applied to other trace elements. The ragnes of Rb, Sr, Ba, Co, Cr, and Sc in the proposed peridotitic source have been calculated and are compared to measured trace-element concentrations in undepleted peridotites (Table 10). Ba and Sr contents of the predicted source are higher than that of average undepleted peridotites whereas the remaining trace elements show fair agreement with the literature values. Inaccuracies in the estimated elemental source ranges could be the cause of the anomalous Ba and Sr.

The strontium isotope ratio of the alkali-olivine basalt is 0.7060 while the tholeiitic basalt has a ratio of 0.7114. The isotopic discrepancy between the two basalts could arise from the contamination of the tholeiitic magma by radiogenic Sr. The evidence for contamination may be substantiated by the fact that the basalt with the high Rb/Sr ratio also has the higher initial $^{87}Sr/^{86}Sr$ ratios.

DACITE-GRANODIORITE-RHYODACITE GENESIS

Origins of silicic magmas at continental margins and in intraplate areas have been discussed by numerous authors. Magma of silicic composition similar to the rocks of the Ravenna area could have formed by: (1) fractional crystallization of parent basaltic magma (Green and Ringwood, 1967); (2) partial melting of subducted oceanic crust (Gilluly, 1971); (3) assimilation of crustal material by basaltic liquids (Gilluly, 1971; Hamilton and Meyers,

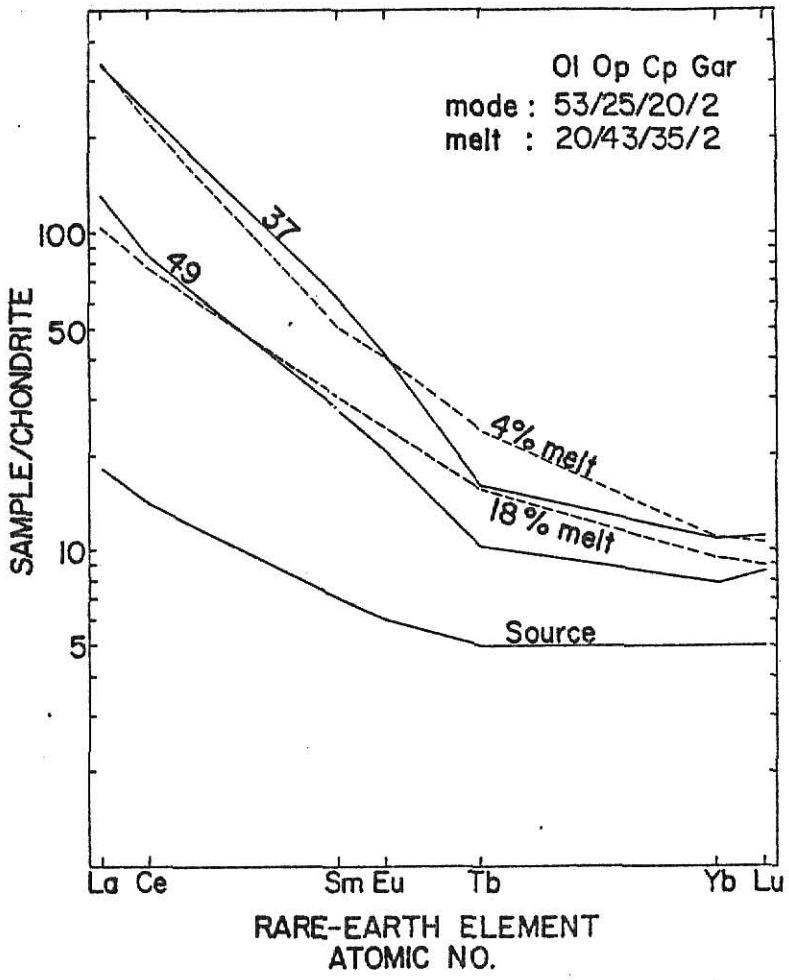

Figure 24. Basalt genesis by varied degrees of melt (dashed lines) of a garnet peridotite source.

1967; and (4) partial melting of crustal material (Armstrong et al., 1969). Gill (1968) believes that intermediate magmas may be generated by more than one of the processes outlined above, whereas Zielinski and Lipman (1976) believe that fusion of subducted eclogite followed by crystal fractionation can produce a range of silicic compositions. Experimental petrology supports the genesis of silicic magmas by melting of eclogite or chemically similar sources in a lower-crust or upper-mantle environment (Green and Ringwood, 1967).

Major element oxide variation diagrams generally show well-developed linear trends which could be produced by fractional crystallization or varied partial fusion of similar sources. Chemical disequilibrium within dacitic units is demonstrated by plagioclase zonations observed petrographically,

Table 10. Literature values of trace-element concentrations in proposed sources compared to calculated trace-element ranges of hypothetical sources of the Ravenna area igneous units (concentrations in ppm).

	Undepleted Peridotite Range (1)	Calc. Basalt Source Range	Oceanic Tholeiite Range (2)	Contin. Rift Tholeiite Avg. (3)	Calc. Dacite Source Range	Undepleted Peridotite Range (1)	Calc. Gabbro Source Range
Rb	2-8	1-6	3.5-9.5	31	18-27	2-8	5-8
Sr	10-40	100-130	120-180	350	185-350	10-40	27-50
Ba	4-5	50-120	21-43	170	360-630	4-5	12-27
Co	35-120	80-90	38-52	38	5-76	35-120	135-145
Cr	2800-3400	600-1200	230-410	160	38-1000	2800-3400	85-310
Sc	5-15	12-13	36-52	--	5-72	5-15	25-30

	Plag.-rich Hybrid Source Range (4)	Calc. Plag.-rich Hybrid Source Range	K.-rich Hybrid Source Range (4)	Calc. K.-rich Hybrid Source Range
Rb	90-136	10-12	90-136	195-200
Sr	225-425	12-14	225-375	120-130
Ba	425-1070	165-170	425-1070	3500-3800
Co	5-73	35-36	5-73	15-16
Cr	5-83	29-30	5-83	35-36
Sc	5-9	11-12	5-9	12-13

(1) From Kilbane (1978). Cr values from Nesbitt and Sun (1976).
(2) Compiled manily from: Frey et al. (1974), Batiza (1978), Engel and Fisher (1975), and Bryan et al. (1977).
(3) From Cullers (personal communication).
(4) Compiled from Shaw et al. (1976), Eade and Fahrig (1973), and Taylor (1964a,b).

which support the possibility of fractionation. Major-element data can be used to test the theory of large-scale crystal fractionation of phenocrysts present in the rocks with the use of extract polygon methods outlined by Cox et al. (1979). Estimated and known phenocryst compositions (Table 11) and whole-rock oxide contents are plotted with respect to two major-element oxides. A plot of CaO versus MgO (Fig. 25) demonstrates that fractionation of Pl + Bt, Hb + Bt, or Pl + Bt + Hb but not Pl + Hb could produce the linear dacitic trend. A second diagram of Al_2O_3 versus SiO_2 (Fig. 25) eliminates the possibility of Hb + Bt fractionation. Thus, the removal of Pl + Bt or Pl + Bt + Hb could be responsible for major-element variations, although similar trends could also be produced by varied degrees of partial melt of the source region. REE trends raise serious questions about the major-element fractionation models. Fractional crystallization of a parent melt could not involve significant quantities of plagioclase given the lack of europium anomalies on the dacitic REE patterns (Fig. 20b). This fact effectively eliminates the remaining two mineral assemblages (i.e. Pl + Bt and Pl + Bt + Hb) which could have produced the major element variations. The role of fractional crystallization of a parent melt in the evolution of the silicic suite can also be discounted on the basis of varied initial strontium isotopic composition of the rocks, unless the isotopic data are reflections of crustal contamination.

The linear major-element oxide trends can be explained by a fusion model given appropriate choice of the source rock. The selection of source mineralogies and compositions is constrained by tectonic regime, isotopic data, and the elemental chemistry of the derived phases. An eclogite is a possible source for the intermediate to silicic magmas of the Ravenna area based on recent studies which indicate that during the Upper Cretaceous

Table 11. Representative major-element contents of minerals used in extract polygon calculations. Plagioclase and olivine values are extrapolated; data is from Cox et al. (1979).

OXIDE	Horn-blende	Biotite	Plagio-clase, An_{35}	Plagio-clase, An_{50}	Augite	Olivine
SiO_2	44.99	37.17	60.34	56.58	52.92	35.22
TiO_2	1.46	3.14	---	---	0.50	0.38
Al_2O_3	11.21	14.60	25.03	27.40	2.80	0.04
Fe_2O_3	3.33	3.75	0.17	0.20	0.85	0.48
FeO	13.17	26.85	0.13	0.08	5.57	37.01
MnO	0.31	0.06	---	---	0.15	1.82
MgO	10.41	4.23	0.24	0.22	16.40	24.42
CaO	12.11	0.17	6.29	9.32	19.97	0.69
Na_2O	0.97	0.15	8.06	6.23	0.35	0.02
K_2O	0.76	8.25	0.08	0.11	0.01	---
H_2O+	1.48	1.35	0.16	0.15	0.10	0.16
H_2O^-	0.04	---	0.05	0.04	0.07	0.05
TOTAL:	100.41	100.57	100.55	100.33	100.67	100.29

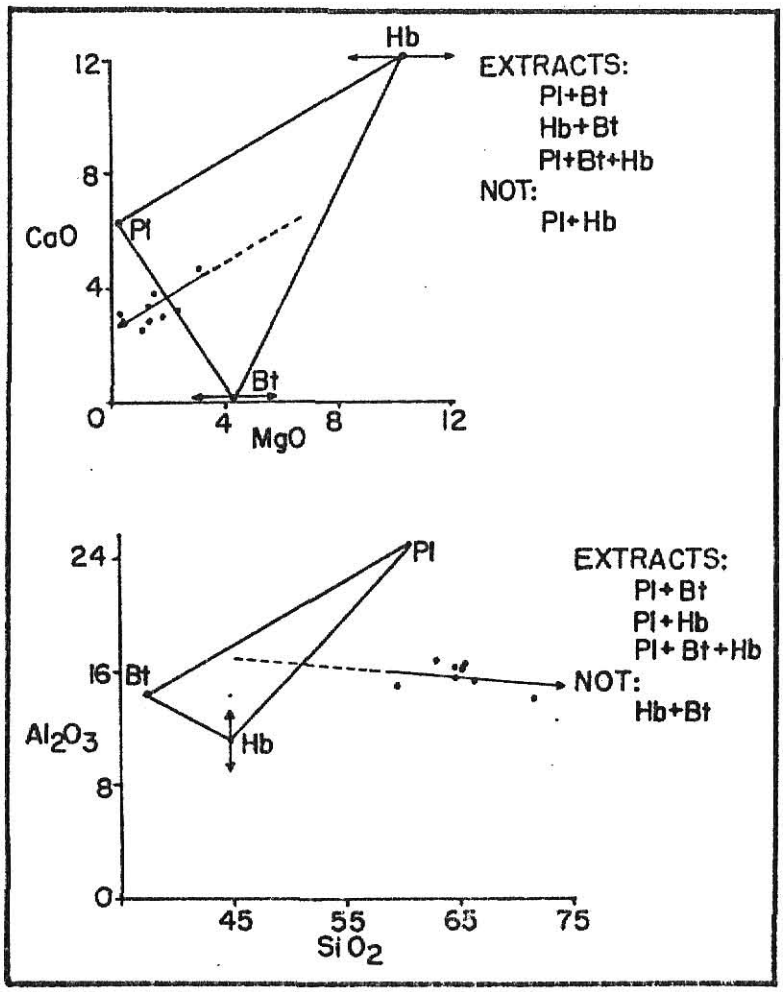

Figure 25. Major element extract polygons which demonstrate the evolutionary trend of the dacite-granodiorite-rhyodacite group and possible mineral assemblages which may have fractionated to produce the observed trends.

a subduction environment was present to the west of the Idaho batholith area (Hyndman, 1979; Scholton and Onasch, 1976). LREE depleted tholeiite typical of most of the present-day ocean floor can be excluded as a source. Alternatively, a lower-crustal source composed primarily of pyroxene and small amounts of garnet and feldspar such as a granulite, could also be a possible source. Approximately thirty percent fusion of a LREE enriched eclogitic source could produce REE patterns similar to those of the Ravenna area silicic units (Figs. 26, 27, and 28). The parallel to sub-parallel trends displayed by the different silicic units could be the result of varied degrees of partial melt, mineralogy, or trace-element content of the source region, mixing of two end members, or small degrees of crystal fractionation. Varied amounts of garnet in the source (Fig. 26) and varied degrees of partial melt (Fig. 27) may result in cross-over fractionation patterns, while parallel trace-element patterns could be produced by varied trace-element contents of a source or sources (Fig, 28).

Strontium isotope data set constraints on the source of the magmas. A plot of $^{87}Sr/^{86}Sr$ versus 1/Sr (Fig. 23) shows a steep positive linear trend among the dacite, granodiorite, and rhyodacite, which could be a reflection of two component mixing of two isotopically distinct sources (Faure, 1977), but the trend is not conclusive due to considerable scatter of the data points. Samples 46 and 58, a granodiorite with Sr_i = 0.7067 and a dacite porphyry with Sr_i = 0.7065 respectively, are taken from apparent extrusive centers and represent the youngest extrusive events, whereas remaining dacite porphyry samples are taken from older dacitic flows (Fig. 29). A source high in Rb/Sr ratios could have generated the older dacite extrusions while a source lower in Rb/Sr may be the parent of the younger igneous material.

Theoretical concentrations of Ba, Rb, Sr, Co, Cr, and Sc in the dacite-granodiorite-rhyodacite source have been calculated (Table 10).

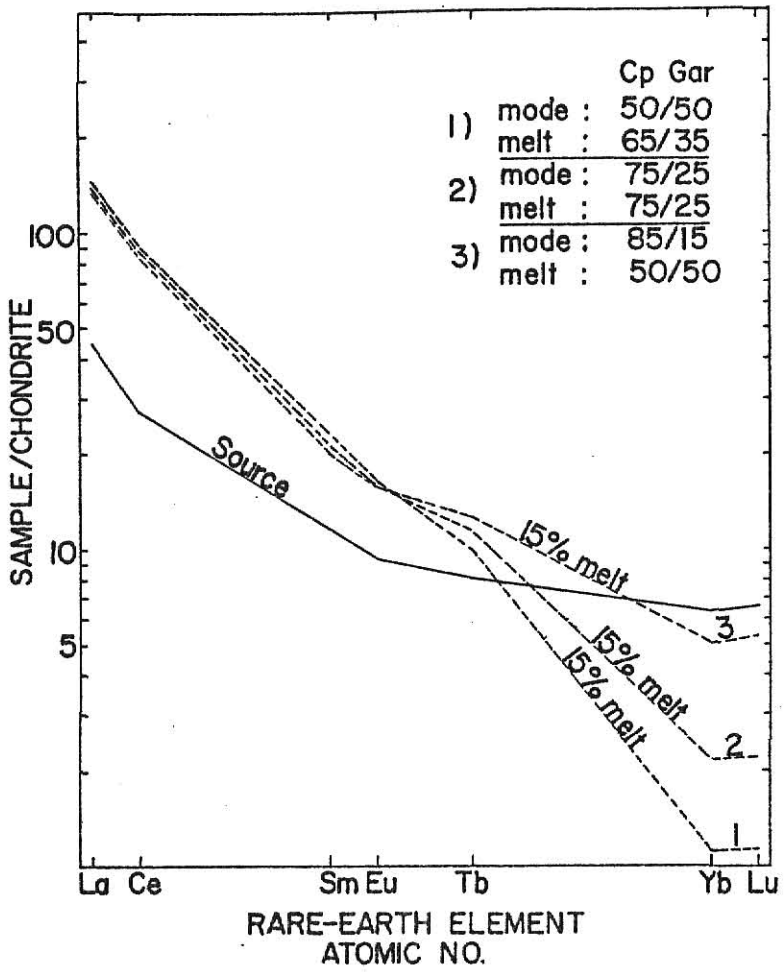

Figure 26. Varied proportions of clinopyroxene-garnet melting of eclogitic sources which produce a cross-over fractionation pattern (dashed lines = hypothetical melts).

Rb, Sr, and Ba values in the predicted source are consistantly high compared to the range of concentrations expected in an oceanic tholeiite source. The assimilation of continental crust rich in Ba, Rb, and Sr could be responsible for the high concentrations of these elements in the silicic units, or the source values may be inaccurately estimated. Alternatively, source compositions may be more similar to those of continental tholeiite (Table 10), which characteristically has high LREE contents. However, poor agreement is again obtained in terms of Ba and Rb values. The concentrations of Co, Cr, and Sc in the hypothetical source agree with contents of either plausible source.

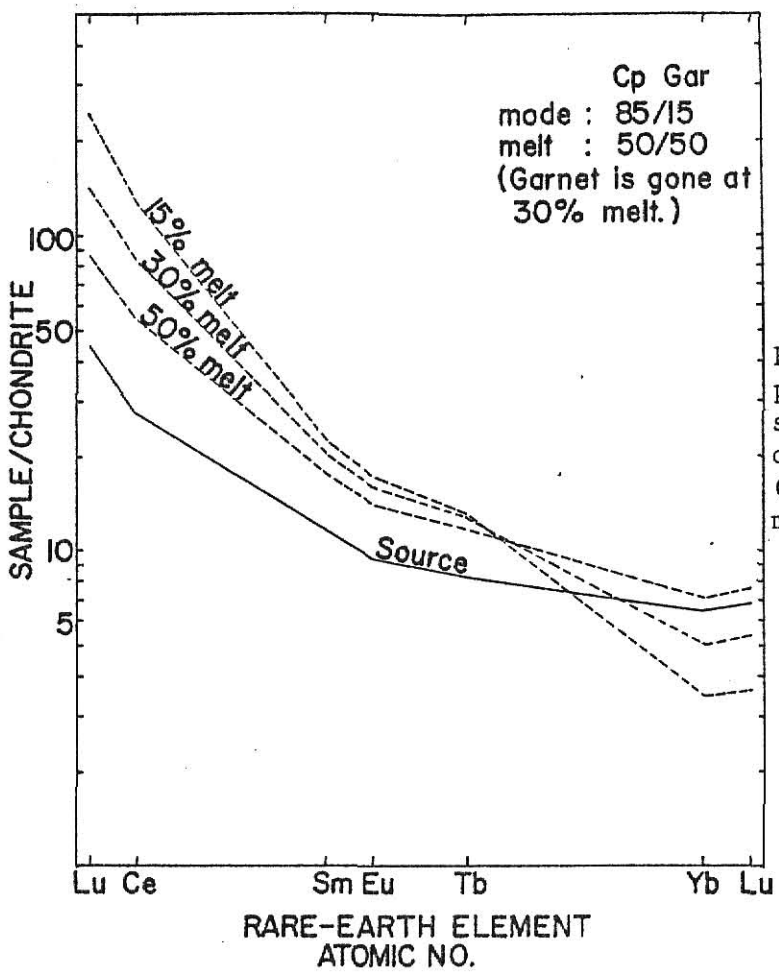

Figure 27. Varied degrees of partial melt of a homogenous source which produces a cross-over fractionation pattern (dashed lines= hypothetical melts).

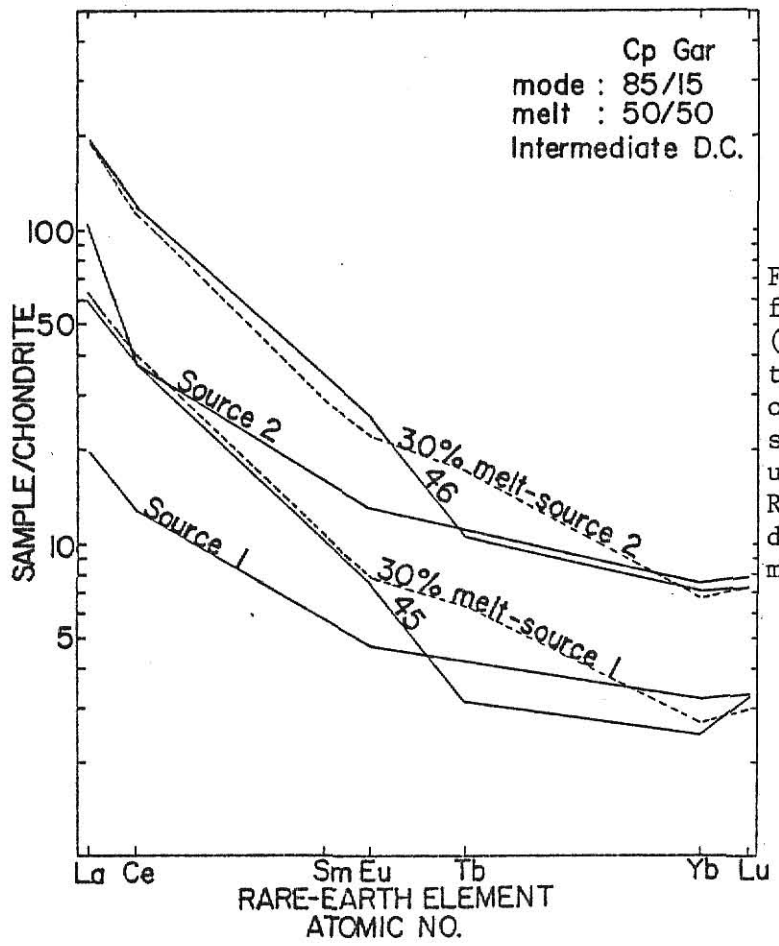

Figure 28. Thirty percent fusion of eclogitic sources (1 and 2) with varied REE concentrations which could produce the observed REE contents in the silicic group (46 and 45 = the upper and lower limits of silicic REE contents, respectively; dashed lines = hypothetical melts).

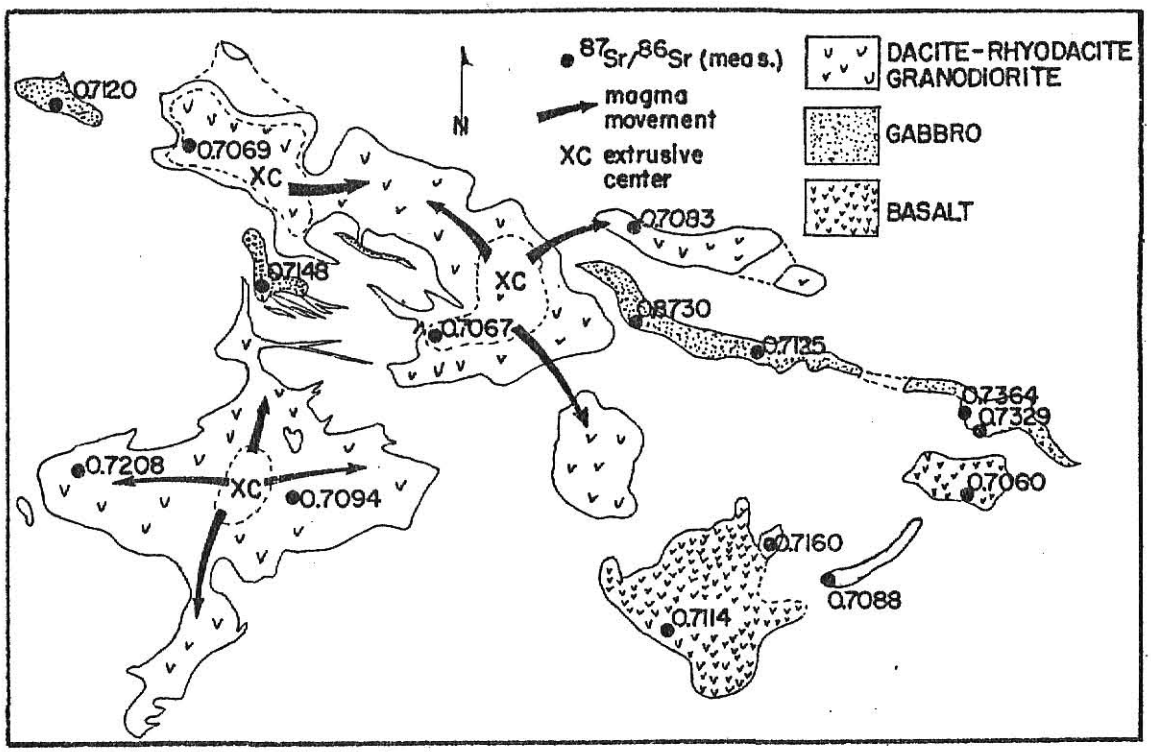

Figure 29. Isotopic data in relation to locations of proposed extrusive centers in the Ravenna area.

Based on major-element, trace-element, and isotopic considerations, source inhomogeneities in a predominantly eclogitic assemblage could have produced the observed chemical variations. Since the isotopic data provide ambiguous answers, the precise role of crustal contamination cannot be ascertained

GABBRO GENESIS

The gabbroic plugs and sills which crop out in the Ravenna area are of tholeiitic composition. Theories of tholeiitic magma genesis have been previuosly outlined.

Variations in major-element chemistry between the gabbros are generally colinear and may represent a liquid line of descent. Extract polygons constructed with minerals observed in the gabbro show that the

evolutionary trend could be caused by fractionation of olivine plus plagioclase from a single magma (Fig. 30). This conclusion is subject to the accuracy of estimated olivine and augite compositions, which may vary considerably. Further constraints upon the crystal fractionation model are set by the REE patterns. The lack of an Eu anomaly suggests significant quantities of plagioclase have not been removed from the primary melt, thereby, eliminating the possibility of fractionation allowed by extract polygons.

The REE patterns of the two gabbro samples analyzed are distinctly different from the pattern of the tholeiitic basalt (Figs. 20a and 20b). Gabbroic REE contents are about 30 times those of chondrites, with La/Lu ratios of about 2 and no Eu anomalies. A spinel peridotite composed of 65 percent olivine, 15 percent orthopyroxene, 15 percent clinopyroxene, and 5 percent spinel is a possible source. Twenty to thirty percent non-modal melts of a LREE-enriched peridotitic assemblage could produce REE patterns and overall compositions similar to those of the gabbros (Fig. 31).

Calculated source compositions of Ba, Rb, Sr, Co, and Sc correlate well with the measured ranges in undepleted peridotites (Table 10), and support the proposed mode of genesis.

The gabbro tends to have an homogeneous initial strontium isotopic composition of about 0.7120. The slightly higher initial $^{87}Sr/^{86}Sr$ of sample 21-G may be due to secondary alteration, whereas the fresher samples 34 and G-4 have isotopic ratios of 0.7120 and 0.7116 respectively which are identical within the range of experimental error. Isotopic values of the gabbros indicate a lower crustal source is feasible (Brooks et al, 1976), and peridotites with crustal histories can have $^{87}Sr/^{86}Sr$

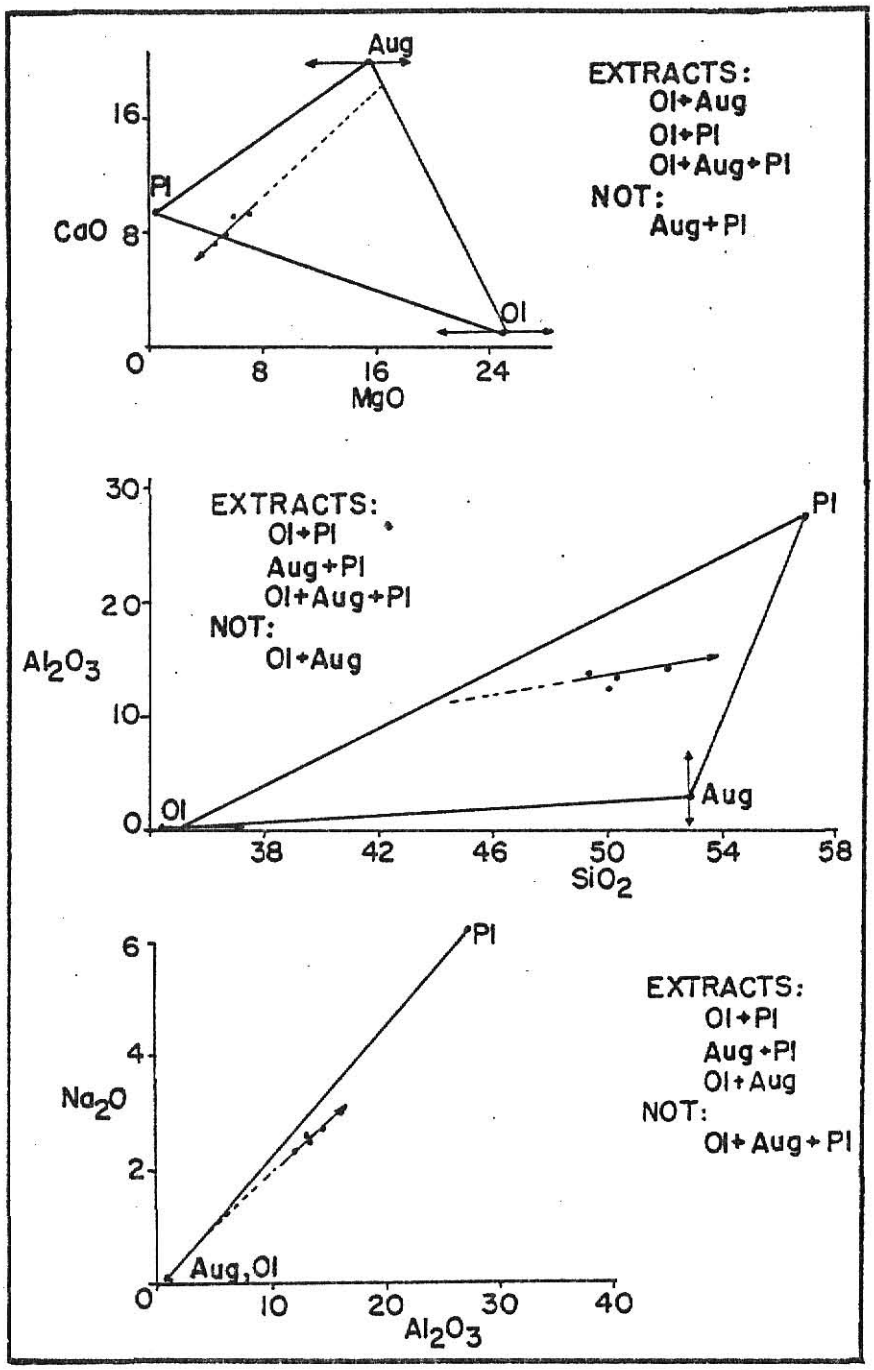

Figure 30. Major-element extract polygons which demonstrate the evolutionary trend of the gabbro group and possible mineral assemblages which could have fractionated to produce the trend.

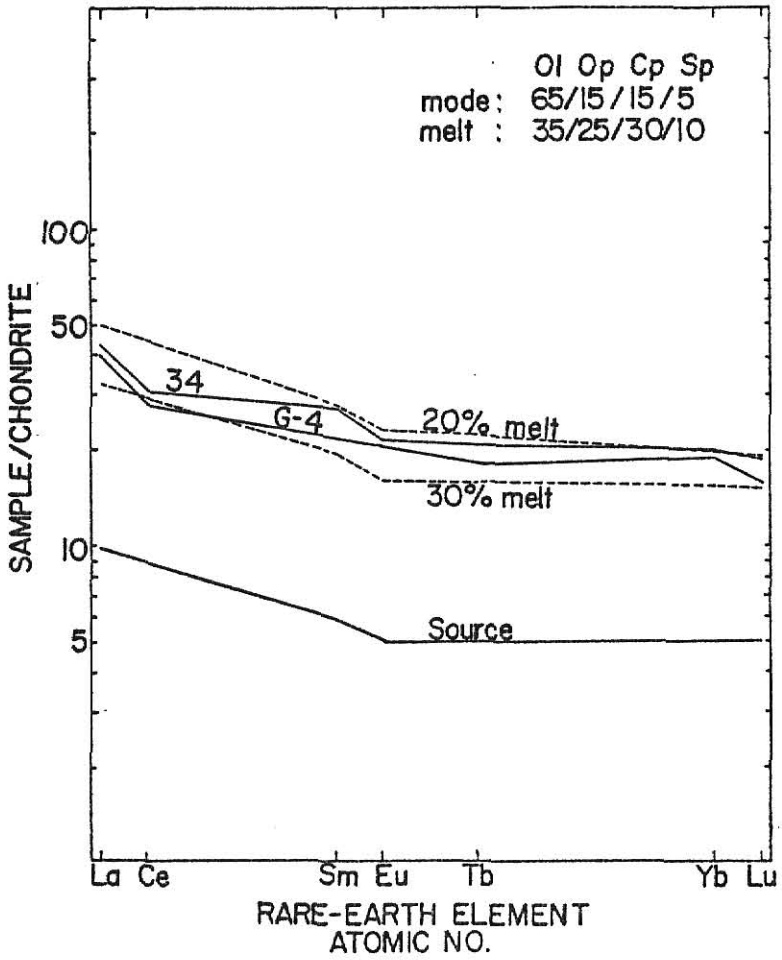

Figure 31. Gabbro (G-4 and 34) genesis by varied degrees of partial melt (dashed lines) of a LREE enriched spinel peridotite.

ratios as high as 0.7240 (Faure and Powell, 1972). Thus, the isotopic values and the variations in the gabbro's major-element and trace-element contents could be caused by 20 to 30 percent fusion in the lower crust of a peridotite of relatively homogenous composition.

HYBRID ROCK GENESIS

Two distinct hybrid rock types occur in association with the gabbro sill. The first is a plagioclase-rich assemblage which is found at the upper contact of the sill and as a narrow, thinly-jointed lens within the sill. The outcrop characteristics indicate that the intrusion of portions of the plagioclase hybrid may have occured subsequent to the solidification

of the sill. The second hybrid rock type is an orthoclase-muscovite assemblage which occurs at the upper contact of the sill and the Garnet Range Formation. The magmatic character of this material is suggested in some places where brecciation and intrusion of the Precambrian Garnet Range Formation occurs. Elsewhere, the orthoclase-muscovite rocks tend to form a gradational contact with the sedimentary units and display relict bedding.

The plagioclase-rich rocks have been found to contain small amounts of carbonate, which has an $^{87}Sr/^{86}Sr$ ratio of 0.7261. The presence of quantities of this carbonate could only lower the observed $^{87}Sr/^{86}Sr$ ratio of the hybrid rocks. Hence the calculated initial $^{87}Sr/^{86}Sr$ ratio is a minimum estimate of the isotopic composition of strontium at the time of formation of the hybrid rocks. The high initial $^{87}Sr/^{86}Sr$ isotopic ratios of 0.7286 and 0.7334 of the plagioclase-rich hybrid rocks are, therefore, an indication of derivation of the magma from a source or sources having distinctly different isotopic compositions than the gabbros. If two sources are involved, at least one must be crustal in origin.

The plagioclase-rich hybrid rock has a REE pattern with low La/Lu ratios of 2 to 3 and a large negative europium anomaly. In the event of fusion of a single source, either feldspar fractionation or partial melt of a source with a high percentage of feldspar could produce the europium anomalies. Additionally, the source region could have a small degree of europium depletion, in which case the requirement for feldspar fractionation or the percentage of feldspar in equilibrium with the melt would be less. Quantative models which produce the albite-rich hybrid rocks from a single source have been derived. Proposed source mineralogy was estimated from data of Koch (1978) and the REE contents of the source are taken to be that of average Precambrian sedimentary units compiled by Wildman and Haskin(1973). Thirty to forty percent fusion of a plagioclase-rich source

could produce REE patterns similar to that of the albite-rich rock (Fig. 32). The hypothetical concentrations of Ba, Rb, Sr, Co, Cr, and Sc in the proposed source have been calculated but they agree poorly with this theoretical model.

Qualitative examination of a second model demonstrates that a more complex origin for the plagioclase-rich rocks is possible. The chemical and isotopic characteristics of the albite-rich hybrid rocks could also be explained by a magma which has a history of assimilation of crustal material. Magma-country rock interactions could have produced the hybrid materials from gabbroic magma which incorporated crustal materials, possibly from the Garnet Range Formation. Initial strontium isotopic compositions of 0.7286 to 0.7334 could result from mixing of the gabbroic ratio of 0.7120 and the Precambrian ratio of 0.8220. The major chemical data can possibly be explained by removal of carbonate and iron-rich phases during crystallization of the hybrid rock melt. Assuming the REE patterns of the Garnet Range Formation are similar to the one observed for sample 33, which may be thermally altered sediments, the REE abundances of the albite-rich rock can also be explained by assimilation and later carbonate removal.

The orthoclase-muscovite rock has an initial strontium isotope ratio of 0.8614, suggestive of a radiogenic crustal origin. REE have a chondrite-normalized La/Lu ratio of about 5 and a large negative Eu anomaly within the orthoclase-rich hybrid rocks. Mobile magmatic portions of this hybrid type could have been produced by twenty to thirty percent fusion of an orthoclase-rich source with relatively high REE contents (Fig. 33). Non-mobile portions of this hybrid type have varied degrees of metamorphic texture and initial strontium isotope ratios similar to the Garnet Range Formation, implying this hybrid type is the direct result of

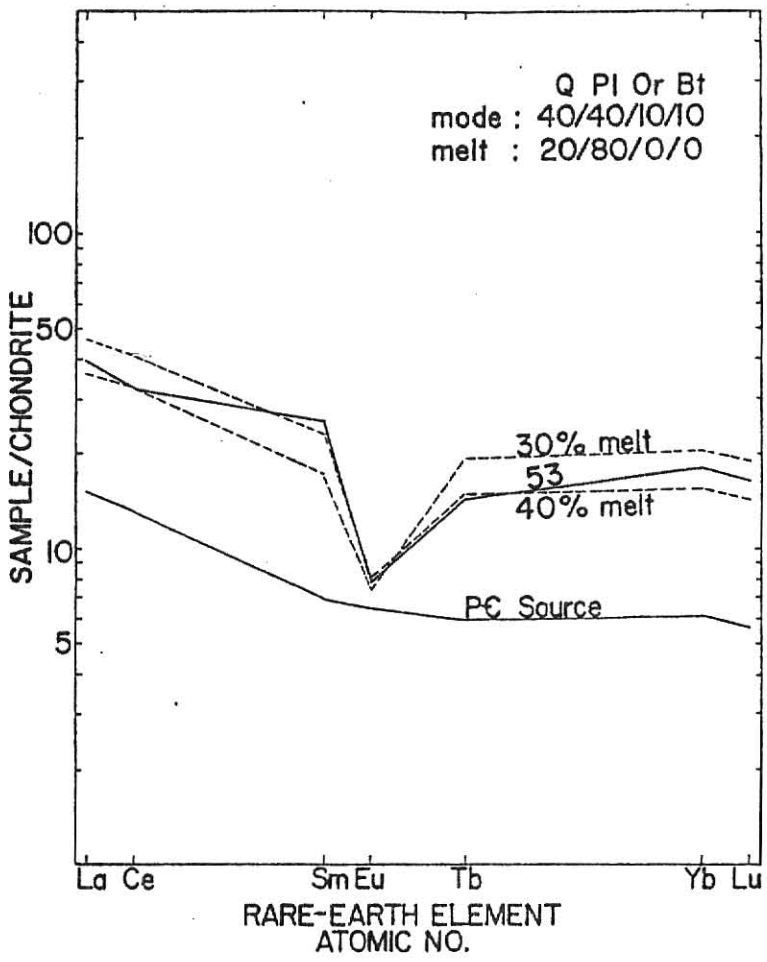

Figure 32. Plagioclase-rich hybrid (53) genesis by partial melt of a crustal source with a REE content similar to that of average Precambrian sediments (dashed lines = hypothetical melts).

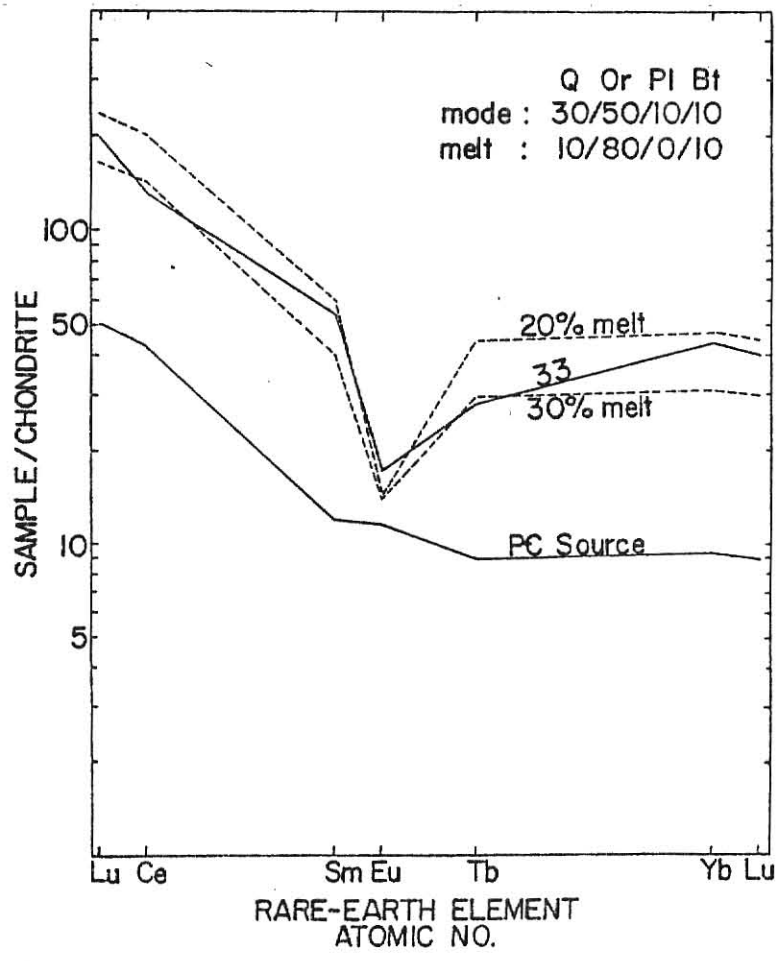

Figure 33. Orthoclase-muscovite-rich hybrid rock (33) genesis by partial melt of a crustal source which has a REE content similar to that of the upper limit of Precambrian sediments (dashed lines = hypothetical melts).

magmatic interactions with the country rock. The REE trends of the orthoclase-muscovite hybrid rocks would thus be a reflection of the REE contents of the Garnet Range Formation.

The theories of simple partial fusion to produce the 'hybrid' rocks can be tested with the use of the experimental five-component system Qz - An - Or - Ab - H_2O of Winkler (1976). Due to the high albite content of the orthoclase-muscovite rock, normative mineral compositions of the hybrid rocks within the system plot off the cotectic surfaces and lines as defined by ideal equilibrium melts. Departures from early eutectic and cotectic melts are possible in the following three cases: (1) presence of HCl on the system, (2) consumption of a component in the solid phase, and (3) absence of alkali-feldspar, anorthite, or albite in the source. Thus, the total absence or very low concentration of one or more of the five components in the system is required to produce melts similar to those of the hybrid rocks. Although this case could occur, magmatic interactions, perhaps followed by fractionation, seem to offer a more feasible path of evolution.

Concentrations of other trace elements (Ba, Rb, Sr, Co, Cr, and Cs) in the one-component sources were calculated and are compared to average Precambrian trace-element values in Table 10. The majority of the calculated values approximate the ranges observed in Precambrian sedimentary units, although actual source compositions are quite varied. The other trace elements cannot be used to support or refute the single-component or multiple-component histories.

RELATIONS TO SURROUNDING IGNEOUS BODIES

A paucity of geochemical data from igneous units immediately surrounding the present study area prohibits elemental and isotopic comparisons on a local scale. However, numerous chemical and isotopic studies have been conducted on the Boulder batholith (Doe et al., 1968; Tilling, 1973; 1974), on the Idaho batholith (Armstrong, 1974; Heitanen, 1962; 1963; Scholton and Onasch; 1976) and on plutonic rocks of the Flint Creek Range (Baty, 1975; Benoit; 1974; Ehinger, 1972; Hawley, 1975; Hyndman et al., 1972; Winegar, 1975). Structural studies relating to the origin of the Boulder batholith include those of Hamilton and Meyers (1974) and Klepper et al. (1971; 1974).

The intermediate to silicic units of the eastern Idaho batholith, the Sapphire tectonic block, the Flint Creek Range, and the Boulder batholith may be related to a common source (Hyndman, 1979). Uplift which resulted from intrusion of the Idaho batholith during the Late Cretaceous was sufficient to cause detachment and gravity sliding of a large block of Beltian sedimentary units. Magma beneath the detached Sapphire tectonic block intruded the Beltan units and was ejected into a broad basin to the east of the toe of the Sapphire block (Figs. 34 and 35). A series of flows several kilometers thick, mantled with its own ejecta, solidified to form the Boulder batholith (Hyndman et al., 1975). If the igneous rocks in and between the Idaho batholith and Boulder batholith are related by such a model, geochemical and isotopic ividence should reflect common origins.

Uncontaminated strontium isotopic initial ratios for granodiorite and dacite within the Ravenna area are about 0.7065 to 0.7067, similar to

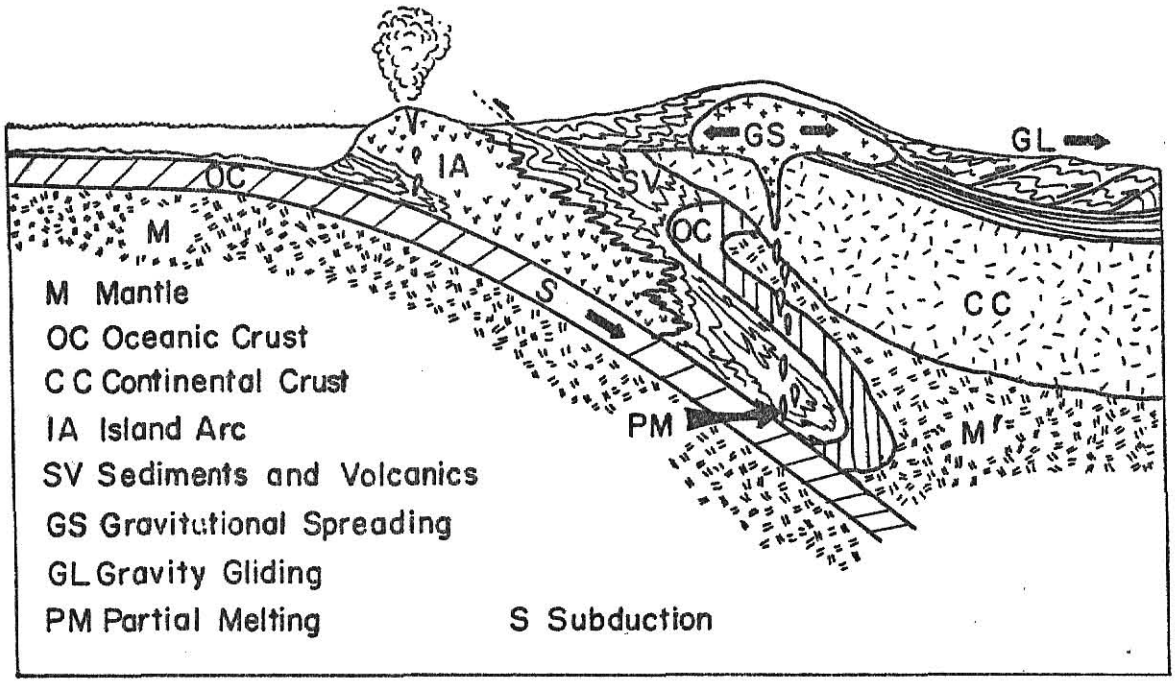

Figure 34. Interpretive sketch of the western North America continental margin during the Jurassic and Cretaceous Periods (after Scholton and Onasch, 1976).

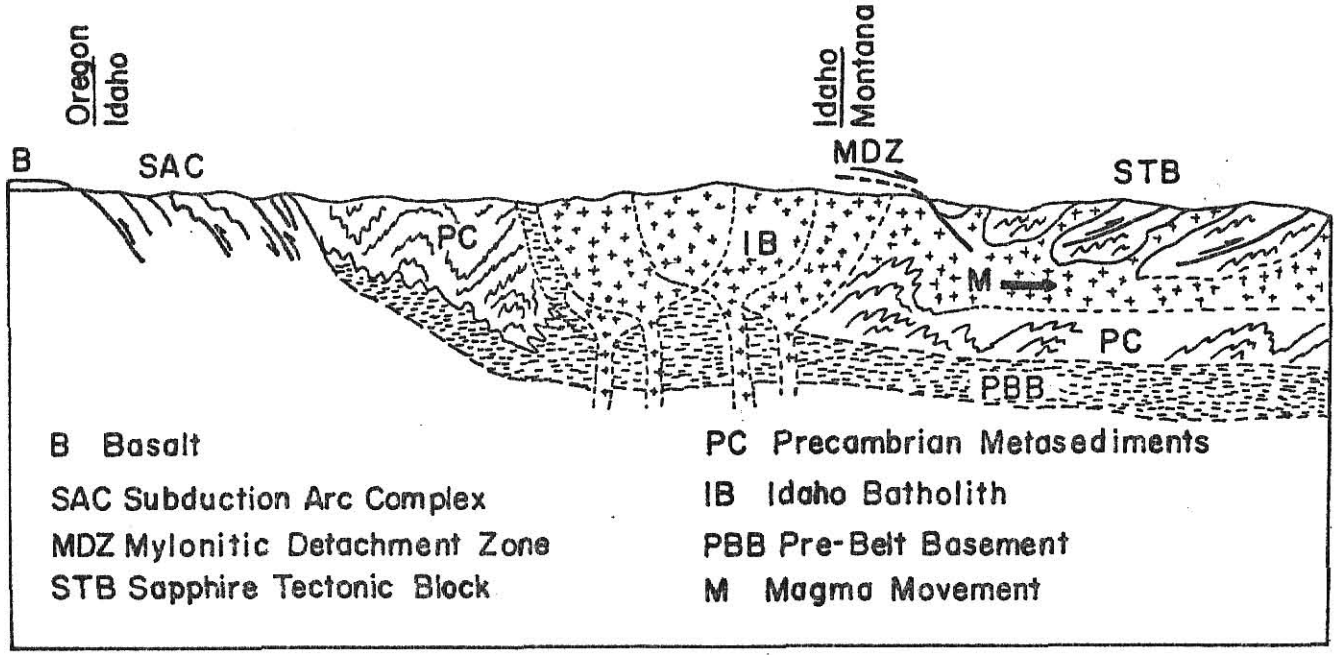

Figure 35. Generalized geologic cross-section from western Oregon to west-central Montana (after Hyndman, 1979).

granodioritic ratios of the Boulder batholith (0.7061 to 0.7072) (Doe et al., 1968). These ranges are similar to the isotopic values of most Cenozoic batholithic rocks in the northwestern United States.

Average major-element chemistry of gabbroic and granodioritic igneous units from the Flint Creek Range (45 km east of the study area), the Elkhorn Mountains (east of the Boulder batholith) and the Idaho and Boulder batholiths are summarized in Table 12. Rocks with SiO_2 contents between 63 and 65 percent have broadly similar major-element contents overall, whereas the gabbro compositions have considerable deviation in Al_2O_3 and $FeO + Fe_2O_3$ contents. The regionally similar silicic compositions support genesis in similar tectonic regimes from similar sources. On a regional scale, the gabbros may be related by fractionation processes, or may be derived from different sources. Ages, proposed origins, isotopic ratios, and bulk chemistry of the dacitic Ravenna units tend to support western batholithic origins proposed by Hyndman (1979). The Ravenna gabbros' bulk chemical dissimilarities compared to other gabbroic rocks is amgibuous and neither supports nor refutes proposed tectonic regimes.

The basaltic units of Ravenna were emplaced near or at the end of orogenic activity within the Montana area, and are unrelated to older, orogenic igneous units. The eruption of alkali-olivine basalts is commonly associated with extensional tectonic activity (Christiansen and Lipman, 1972). Mid-Tertiary volcanism in the central Montana region may be controlled in part by extensional couples along fundamental shear zones within the earth's crust (Smith, 1965), one of which passes beneath the present study area.

Table 12. Comparison of average major-element compositions of Upper Cretaceous gabbroic and granodioritic igneous rocks from central Idaho to central-western Montana (values in weight percent).

	(1) Gabbros, Idaho Bath.	(2) Gabbros, Elkhorn Mts.	(3) Gabbros, Race-track Pluton	(4) Gabbros, Ravenna Area	(5) Diorites, Idaho Bath.	(6) Monzon-ites, Boulder Bath.	(7) Grano-diorites, Boulder Bath.	(8) Grano-diorites, Elkhorn Mts.	(9) Silicics, Race-track Pluton	(10) Dacites, Ravenna Area
SiO_2	51.57	49.98	49.75	50.46	65.18	64.76	62.98	63.18	63.29	63.97
Al_2O_3	18.02	11.40	19.65	13.49	16.90	14.98	16.28	16.88	16.37	16.14
Fe_2O_3	2.16	3.92	---	16.49	1.36	2.66	2.45	2.52	---	2.79
FeO	6.72	6.15	10.51	---	2.46	2.28	2.75	2.35	6.51	---
MnO	0.14	0.15	---	0.23	0.05	0.08	0.13	0.10	---	0.056
MgO	5.85	7.71	5.94	5.14	1.73	2.13	2.20	2.39	1.91	1.79
CaO	8.36	11.86	10.23	8.38	4.41	3.71	4.72	5.30	4.99	3.32
Na_2O	3.27	2.06	2.58	2.52	4.42	2.94	3.48	3.32	5.22	3.75
K_2O	0.89	1.13	0.86	0.71	1.80	4.27	3.35	2.40	3.52	3.33
TiO_2	1.26	1.18	1.16	2.13	0.51	0.56	0.54	0.58	0.78	0.39
H_2O	1.26	0.88	---	0.82	0.77	0.94	0.71	1.19	---	2.95
TOTAL	99.50	99.42	100.68	100.32	99.59	99.31	99.59	100.20	102.59	98.49

References: (1) Average of four gabbros, northwest Idaho Batholith (Hietanen, 1962; 1963). (2) Average of three gabbros, Elkhorn Mountains (Klepper at al., 1957). (3) Average of four mafic rocks, Racetrack Pluton, Flint Creek Range. Similar to analyses from the Philipsburg and Mount Powell Batholiths (Hawley, 1975). (4) Average of four gabbros, this study. (5) Average of seven diorites and tonalites, northwest Idaho Batholith (Hietanen, 1962; 1963). (6) Average of seven quartz monzonites, Boulder Batholith (Ruppel, 1963). (7) Average of four granodiorites and quartz monzonites, Boulder Batholith (Smedes, 1966) (8) Average of four granodiorites, Elkhorn Mountains (Klepper et al., 1957). (9) Average of four silicic rocks, Racetrack Pluton, Flint Creek Range. Similar to analyses from the Phlipsburg and Mount Powell Batholiths (Hawley. 1975). (10) Average of seven dacites and granodiorite, this study.

C O N C L U S I O N

On the basis of petrographic and chemical data, three major distinct rock groups have been defined: (1) the basalt group, (2) the dacite-granodiorite-rhyodacite group, and (3) the gabbro group. The hybrid rocks found in association with the gabbro sill constitute a fourth, but volumetrically minor, rock group. The proposed parent rocks, genetic histories and tectonic sources for the various igneous groups are summarized below:

(1a) Alkali-olivine basalt: An Eocene age of emplacement is suggested by association of Eocene basalt and geochemical similarities to the tholeiitic basalt unit. Small quantities (about 4 percent) of partial melt of a LREE-enriched garnet peridotite within the upper mantle (30 to 40 km depth) could produce the observed major-element, trace-element, and isotopic concentrations. Melting may have been the result of tensional stresses generated by movement along deep-seated shear zones.

(1b) Tholeiitic basalt: An Eocene age is assigned to the tholeiitic basalt because of geomorphic evidence and the association of basaltic material of similar age. Large quantities (about 18 percent) of partial melt of an upper-mantle garnet peridotite enriched in LREE followed by small degrees of crustal contamination would produce the elemental contents. Magma generation processes may have been similar to that of the alkali-olivine basalt.

(2) Dacite-granodiorite-rhyodacite: Several episodes of dacitic volcanism occured within the study area after the emplacement of the

Sapphire tectonic block 78 m.y. B.P. Partial melts of a compositionally varied eclogitic source enriched in trace elements, perhaps similar to the subduction regime which produced the Idaho batholith and possibly augmented by varied degrees of crustal contamination, could have produced these units.

(3) Gabbro: The tholeiitic gabbro units are intimately associated with dacitic units in space and time but do not appear to be the result of subduction processes. Twenty to thirty percent melt of a lower-crust or upper-mantle peridotite could produce the gabbroic compositions. Linear geochemical trends observed between the gabbros are the result of varied degrees of partial melt of a spinel peridotite.

(4) Hybrid rocks: The hybrid rocks are not the result of crystal fractionation processes within the large gabbro sill. Leucocratic hybrid rocks could be the result of mixing of gabbroic and crustal material followed by fractionation, whereas potassium-rich hybrid rocks are primarily the result of contact metamorphism of the Garnet Range Formation, perhaps accompanied by mixing of gabbroic components.

A P P E N D I X

A: SAMPLE LOCATIONS

BR-79-12: SW¼, SE¼, NW¼; Sec. 26; T. 11 N.; R. 16 W.; prospect pit in dacite porphyry north of the road at Gillespie saddle.

BR-79-20: NE¼, NE¼, SE¼; Sec. 25; T. 11 N.; R. 16 W.; roadcut through base of massive natural outcrop of dacite porphyry.

BR-79-26: SW¼, NE¼, NW¼; Sec. 28; T. 11 N.; R. 15 W.; natural outcrop of dacite porphyry on the crest of the shoulder at about 5000 ft elevation.

BR-79-45: NW¼, SE¼, SW¼; Sec. 16; T. 11 N.; R. 15 W.; west side of roadcut through dacite porphyry.

BR-79-46-B: SW¼, SE¼, SW¼; Sec. 27; T. 11 N.; R. 15 W.; west side of roadcut through dacite porphyry.

BR-79-58: SE¼, SE¼, NE¼; Sec. 19; T. 11 N.; R. 15 W.; south side of roadcut through dacite porphyry.

BR-79-46: SE¼, NW¼, NW¼; Sec. 13; T. 11 N.; R. 16 W.; Roadcut through massive granodiorite on the north side of Gillespie Creek.

BR-79-51: SW¼, NE¼, NE¼; Sec. 34; T 11 N.; R. 15 W.; natural outcrop on the west bank of Tyler Creek.

BR-79-G-4: SW¼, SW¼, SW¼; Sec. 11; T. 11 N.; R. 16 W.; north side of roadcut through gabbro and dacite near the southern end of Beavertail Hill.

BR-79-21-G: SW¼, NW¼, NE¼; Sec. 24; T. 11 N.; R. 16 W.; roadcut through massive gabbro on the west bank of Gillespie Creek.

BR-79-24: NE¼, NW¼, NE¼; Sec. 19; T. 11 N.; R. 16 W.; natural massive outcrop of gabbro on the south side of a small stream channel.

BR-79-34: SE¼, NE¼, SW¼; Sec. 22; T. 11 N.; R. 15 W.; outcrop on crest of shoulder west of creek at about 4100 ft elevation.

BR-79-37: SW¼, NE¼, SE¼; Sec. 26; T. 11 N.; R. 15 W.; outcrop in small clearing east of access road.

BR-79-49: NE¼, NW¼, SE¼; Sec. 33; T. 11 N.; R. 15 W.; west side of roadcut through basalt as about 5300 ft elevation.

BR-79-33: SE¼, SE¼, NW¼; Sec. 21; T. 11 N.; R. 15 W.; outcrop in cattle path on the west side of Bateman Creek.

BR-79-53: SE¼, NE¼, NE¼; Sec. 26; T. 11 N.; R. 15 W.; outcrop near prospecr drift, east side of Tyler Creek.

BR-79-54: SW¼, NE¼, NE¼; Sec. 26; T. 11 N.; R. 15 W.; massive outcrop on the west bank of Tyler creek.

BR-79-YGR: SW¼, NE¼, NE¼; Sec. 26; T. 11 N.; R. 15 W.; Precambrian Garnet Range Formation west of sample location 54.

REFERENCES

Armstrong, R.L., 1974, Geochronometry of the Eocene volcanic-plutonic episode in Idaho. Northwest Geol. 3, 1-11.

Armstrong, R.L., Ekren, E.B., McKee, E.H., Noble, D.C., 1969, Space-time relations of Cenozoic silicic volcanism in the great basin of the western United States. Am. Jour. Sci. 267, 478-490.

Batiza, R., 1978, Geology, petrology, and geochemistry of Isla Tortuga, a recently formed tholeiitic island in the Gulf of California. Geol. Soc. Am. Bull. 89, 1309-1324.

Baty, B., 1975, Fission track age dates from three granitic plutons in the Flint Creek Range, western Montana. Northwest Geol. 4, 34-41.

Benoit, W.R., 1974, Chemistry and genetic relationship of the Royal Stock and the Mount Powell batholith, western Montana. Northwest Geol. 3, 53-58.

Brooks, C. James, D.E., Hart, S.R., 1976, Ancient lithosphere: its role in young continental volcanism. Science 193, 1086-1094.

Bryan, W.B., Frey, F.A., Thompson, G., 1977, Oldest Atlantic seafloor Mesozoic basalts from western north Atlantic margin and eastern north America. Contrib. Mineral. Petrol. 64, 223-242.

Christiansen. R.L., Lipman, P.W., 1972, Cenozoic volcanism and plate tectonic evolution of the western United States II, late Cenozoic. Phil. Trans. Roy. Soc. London A 271, 249-284.

Cox, K.G., Bell, J.D., Pankhurst, R.J., 1979, The Interpretation of Igneous Rocks. London: George Allen and Unwin, 450 p.

Desormier, W.L., 1975, A section of the northern boundary of the Sapphire tectonic block. M.S thesis, University of Montana, 65 p.

Doe, B.R., Tilling, R.I., Hedge, C.E., Klepper, M.R., 1968, Lead and strontium isotope studies of the Boulder batholith, southwestern Montana. Econ. Geol. 63, 884-906.

Eade, K.E., Fahrig, W.F., 1973, Regional, lithological and temporal variation in the abundances of some trace elements in the Canadian Shield. Geol. Surv. Can. Paper 72-46, 46 p.

Ehinger, R.F., 1972, Magmatic processes in the Philipsburg batholith, Montana. Northwest Geol. 1, 47-51.

Engel, C.G., Fisher, R.L., 1975, Granitic to ultramafic rock complexes of the Indian Ocean ridge system, western Indian Ocean. Geol. Soc. Am. Bull. 86, 1553-1578.

Faure, G., 1977, Principles of Isotope Geology. New York: John Wiley and Sons, 464 p.

Flanagan, F.J., 1973, 1972 values for international geochemical reference samples. Geochim. Cosmochim. Acta 37, 1189-1200.

Flanagan, F.J., 1976, Descriptions and analyses of 8 new U. S. Geological Survey rock standards. U. S. Geol. Surv. Prof. Paper 840, 192 p.

Frey, F.A., 1979, Trace element geochemistry: applications to the igneous petrogenesis of terrestial rocks. Rev. Geophy. Space Phy. 17, 803-823.

Frey, F.A., Bryan, W.B., Thompson, G., 1974, Atlantic Ocean floor: geochemistry and petrology of basalts from legs 2 and 3 of the Deep-Sea Drilling Project. J. Geophys. Res. 79, 5507-5527.

Gill, J.B., 1978, Role of trace element partition coeffieients in models of andesite genesis. Geochim. Cosmochim. Acta 42, 709-724.

Gilluly, J., 1971, Plate tectonics and magma evolution. Geol. Soc. Am. Bull. 82, 2383-2396.

Green, D.H., Ringwood, A.E., 1967, The genesis of basaltic magmas. Contrib. Mineral. Petrol. 15, 103-190.

Hamilton, W.B., Meyers, W.B., 1967, The nature of batholiths. U. S. Geol. Surv. Prof. Paper 554-C, C-1-C-30.

Hamilton W.B., Meyers, W.B., 1974, Nature of the Boulder batholith of Montana. Geol. Soc. Am. Bull. 85, 365-378.

Haskin, L.A., Frey, F.A., Wildeman, T.R., 1968, Relative and absolute terrestial abundances of the rare earths. In: Origin and Distribution of the Elements, Ahrens, C.H., Ed., Intern. Ser. Monography Earth Sc. 30, 889-912.

Hawley, K.T., 1975, The Racetrack pluton-- a newly defined Flint Creek pluton. Northwest Geol. 4, 1-9.

Hietanen, A., 1962, Metasomatic metamorphism in western Clearwater County, Idaho. U. S. Geol. Surv. Prof. Paper 344-A. A1-A116.

Hietanen, A., 1963, Metamorphic and igneous rocks along the Idaho batholith near Pierce and Bungalow, Clearwater County, Idaho. U. S. Geol. Surv. Prof. Paper 344-D, D1-D42.

Hyndman, D.W., 1972, Petrogenesis of Igneous and Metamorphic Rocks. New York: McGraw-Hill, 533 p.

Hyndman, D.W., 1979, Major tectonic elements and tectonic problems along the line of section from northeastern Oregon to west-central Montana. Geol. Soc. Am. Map and Chart Series MC-28-C, 11 p.

Hyndman, D.W., Obradovich, J.D.,hinger, R., 1972, Potassium-argon age determinations of the Philipsburg batholith. Geol. Soc. Am. Bull. 83, 473-474.

Hyndman, D.W., Talbot, J.L., Chase, R.B., 1975, Boulder batholith: A result of emplacement of a block detached from the Idaho batholith infrastructure? Geology 3, 401-404.

Jacobs, J.W., Korstev, R.L., Blanchard, D.P., Haskin, L.A., 1977, A well-tested procedure for instrumental neutron activation analyses of silicate rocks and minerals. J. Radioanal. Chem. 40, 93-114.

Kilbane, N.K., 1978, Petrogenesis of the McClure mountain mafic-ultramafic and alkalic complex, Fremont County, Colorado. M.S. thesis, Kansas State University, 158 p.

Klepper, M.R., Robinson, G.D., Smedes, H.W., 1971, On the nature of the Boulder batholith of Montana. Geol.Soc. Am. Bull. 82, 1563-1580.

Klepper, M.R., Robinson, G.D., Smedes, H.W., 1974, Nature of the Boulder batholith of Montana: discussion. Geol. Soc. Am. Bull. 85, 1953-1960.

Klepper, M.R., Weeks, R.A., Ruppel, E.T., 1957, Geology of the southern Elkhorn mountains, Jefferson and Broadwater Counties, Montana. U. S. Geol. Surv. Prof. Paper 292, 81 p.

Koch, R., 1978, Petrogenesis of the Precambrian Bevos and Musco groups, St. Francois mountains igneous complex, Missouri. M.S. thesis, Kansas State University, 104 p.

Leeman, W.P., 1976, Petrogenesis of the McKinney (Snake River) olivine tholeiite in light of rare-earth element and Cr/Ni distributions. Geol. Soc. Am. Bull. 87, 1583-1586.

Leeman, W.P., Rogers, J.J.W., 1970, Late Cenozoic alkali-olivine basalts of the Basin-Range province, U.S.A. Contrib. Minreal. Petrol. 25, 1-24.

MacDonald, G.A., Katsura, T., 1964, Chemical conposition of Hawaiian lavas. J. Petrol. 5, 82-133.

McBirney, A.R., Williams, H., 1969, Geology and petrology of the Galapagos Islands. Geol. Soc. Am. Mem. 118, 197 p.

Medlin, J.H., Suhr, N.H., Bodkin. J.B., 1969, Atomic absorption analysis of silicates employing $LiBO_2$ fusion. Atom. Absorp. News. 8, 25-29.

Montgomery, J.K., 1958, Geology of the Nimrod area, Granite County, Montana. M.S. thesis, Montana State University, 61 p.

Nesbitt, R.W., Sun, S.-S., 1976, Geochemistry of Archean spinifex-textured peridotites and magnesian and low-magnesian tholeiites. Earth Planet. Sci. Lett. 31, 433-453.

Pardee, J.T., 1918, Ore deposits of the northwestren part of the Garnet Range, Montana. U.S. Geol. Surv. Bull. 660-F, 195-239.

Peacock, M.A., 1931, Classification of igneous rock series. J. Geol. 39, 54-67.

Philpotts, J.A., Schnetzler, C.C., 1970a, Phenocryst-matrix partition coefficients for K, Rb, Sr, and Ba, with applications to anorthosite and basalt genesis. Geochim. Cosmochim. Acta 34, 307-322.

Philpotts, J.A., Schnetzler, C.C., 1970b, Speculations on the genesis of alkaline and sub-alkaline basalts following exodus of the continental crust. Can. Mineral. 10, 374-379.

Ruppel, E.T., 1963, Geology of the Basin quadrangle, Jefferson, Lewis and Clark, and Powell Counties, Montana. U.S. Geol. Surv. Bull. 1151, 121 p.

Schnetzler, C.C., Philpotts, J.A., 1968, Partition coefficients of REE and Ba between igneous matrix material and rock-forming mineral phenocrysts. In: Origin and Distribution of the Elements, Ahrens, L.H., Ed. Pergamon Press, 929-938.

Schnetzler, C.C., Philpotts. J.A., 1970, Partition coefficients of REE between igneous matrix material and rock-forming phenocrysts II. Geochim. Cosmochim. Acta 34, 331-340.

Scholten, R., Onasch, C.M., 1976, Genetic relations between the Idaho batholith and its deformed eastern and western margins. Northwest Geol. 5, 25-37.

Shaw, D.M., 1970, Trace element fractionation during anatexis. Geochim. Cosmochim. Acta 34, 237-248.

Shaw, D.M., Dostal. J., Keays, R.R., 1976, Additional estimates of continental surface Precambrian shield composition in Canada. Geochim. Cosmochim. Acta 40, 73-83.

Smedes, H.W., 1966, Geology and igneous petrology of the northern Elkhorn mountains, Jefferson and Broadwater Counties, Montana. U.S. Geol. Surv. Pro. Paper 510, 116 p.

Smith, J.G., 1965, Fundamental transcurrent faulting in the northern Rocky mountains. Amer. Assoc. Petrol. Geol. Bull. 49, 1398-1409.

Suhr, N.H., Ingamells, C.O., 1966, Solution technique for analysis of silicates. Anal. Chem. 38, 730-734.

Taylor, S.R., 1964a, Trace element abundances and the chondritic earth model. Geochim. Cosmochim. Acta 28, 1984-1998.

Taylor, S.R., 1964b, Abundances of chemical elements in the continental crust: a new table. Geochim. Cosmochim. Acta 28, 1273-1285.

Tilling. R.I., 1973, Boulder batholith, Montana: A product of two contemporaneous but chemically distinct magma series. Geol. Soc. Am. Bull. 84, 3879-3900.

Tilling, R.I., 1974, Composition and time relations of plutonic and associated volcanic rocks, Boulder batholith region, Montana. Geol. Soc. Am. Bull. 85, 1925-1930.

Wallace, C.A., Klepper, M.R., French, A.B., Scarborough, D.M., 1978, Preliminary geologic map of the northwestern part of the Butte 1° x 2° quadrangle, Montana. U.S. Geol. Surv. Open File Report 78-371.

Weidman, R.M., 1965, The Montana lineament. Billings Geological Society Sixteenth Annual Field Conference, p. 137-143.

Wildeman, T.R., Haskin, L.A., 1973, Rare earths in Precambrian sediments. Geochim. Cosmochim. Acta 37, 419-438.

Williams, T.R., 1976, Geothermal potential in the Bearmouth area, Montana. M.S. Thesis, University of Montana, 62 p.

Winegar, R.C., 1975, Evidence of eastward movement of magma near the eastern boundary of the Sapphire plate. Northwest Geol. 4, 50-53.

Zielinski, R.A., Lipman, P.W., 1976, Trace element variations at Summer Coon volcano, San Juan mountains, Colorado, and the origin of continental-interior andesite. Geol. Soc. Am. Bull. 87, 1477-1485.

EVOLUTION OF TERTIARY PLUTONIC AND VOLCANIC ROCKS NEAR RAVENNA, GRANITE COUNTY, MONTANA

by

BRUCE KEVIN REITZ

B.S., Wright State University, 1978

AN ABSTRACT OF A MASTER'S THESIS

submitted in partial fulfillment of the

requirements of the degree

MASTER OF SCIENCE

Department of Geology

KANSAS STATE UNIVERSITY
Manhattan, Kansas
1980

ABSTRACT

The plutonic and volcanic units which occur within an area of about thirty square miles in northeastern Granite County, Montana, have been mapped and examined for their petrogenetic history. Major igneous rock types include Eocene basalt and Tertiary dacite porphyry, granodiorite, rhyodacite, and gabbro. Very minor quantities of two distinct hybrid rocks, are found in association with a large gabbro sill. Igneous stratigraphic succession from oldest to youngest is as follows: granodiorite and dacite porphyry, gabbro, dacite porphyry, and basalt.

On the basis of data of major elements, Ba, Sr, Rb, Co, Cr, Cs, Hf, Sb Sc, Se, Ta, Th, U, Zn, REE (rare-earth element) content, and strontium isotopic composition, three major rock groups are defined: the basalt, the dacite-granodiorite-rhyodacite, and the gabbro groups. The volumetrically minor hybrid rocks constitute a small fourth group.

Alakli-olivine and tholeiitic basalt may have been generated by 4 and 18 percent non-modal melting, respectively, of an upper-mantle garnet peridotite composed of 53 percent olivine, 25 percent orthopyroxene, 20 percent clinopyroxene, and 2 percent garnet. High ΣREE contents (alk.-ol. = 428 ppm; thol. = 163 ppm) and highly fractionated chondrite-normalized REE patterns (La/Lu = 15 to 30 ppm) are characteristic of the basalt. Crustal contamination of the tholeiite is possible given the high $^{87}Sr/^{86}Sr$ initial ratio (0.7113) and the high Rb/Sr ratio (0.05) compared to those of the alkali-olivine basalt ($^{87}Sr/^{86}Sr_i$ = 0.7060; Rb/Sr = 0.02). The dacite-granodiorite-rhyodacite group has relatively diverse elemental and isotopic

compositions (ΣREE = 87-244 ppm; La/Lu = 25-35; $^{87}Sr/^{86}Sr$ = 0.7065-0.7206; Rb/Sr = 0.05-0.15). Approximately thirty percent fusion of a trace-element enriched, compositionally varied eclogite, possible accompanied by minor degrees of crustal contamination, could have formed the silicic units. The tholeiitic gabbros are relatively homogeneous in terms of major-element, trace-element, and isotopic chemistry (ΣREE = 80-89 ppm; La/Lu = 2-3; $^{87}Sr/^{86}Sr_i$ = 0.7116-0.7143; Rb/Sr = 0.15-0.19). REE models suggest that twenty to thirty percent non-modal fusion of a lower crustal spinel peridotite composed of 65 percent olivine, 15 percent clinopyroxene, 15 percent orthopyroxene, and 5 percent spinel could produce the parent magma of the gabbro. Complex genetic histories are involved in the origin of minor volumes of hybrid rocks. Large degrees of crustal assimilation by gabbro magmas is suggested by trace-element and isotopic data (ΣREE = 80-272 ppm; La/Lu = 2-5; $^{87}Sr/^{86}Sr_i$ = 0.7286-0.8614; Rb/Sr = 1.16-4.44).

Comparison of the major-element and isotopic data of the Ravenna area with similar data of Upper Cretaceous igneous units from the Idaho and Boulder batholiths, the Flint Creek Range, and the Elkhorn Mountains demonstrate a regional continuum of rocks of silicic chemical composition but a lack of chemical correlation between gabbro rocks of the region. The data support the evolutionary model of the Late Cretaceous and Early Tertiary igneous terrain in Montana and Idaho proposed by Hyndman (1979).